REPUBLIQUE DU CAMEROUN
Paix – Travail – Patrie
****
UNIVERSITE DE YAOUNDE I
FACULTE DES SCIENCES
DEPARTEMENT DE PHYSIQUE
****
CENTRE DE RECHERCHE ET DE FORMATION DOCTORALE EN SCIENCES, TECHNOLOGIES ET GEOSCIENCE
LABORATOIRE DE MECANIQUE, MATERIAUX ET STRUCTURES

REPUBLIC OF CAMEROUN
Peace – Work – Fatherland
****
UNIVERSITY OF YAOUNDE I
FACULTY OF SCIENCE
DEPARTMENT OF PHYSICS
****
POSTGRADUATE SCHOOL FOR SCIENCES, TECHNOLOGY AND GEOSCIENCES
LABORATORY OF MECHANICS, MATERIALS AND STRUCTURES

SYNCHRONIZATION DYNAMICS AND DIFFUSION-INDUCED SPATIOTEMPORAL PATTERNS IN CELLS WITH ACTIVATOR-INHIBITOR PATHWAYS

Thesis
Submitted and defended in fulfillment of the requirements for the award of the degree of Doctor of Philosophy in Physics

Par : **GUEMKAM GHOMSI PATRICK**
Master of Science in Physics, Specialty: Mechanics

Sous la direction de
KOFANE Timoléon Crépin
Professor
University of Yaounde I

Année Académique : 2017 - 2018

BIBLIOTHEQUE UNIVERSITAIRE UYI

UNIVERSITÉ DE YAOUNDÉ I
UNIVERSITY OF YAOUNDE I

FACULTÉ DES SCIENCES
FACULTY OF SCIENCE

DÉPARTEMENT DE PHYSIQUE
DEPARTMENT OF PHYSICS

ATTESTATION DE CORRECTION DE LA THÈSE DE DOCTORAT/Ph.D

Nous, Professeur **TCHAWOUA Clément** et Professeur **WOAFO Paul**, respectivement Examinateur et Président du jury de la Thèse de Doctorat/Ph.D de Monsieur **GUEMKAM GHOMSI Patrick**, Matricule **98X384**, préparée sous la supervision du Professeur **KOFANE Timoléon Crépin,** intitulée : « **SYNCHRONIZATION DYNAMICS AND DIFFUSION-INDUCED SPATIOTEMPORAL PATTERNS IN CELLS WITH ACTIVATOR-INHIBITOR PATHWAYS** », soutenue le **Jeudi, 01 Novembre 2018**, en vue de l'obtention du grade de Docteur/Ph.D en Physique, Spécialité **Mécanique, Matériaux et Structures,** Option **Mécanique Fondamentale et Systèmes Complexes,** attestons que toutes les corrections demandées par le jury de soutenance ont été effectuées.

En foi de quoi, la présente attestation lui est délivrée pour servir et valoir ce que de droit.

Fait à Yaoundé le 09 NOV 2018

Examinateur	Le Président du jury	Le Chef de Département de Physique
Prof. TCHAWOUA Clément	Prof. WOAFO Paul	Prof. NDJAKA Jean-Marie Bienvenue

University of Yaoundé I

Faculty of Science

Department of Physics

SYNCHRONIZATION DYNAMICS AND DIFFUSION-INDUCED SPATIOTEMPORAL PATTERNS IN CELLS WITH ACTIVATOR-INHIBITOR PATHWAYS

Submitted and defended in Fulfillment of the Requirements for the Degree of Doctor of Philosophy/PhD in Physics

Specialty: Mechanics, Materials and Structures

By

GUEMKAM GHOMSI Patrick

Registration number: 98X384

M. Sc. in Physics

Supervisor

Prof. KOFANE Timoléon Crépin

Laboratory of Mechanics, Materials and Structures

Year 2017

Dedication

This work is dedicated to:

- my dear mother **GHOMSI Philomène** born **MEYUE**
- my dear late father **GHOMSI Gérard**
- my beloved wife **GUEMKAM Monique Chimène** born **MBOUS**
- my beloved brothers and sisters: **NONO Eric, SANDJO Christian, TCHUENTE Alain, MAYOU Linda, KAMGAIN Valerie**
- my beloved son **GHOMSI GUEMKAM Maxime Andy Isaac**

Acknowledgements

This thesis has been realized concomitantly in the Laboratory of Mechanics, Materials and Structures at the University of Yaounde *I*; and in the Laboratory of Research on Advanced Materials and Nonlinear Science (LaRAMaNS) at the University of Buea.

I would like to express my sincere gratitude to my supervisor, Professor KOFANE Timoléon Crépin, Head of the Laboratory of Mechanics. Before being my Ph.D. thesis supervisor, I first met Professor KOFANE in 2007 as my lecturer in the master of science degree programme in Physics, where he initiated me in several courses dealing with nonlinear phenomena, including the course on chaos and dynamical systems which have high relevance in the present research work. Since that meeting, I have been appreciating his exceptional personality as well as his scientific and human qualities. First and foremost, Professor KOFANE is a physicist with a very large culture. His formidable knowledge of problems involving nonlinear physics and his curiosity to new ideas make of him a fascinating scientist: his ideas and suggestions brought clarity and insight to our work. His pedagogic attitude and permanent need of grasping knowledge stand as a reference model for me. He constantly comforted me and has also been a patient advisor, with the tact and the ability to understand the finer details of theoretical methods. He has guided me through difficult challenges with empathy, and openly shared the excitement of our successes.

I would like to address warm cheers to my research director and coordinator of the LaRAMaNS Lab, Professor MOUKAM KAKMENI François Marie at the University of Buea, for his great human virtues, guidance and constant support during this research work. He gave me the opportunity to work very closely to him, and took it on him to see me through my postgraduate studies. In spite of his huge academic duties, he always found time to discuss with me and answer my queries. Beyond the academic realm, he has always had a fatherly attitude toward me. For the key role I do believe he plays in this evolution, I would like to express my sincere gratitude to Professor MOUKAM KAKMENI.

Next, I am profoundly indebted to Professor TCHAWOUA Clément who entrusted me in engaging in a scientific career. The numerous discussions I had with him, in spite of his huge academic and administrative duties, tremendously imparted me with knowledge and skills crucial for a better perception of some physical phenomena. At the end of this research work, I am aware of having improved largely, both scientifically and personally since the beginnings.

I wish to express special thanks to Professor DIKANDE Alain Moïse of the University of Buea for his scientific proficiency, support and friendship. I have benefited greatly from the countless discussions we have had. His advice and constant encouragements have undoubtedly driven me towards achieving my goals in reasonable time. He has equally accepted to bring

his great expertise in reviewing the present thesis. I have equally gained greatly from countless discussions with Doctor MKAM TCHOUOBIAP Serges Eric. I would like to thank him for his patience and concerns towards me.

My deepest thankfulness goes to my mother Madame GHOMSI born MEYUE Philomène who groomed me scientifically in the field of physical sciences right from the onset, in her capacity of skilled educator in the fields of physics and chemistry. She is the one who inducted me in the scope of Physics, and she has never spared any effort to ensure that I succeed in my endeavors towards meeting my objectives, by laying a strong scientific foundation which has been exceedingly beneficial to me till date. On the same footing, I am profoundly grateful to my deceased father, late Doctor GHOMSI GERARD who never relented in prompting me to work hard toward defending my Ph.D. thesis in satisfactory time.

I am equally thankful to late Doctor MOUSSA ILDOKO who supervised me for my master of science degree dissertation, making it possible for me to explore new challenges. I owe a lot of gratitude to all the teachers of the Department of Physics of the University of Yaounde I and the University of Buea. I am thankful to Professor SIEWE SIEWE Martin who kindly responded to some of my querries whenever we discussed. I would like to thank all the former and present members of the Laboratory of Mechanics for their help and the friendship I shared with them there. Among them are Dr. TOGUEU MOTCHEYO Alain Bertrand, TCHINANG TCHAMEU Joel Durel, TCHUISSEU Roni Martial, KUIKA NGATCHA Sophia Durdovic.

I am also grateful to all the friends I met during this work at the Department of Physics. I wish to express here my sincere gratitude to Mr SIMO Bernard and his family, Mme SOB Luçienne and her family, Mrs KOUOBOU Honorine, Mr TAME Abel and his family, Mme NDASSI marie and her family, Mr SENDJONG François and his family, Mr TCHIMCHOU Pascal and his family for the support and love they have been giving to my person. I acknowledge the support and encouragement from my brothers NONO Eric, SANDJO Christian, TCHUENTE Alain, my sisters MAYOU Linda, KAMGAIN Valerie, my wife MBOUS Monique Chimene and my son GHOMSI GUEMKAM Maxime Andy Isaac, whose erratic behavior made me to have a clear practical experience of the phenomenon of chaos in dynamical systems.

List of Abbreviations

CS: Complete Synchronization

1-D: One-dimensional

2-D: Two-dimensional

PS: Phase Synchronization

TW: Travelling Wave

P_1: Period one

P_2: Period two

P_4: Period four

Contents

List of Figures

Abstract

The cellular transport through the plasma membrane determines cells' fate, function and phenotype. It controls what enters or leaves the cells through both active and passive transport processes such as diffusion and osmosis, while relying on several important signaling schemes involving both short and long range interactions. In this thesis, we contribute to the understanding, on one part, of the impact of these two types of coupling on the synchronization and control of the cellular rhythms crucial for their coordinated collective behavior, in order to preserve homeostasis and enhance cellular communication. On the other part, to highlight the emergence of both stable and unstable patterns which are fundamental in cellular exchange, organisms morphology, and specialization amid living beings. In this framework, cells with activator-inhibitor pathways stand as our core biochemical models for these investigations. Firstly, synchronization - wise, while bearing in mind the adaptive character of the extracellular medium, we start by analyzing the effects of chemical, electrical and environment-mediated coupling types on the exchange of metabolites across concentrations of cells, in order to study the onset of phase and complete synchronization in the chaotic biochemical system. In these contexts, the stability of the synchronization manifold is studied by means of both mathematical and numerical tools such as the master stability function approach, the conditional Lyapunov exponents, the rate of change of the Lyapunov function, the construction of localized sets via Poincare sections, the phase difference, the Kuramoto parameter for phase entrainment, and the phase space conditional observation spreading parameter for stroboscopic maps. All these indicators continuously advocate for the prevalence of a phase synchronized dynamics among the interacting cells in the phase space. Yet, the results indicate that the system cannot completely synchronize under the sole action of the chemical coupling. Both the combined effects of the chemical and electrical couplings on one side, and the adaptive environment-mediated coupling scheme with feedbacks and control mechanisms on the other side, are found to be of capital importance in the onset of complete synchronization and high quality synchronization in the system. Secondly, we ascertain the emergence of spatiotemporal structures in $1-D$ and $2-D$ spatial lattices of the biochemical system. In $1-D$ ensembles, we report several phenomena of patterns formation with and without suppression of chaos in the heterogeneous lattices, with bubbling scenarios. Next, we also construct

a normalized formalism emulating the dynamics of the morphogens concentrations in two-dimensional spatial arrays of such pathways. The stability analysis of the spatially homogeneous equilibrium state of our biochemical lattice is performed both analytically and numerically. Some suitable parameter conditions are highlighted as conducive for the occurrence of diffusion-driven instabilities, crucial for the emergence of spatiotemporal patterns. The patterning events include inhomogeneous stationary (Turing) spatial patterns and oscillatory spatial patterns encompassing travelling wave phenomena and spatiotemporal chaos. Their relevance in biology stems from their staple prevalence in the communicative and developmental processes of cells.

Keywords: *Chaos, synchronization, cell-cell communication, biochemical systems, Lyapunov stability, spatiotemporal patterns, Turing instability.*

Résumé

Le transport cellulaire via la membrane plasmique determine le destin, les fonctions et les caractéristiques visibles des cellules qui resultent des interactions entre leurs constituants génétiques et leur environnement. Il contrôle les échanges cellulaires par des processus de transport actifs et passifs tels que la diffusion et l'osmose, tout en s'appuyant sur plusieurs mécanismes de couplages impliquant à la fois des interactions directes et indirectes, à courtes et à longues portées. Dans cette thèse, nous contribuons à la compréhension, d'une part, de l'impact de ces differents types de couplages sur la synchronisation et le contrôle des rythmes cellulaires, cruciaux pour la coordination de leurs activités, afin de préserver l'homéostasie et d'améliorer la communication cellulaire. D'une autre part, nous mettons en exergue l'émergence des structures stables et instables qui sont fondamentaux au cours des échanges cellulaires, pour la morphologie des organismes, et pour la spécialisation entre les êtres vivants. Dans le cadre de cette investigation, les cellules incorporant des séries de reactions biochimiques, et qui régulent leurs concentrations internes en produits finis par rétrocontrôles, font l'objet de notre étude. Premièrement, en ce qui concerne la synchronisation, tout en gardant en vue le caractère adaptatif du milieu extracellulaire, nous analysons les effets des couplages de types chimique, electrique, et adaptatif par le biais de l'environnement, sur les échanges métaboliques dues aux différences de concentrations entre les cellules, dans le but d'identifier l'apparition des phénomènes de synchronisation de phase et synchronisation complète au sein d'un système biochimique à caractère chaotique. Dans ces contextes, la stabilité de la solution synchrône est etudiée sur la base d'outils mathématiques et numériques tels que la méthode de la fonction principale de stabilité, le taux de variation de la fonction de Lyapunov, la construction géométrique de sous-espaces localisés par des sections de Poincaré, la différence de phase, le paramètre de Kuramoto pour l'entrainement de phase, le paramètre de dispersion des observations conditionnelles de l'espace de phase par stroboscopie. Tous ces indicateurs montrent la prévalence d'un état de synchronisation de phase entre les cellules couplées dans l'espace de phase. Cependant, les résultats indiquent que la synchronisation complète n'est pas accessible sous l'unique action du couplage chimique. Seules les actions combinées des couplages chimique et électrique d'une part, et du couplage adaptatif par médiation de l'environnement d'une autre part, s'avèrent être d'une importance capitale pour

l'instauration des états de synchronisation complets et robustes au sein du système couplé. Deuxièmement, nous découvrons l'émergence de structures spatiotemporelles dans les réseaux cellulaires en une et deux dimensions spatiales. Dans les réseaux unidimensionnels hétérogènes, nous montrons plusieurs phénomènes de formations de structures, avec et sans suppression de chaos, et formation de bulles. En proçédant à une normalisation du modèle mathématique des concentrations du système cellulaire diffusément couplé en deux dimensions spatiales, nous étudions analytiquement et numériquement la stabilité de l'état stationnaire spatialement homogène de notre reseau biochimique. Des conditions paramétriques promouvant une instabilité de l'état stationnaire, induite par diffusion et pertinente pour l'apparition des motifs spatiotemporels, sont indiquées. Ces structures spatiotemporelles incorporent des motifs stationnaires de Turing spatialement hétérogènes, et des phénomènes oscillatoires tels que des cas de propagation d'ondes et des états de chaos spatiotemporel. L'importance de ces phénomènes en biologie vient de leur prévalence fondamentale au cours des processus communicatifs et développementaux des cellules.

Mots clés: *Chaos, synchronisation, communication cellulaire, systèmes biochimiques, stabilité de Lyapunov, motifs spatiotemporels, instabilité de Turing.*

General Introduction

One of the prominent challenges formulated nowadays by many scientists in the fields of biological and nonlinear science, is the issue of understanding the functioning and failure of the vital in-built biochemical pathways found in living cells. A pathway is a collection of step by step modifications, whereby an initial substance used as substrate by an enzyme is transformed into a product. This product will then become the substrate for the next reaction, until the exact chemical structure necessary for the cell is reached. The biochemical pathways involved in cellular metabolism can, depending on their parameter values, exhibit regular or chaotic dynamics. This latter erratic behavior is more naturally and widely observed in many biological systems such as neural networks, cardiac pacemaker cells, animal gaits, metabolic networks [1, 2, 3, 4, 5, 6, 7, 8, 9, 10], etc. The latter set includes arrays of cells with activator-inhibitor pathways [1, 11, 12]. In reality, there is nothing strange about this as it is well known that in nature, disorder is more likely than order. Disorder happens more spontaneously while organization requires energy. Thus, energy and organization are closely related. Epitome of the latter concept is synchronization, which is a prerequisite for the coordinated collective behavior of cells. In a pioneering work on oscillating biochemical reactions, Higgins [13, 14, 15, 16] addressed the problem of the way in which a coupling between individual cells can affect the resulting dynamics, for example, by synchronizing their oscillations.

Synchronization, that is, the ability of coupled oscillators to lock to a common frequency, is a general and ubiquitous feature of nature, since it occurs for mechanical or electrical oscillators, lasers, chemical reactions and biological clocks, to mention just some well-known examples [17, 18, 19, 20, 21, 22, 23, 24, 25, 26, 27, 28, 29, 30, 31]. In the last named fields of studies, it was observed that many living organisms naturally come together, organize themselves into coupled systems, in order to perform certain functions, with the aim of maintaining the equilibrium in their living environment and perpetuate life. This is also actually the case for the basic building blocks of any living organism: the cells [13, 14, 32, 33]. So, the synchronization dynamics of cells with activator-inhibitor pathways entails the existence of a potential energy of interaction among

these biochemical systems, with suitable strength. This energy is brought in through several signaling schemes listed in the literature such as the electrical, chemical, environmental coupling types [1, 11, 12, 34]. Depending on the nature of the interactions involved, these couplings can be of direct(or indirect), linear(or nonlinear) types [11, 12, 34, 35].

During the last decade, Turing instabilities have also been shown to be crucial for the appearance of stationary spatial patterns in physics, chemistry and biology [36, 37, 38]. Similarly, the likelihood of the emergence of spatiotemporal patterns in the neighborhood of Turing-Hopf bifurcations, where the formation of inhomogeneous stationary configurations due to Turing instabilities, interact with the occurrence of oscillations caused by a Hopf bifurcation, has been highlighted [39]. The mechanism pertaining in the emergence of such spatiotemporal patterns has been thoroughly studied not long ago in physical and chemical systems [40, 41, 42]. It is noteworthy that even though the two physical processes may coexist, they are usually separated from one another. The Hopf or wave instability typically appears at significantly lower wave numbers than the Turing mode. Therefore, their interactions may lead more generically to a family of oscillating Turing-like patterns [43].

Since the seminal paper of Turing [44], a lot of attention has been given to theoretical models in order to describe self-organized pattern formation in several different areas of physics, chemistry, biology, geology, ecology, etc [45, 46, 47, 48, 49, 50, 51, 52, 53, 54, 55, 56, 57, 58, 59, 60, 61, 62, 63, 64, 65]. The interesting findings derived from the above mentioned explorations have paved the way for a relatively smooth understanding of processes pertaining in the emergence of spatiotemporal structures. In this regard, recently, Turing instability mediated by voltage and calcium diffusion in paced cardiac cells has been investigated [66]. A similar study has been lately performed in a modified FitzHugh-Nagumo neuronal model for the emergence of spatiotemporal chaos involving wave instability [67].

Furthermore, one fundamental property of coupled cells is that the coupling structure forces the existence of subspaces that are flow-invariant under the associated coupled cell systems: the synchrony subspaces. These should have an important role in the kinds of dynamics that can occur, and represent a significant step in understanding the dynamics forced by the coupling of these patterns of synchrony. Since the chemical coupling between cells is well known to change the cells synchrony subspace [68, 69, 70, 71, 72], the analysis of coupled cells with activator-inhibitor pathways under such circumstances is of capital importance in biological systems. Un-

derstanding both the processes that influence the synchronization of individual biochemical oscillators and how the behaviors of living cells arise out of the properties of coupled populations of cell oscillators are important goals in the study of biological systems, and a field of research with enormous practical applications [73].

The phenomenon of synchronization in electrically coupled cells with activator-inhibitor pathways has been extensively studied in [11, 34]. However, these works on coupled cells with activator-inhibitor pathways limited their analysis on electrical coupling. This scenario, termed short range interaction, suggests that cells are linked through electrical coupling or signal only. However, in nature, the interactions among cells sharing the same living environment are more complex and involve much more than just short range and linear interactions. They are in general nonlinear, deterministic or stochastic and involve long range interactions with one or many other cells. The chemical and electrical coupling schemes have proven their physical importance in neural systems [68, 69, 70, 71]. In the first case (electrical), the coupling is linear and made through gap junction and directly depend on the difference in the normalized concentrations of the substances in the pathway of each cell. While in the second case (chemical), the coupling is often modelled by a threshold nonlinear input or output function. In this last case, coupled cells with activator-inhibitor pathways may exhibit a variety of synchronization behavior including phase, partial and complete synchronization.

Moreover, it is well known that cells live in a common environment through which they interact indirectly with the diffusion and transport of chemical species across their membrane, and with the effects of the activation of receptors on their cellular membranes [13, 14, 15, 74, 75, 76, 77, 78, 79]. For example, Katriel experimentally observed the ability of thousand of cells to synchronize their periodic activity, crucial for the generation of macroscopic oscillations like circadian periodicities [80]. Cells perform numerous functions, and in order to carry out these tasks aiming at perpetuating life, cells need resources, most of which is obtained from their living environment. Competition for resources is therefore likely to occur among cells which interact through the same environment. Cell's fate, function and phenotype are therefore affected by environmental cues. These interactions with the medium create indirect ties between the cells. These connections among the biochemical pathways striving for resources shape biological niches. These interspecific interactions often limit the portion of their niche that they can actually use. Therefore, over time, the cells will make many complex adjustments to community

living, evolving together and forging relationships that give the community its character and stability. Both competition and cooperation then play key roles as cooperation favors available resource partitioning, by this means reducing competition that can lead to extinction. Thus, in order to reach a balance, that is homeostasis in the medium, cells need to communicate. The state of each cell influences the state of the environment, and the environment in turns influences the cells. This phenomenon is called "co-evolution", where different biochemical organisms evolve adjustments to one another over long periods of time. Biological systems have shown in many cases this ability to display a sufficiently rich variety of mechanical regulatory directives bequeathing them with the advantageous and useful skills of adaptation and learning [10].

In spite of the fact that nowadays reaction-diffusion systems are obviously no longer considered a topic of scientific oddity, but rather an important ingredient of the evolving world, it still remains that a variety of pattern formation mechanisms which engender patterns, are nonetheless unknown in a multiplicity of areas, and more specifically in a wide range of biological systems. Many research activities in developmental biology, both theoretical and experimental, have indicated that the underlying processes which produce patterns and structures in early developments are important. Special attention needs to be given to the issue of patterns generation in arrays of cells with activator-inhibitor pathways. Many researchers have recently explored the ability of these complex biochemical systems to exhibit a wide range of local and global dynamical behaviors with spatiotemporal organization, comprising on one hand(locally), alongside with quiescent states, periodic, quasi-periodic and chaotic regimes; and on the other side(collectively), interesting events of occurrence of synchronization and, of emergence of travelling and standing wave structures within one-dimensional spatial lattices [11, 12, 34, 81]. The fact that more significant results could be retrieved from a further exploration of the processes of reaction-diffusion taking place among these cells with activator-inhibitor pathways is motivating. In order to investigate for, and possibly unveil new facts about the advent of pattern-forming scenarios, we will perform our analysis over some relatively large networks of such biochemical systems, in a two-dimensional spatial domain.

Motivated by these facts, the aim of this thesis is to contribute first and foremost, to a better understanding of the effect of the chemical coupling on the dynamics and synchronization of coupled cells with activator-inhibitor pathways, and also to analyze the combined effects of electrical and chemical couplings on the high quality synchronization process of the coupled cells.

It is noteworthy that the method we shall use for the purpose of this inspection is quite appealing. It provides an optimal parameter value for the implementation of robust synchronization, and is based on the rate of change of the Lyapunov function of the coupled system. Secondly, we will explore the capacity of the previously mentioned indirect type of connection through an adaptive dynamic environment to foster a synchronized dynamics among cells with activator-inhibitor pathways as they diffuse in the environment their biochemical species referred to in this case as "synchronizing agents". In our analysis, we shall take into account the ability of these environmental connections to adapt to the biochemical changes occurring in the intercellular medium. This adaptation feature is crucial as we seek the synchronization dynamics of cells with activator-inhibitor pathways in their chaotic regime. Adaptive law have been widely used in the line of synchronization of chaotic systems ranging from chaotic oscillations, chaotic circuits to chaotic biological systems [82, 83, 84, 85]. However, in this case, the adaptation law is brought in the system through environmental coupling. Their respective trajectories are known to continuously distribute along unstable directions in the phase space, due to their extreme sensitivity to initial conditions, inherently biasing them to flout synchronization. Lastly, but not the least, our goal will be to throw more light on pattern generation mechanisms, using reaction-diffusion processes in some biological systems, that can enable us to generate and control both small-scale and large-scale structures, with the goal of mimicking natural processes. In an attempt to do so, the individual cells will be considered to be identical, and assumed to have ostensibly the same initial conditions, except otherwise stated.

This thesis is organized as follows:

In chapter 1, we carry out a comprehensive literature review on cells in general, and a special attention is later on given to cells with activator-inhibitor pathways. We equally highlight some ideas that are basic to our current understanding of the concepts of dynamical systems, chaos, and to the phenomena of synchronization and pattern generation in biochemical pathways. An emphasis is made on the concepts of complexity in dynamical regimes, synchronization, chaos suppression and pattern formation in science as a whole, and in biological systems in particular.

Chapter 2 presents and describes the models, analytical and numerical methods used in the investigation of synchronization and patterns generation phenomena amid cells with activator-inhibitor pathways, under the chemical, adaptive environment-mediated and spatially extended diffusive signalling schemes, respectively. The analytical methods mainly incorporate the linear

stability analysis of the various models, alongside with the variational approach for their stability assessment. Also are reported some numerical methods such as, the fourth-order Runge-Kutta scheme, the Newton-Raphson algorithm and the dichotomy scheme, that have been used to numerically integrate and examine the model equations used in this work.

In chapter 3, we present the main outcomes of this thesis. By performing a linear stability analysis on the single cell model, we investigate for its equilibrium states whose instabilities customarily lead to biochemical oscillatory rhythms via diverse Hopf bifurcation scenarios. By applying the variational approach in the form of the master stability function method, we carefully appraise the stability conditions of the synchronization manifolds in various signalling schemes. In the framework of the coexistence of both synaptical and electrical couplings, we investigate analytically and numerically the impact of their interplay on the synchronized dynamics of the pathways. By means of the Lyapunov function, we look for the requirements needed for the instatement of a high quality synchronization within the coupled system. In the context of the adaptive environment-mediated coupling scheme, both mathematical and numerical methods, via a Lyapunov spectrum approach and a dichotomy scheme among others, provide the parameter prerequisites in terms of coupling threshold, rate of degradation of substrates and maximum velocity of the enzyme, that favors the emergence of a robust synchrony among the pathways. Based on mathematical constructs, we normalize the dimensionless spatially extended model of diffusively connected cells with activator-inhibitor pathways. Subsequently, we conduct a linear stability analysis of the spatially homogeneous equilibrium state of large bi-dimensional spatial networks of biochemical pathways and numerically expose the conditions conducive for diffusion-driven instabilities, crucial in the occurrence of patterns generation in physical systems.

The thesis ends with a general conclusion and provides some future potential avenues of research that could be explored.

CHAPTER I

GENERALITIES ON CELLS AND DYNAMICAL SYSTEMS

I.1 Introduction

A cell is a membrane-bounded unit that contains the DNA hereditary machinery and the cytoplasm. All organisms are cells or aggregates of cells. The general plan of cellular organization varies in the cells of different organisms, but despite these modifications, all cells resemble each other in certain fundamental ways. Before we begin our detailed examination of cell structure, let us first summarize three major features all cells have in common: a plasma membrane, a nucleoid or nucleus, and cytoplasm. The plasma membrane encloses a cell and separates its contents from its surroundings. The plasma membrane is a phospholipid bilayer about 5 to 10 nanometers (5 to 10 billionths of a meter) thick with proteins embedded in it. Viewed in cross-section with the electron microscope, such membranes appear as two dark lines separated by a lighter area. This distinctive appearance arises from the tail-to-tail packing of the phospholipid molecules that make up the membrane. The proteins of a membrane may have large hydrophobic domains, which associate with and become embedded in the phospholipid bilayer. The proteins of the plasma membrane are in large part responsible for a cell's ability to interact with its environment. Transport proteins help molecules and ions move across the plasma membrane, either from the environment to the interior of the cell or vice versa. Receptor proteins induce changes within the cell when they come in contact with specific molecules in the environment, such as hormones. Markers identify the cell as a particular type. This is especially important in multicellular organisms, whose cells must be able to recognize each other as they form tissues.

I.2 Central portion of the cell contains the genetic material

Every cell contains DNA, the hereditary molecule. In prokaryotes (bacteria), most of the genetic material lies in a single circular molecule of DNA. It typically resides near the center of the cell in an area called the nucleoid, but this area is not segregated from the rest of the cell's interior by membranes. By contrast, the DNA of eukaryotes is contained in the nucleus, which is surrounded by two membranes. In both types of organisms, the DNA contains the genes that code for the proteins synthesized by the cell. The cytoplasm comprises the rest of the cell's interior. A semifluid matrix called the cytoplasm fills the interior of the cell, exclusive of the nucleus (nucleoid in prokaryotes) lying within it. The cytoplasm contains the chemical wealth of the cell: the sugars, amino acids, and proteins the cell uses to carry out its everyday activities. In eukaryotic cells, the cytoplasm also contains specialized membrane-bounded compartments called organelles. From the cell theory, a general characteristic of cells is their microscopic size. While there are a few exceptions like the marine alga Acetabularia, which can be up to 5 centimeters long, a typical eukaryotic cell is 10 to 100 micrometers (10 to 100 millionths of a meter) in diameter (Fig. 1); most bacterial cells are only 1 to 10 micrometers in diameter.

Because cells are so small, no one could observe them until microscopes were invented in the mid-seventeenth century. Robert Hooke first described cells in 1665, when he used a microscope he had built to examine a thin slice of cork, a nonliving tissue found in the bark of certain trees. Hooke observed a honeycomb of tiny, empty (because the cells were dead) compartments. He called the compartments in the cork "cellulae" (Latin, "small rooms"), and the term has come down to us as cells. The first living cells were observed a few years later by the Dutch naturalist Antonie van Leeuwenhoek, who called the tiny organisms that he observed "animalcules," meaning little animals. For another century and a half, however, biologists failed to recognize the importance of cells. In 1838, botanist Matthias Schleiden made a careful study of plant tissues and developed the first statement of the cell theory. He stated that all plants "are aggregates of fully individualized, independent, separate beings, namely the cells themselves." In 1839, Theodor Schwann reported that all animal tissues also consist of individual cells. The cell theory, in its modern form, includes the following three principles:

1. All organisms are composed of one or more cells, and the life processes of metabolism and heredity occur within these cells.

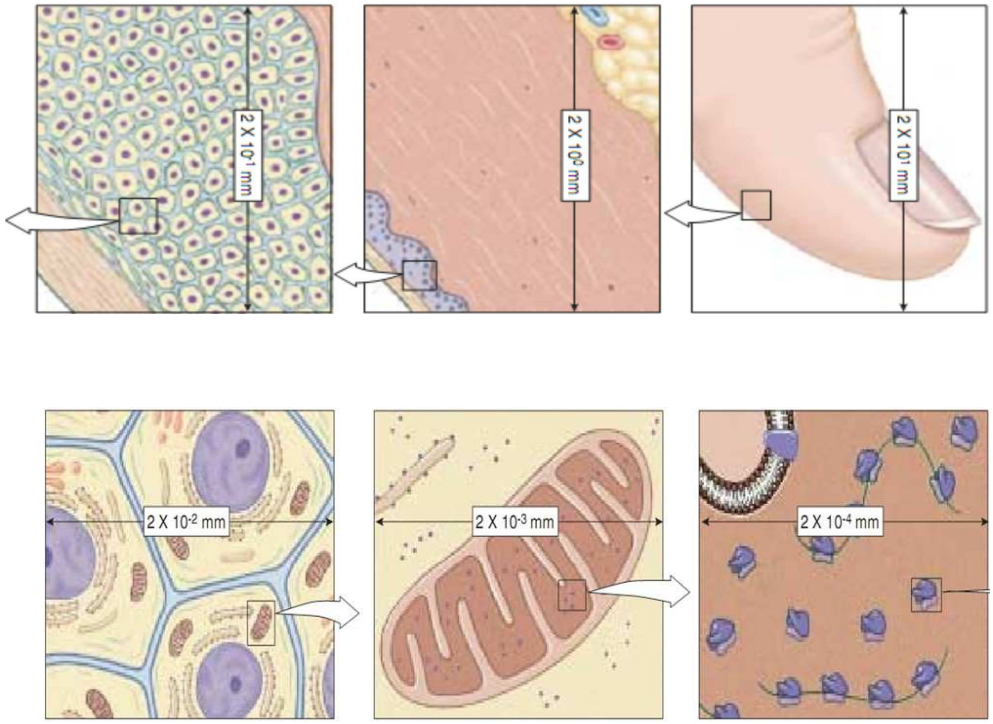

Figure 1: *The size of cells and their contents. This diagram shows the size of human skin cells, organelles, and molecules. In general, the diameter of a human skin cell is* 20 *micrometers* (μm) *or* 2×10^{-2} *mm, that of a mitochondrion is* $2\mu m$ *or* 2×10^{-3} *mm, that of a ribosome is* 20 *nanometers (nm) or* 2×10^{-5} *mm.*

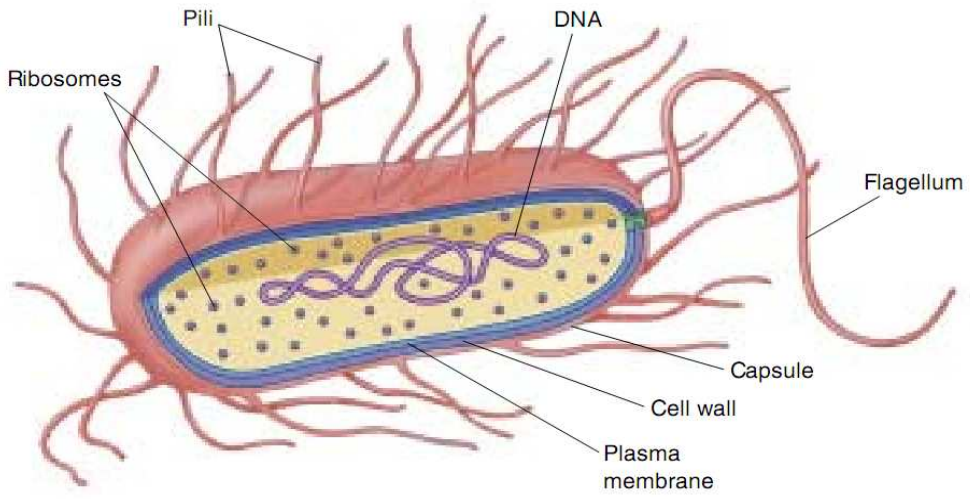

Figure 2: *Structure of a bacterial cell. Generalized cell organization of a bacterium. Some bacteria have hairlike growths outside of the cell called pili.*

2. Cells are the smallest living things, the basic units of organization of all organisms.

3. Cells arise only by division of a previously existing cell. Although life likely evolved spontaneously in the environment of the early earth, biologists have concluded that no additional cells are originating spontaneously at present. Rather, life on earth represents a continuous line of descent from those early cells.

I.3 Complexity of eukaryotic cells: far more complex than bacterial cells

Bacteria Are Simple Cells: Prokaryotes, the bacteria, are the simplest organisms. Prokaryotic cells are small, consisting of cytoplasm surrounded by a plasma membrane and encased within a rigid cell wall, with no distinct interior compartments (Fig. 2). A prokaryotic cell is like a one-room cabin in which eating, sleeping, and watching TV all occur in the same room. Bacteria are very important in the economy of living organisms. They harvest light in photosynthesis, break down dead organisms and recycle their components, cause disease, and are involved in many important industrial processes.

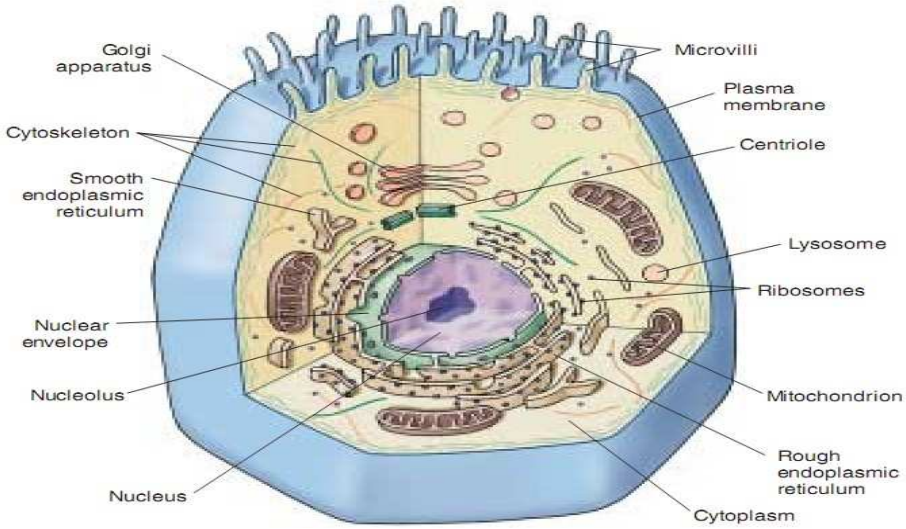

Figure 3: *Structure diagram of an animal cell with its internal organelles. (Generalized illustration)*

Eukaryotic Cells Have Complex Interiors:

Eukaryotic cells (Fig. 3) are far more complex than prokaryotic cells. The hallmark of the eukaryotic cell is compartmentalization. The interiors of eukaryotic cells contain numerous organelles, membrane-bounded structures that close off compartments within which multiple biochemical processes can proceed simultaneously and independently. Plant cells often have a large membrane-bounded sac called a central vacuole, which stores proteins, pigments, and waste materials. Both plant and animal cells contain vesicles, smaller sacs that store and transport a variety of materials. Inside the nucleus, the DNA is wound tightly around proteins and packaged into compact units called chromosomes. All eukaryotic cells are supported by an internal protein scaffold, the cytoskeleton. While the cells of animals and some protists lack cell walls, the cells of fungi, plants, and many protists have strong cell walls composed of cellulose or chitin fibers embedded in a matrix of other polysaccharides and proteins. This composition is very different from the peptidoglycan that makes up bacterial cell walls.

I.4 Membrane and cellular transport

Biological membranes are fluid layers of lipid. Cells are encased by membranes composed of a bilayer of phospholipid. Because individual phospholipid molecules do not bind to one another, the lipid bilayer of membranes is a fluid. Proteins embedded within the plasma membrane determine its character. A varied collection of proteins float within the lipid bilayer. Visualizing a plasma membrane requires a powerful electron microscope. There are many kinds of membrane proteins. These proteins in a membrane function in support, transport, recognition, and reactions. Membrane proteins are anchored into the lipid bilayer by their non-polar regions.

Components of the Cell

A eukaryotic cell contains many membranes. While they are not all identical, they share the same fundamental architecture. Cell membranes are assembled from four components:

1. *Lipid bilayer:* Every cell membrane is composed of a phospholipid bilayer. The other components of the membrane are enmeshed within the bilayer, which provides a flexible matrix and, at the same time, imposes a barrier to permeability.

2. *Transmembrane proteins:* A major component of every membrane is a collection of proteins that float on or in the lipid bilayer. These proteins provide passageways that allow substances and information to cross the membrane.

3. *Network of supporting fibers:* which are intracellular proteins that reinforce the membrane's shape. For example, a red blood cell has a characteristic biconcave shape because a scaffold of proteins called spectrin links proteins in the plasma membrane with actin filaments in the cell's cytoskeleton.

4. *Exterior proteins and glycolipids:* Different cell types exhibit different varieties of glycoproteins and glycolipids on their surfaces, which act as cell identity markers.

Kinds of Membrane Proteins

The plasma membrane is a complex assembly of proteins enmeshed in a fluid array of phospholipid molecules. This enormously flexible design permits a broad range of interactions with the environment, some directly involving membrane proteins (Fig. 4). Though cells interact with their environment through their plasma membranes in many ways, we will focus on six key classes of membrane protein.

1. *Transporters:* Membranes are very selective, allowing only certain substances to enter or

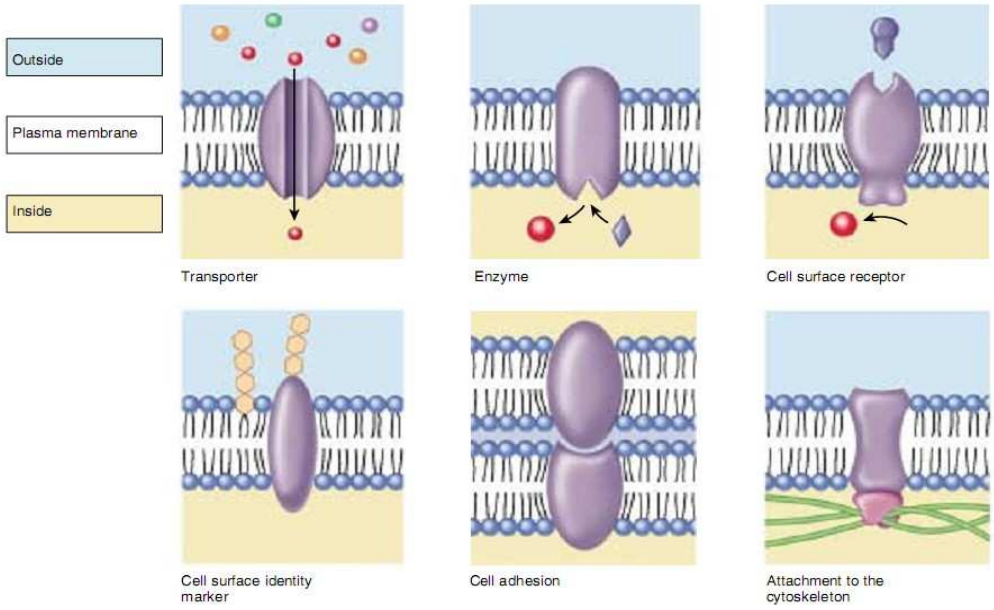

Figure 4: *Functions of plasma membrane proteins. Membrane proteins act as transporters, enzymes, cell surface receptors, and cell surface markers, as well as aiding in cell-to-cell adhesion and securing the cytoskeleton.*

leave the cell, either through channels or carriers. In some instances, they take up molecules already present in the cell in high concentration.

2. *Enzymes:* Cells carry out many chemical reactions on the interior surface of the plasma membrane, using enzymes attached to the membrane.

3. *Cell surface receptors:* Membranes are exquisitely sensitive to chemical messages, detecting them with receptor proteins on their surfaces that act as antennae.

4. *Cell surface identity markers:* Membranes carry cell surface markers that identify them to other cells. Most cell types carry their own identity tags, specific combinations of cell surface proteins characteristic of that cell type.

5. *Cell adhesion proteins:* Cells use specific proteins to glue themselves to one another. Some act like Velcro, while others form a more permanent bond.

6. *Attachments to the cytoskeleton:* Surface proteins that interact with other cells are often anchored to the cytoskeleton by linking proteins. Therefore, the many proteins embedded within a membrane carry out a host of functions, many of which are associated with transport of materials or information across the membrane.

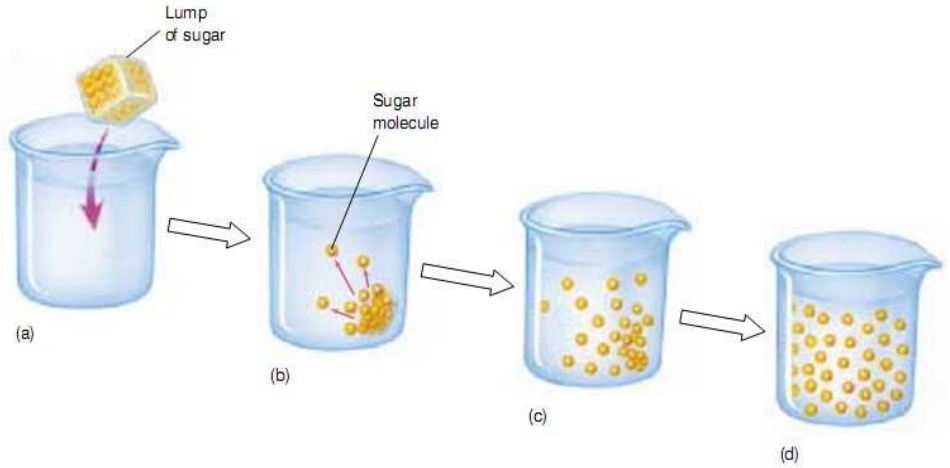

Figure 5: *Diffusion. If a lump of sugar is dropped into a beaker of water (a), its molecules dissolve (b) and diffuse (c). Eventually, diffusion results in an even distribution of sugar molecules throughout the water (d).*

Passive transport across membranes moves down the concentration gradient:

1- *Diffusion* is the random molecular motion which results in a net movement of molecules to regions of lower concentration. Indeed, molecules and ions dissolved in water are in constant motion, moving about randomly. This random motion causes a net movement of these substances from regions where their concentration is high to regions where their concentration is lower, a process called diffusion (Fig. 5). Net movement driven by diffusion will continue until the concentrations in all regions are the same. You can demonstrate diffusion by filling a jar to the brim with ink, capping it, placing it at the bottom of a bucket of water, and then carefully removing the cap. The ink molecules will slowly diffuse out from the jar until there is a uniform concentration in the bucket and the jar. This uniformity in the concentration of molecules is a type of equilibrium.

Facilitated transport:

Many molecules that cells require, including glucose and other energy sources, are polar and cannot pass through the non-polar interior of the phospholipid bilayer. These molecules enter the cell through specific channels in the plasma membrane. The inside of the channel is po-

lar and thus "friendly" to the polar molecules, facilitating their transport across the membrane. Each type of biomolecule that is transported across the plasma membrane has its own type of transporter (that is, it has its own channel which fits it like a glove and cannot be used by other molecules). Each channel is said to be selective for that type of molecule, and thus to be selectively permeable, as only molecules admitted by the channels it possesses can enter it. The plasma membrane of a cell has many types of channels, each selective for a different type of molecule.

Facilitated diffusion refers to a passive movement across a membrane which often takes place through specific carrier proteins.

Diffusion of ions through channels: One of the simplest ways for a substance to diffuse across a cell membrane is through a channel, as ions do. Ions are solutes (substances dissolved in water) with an unequal number of protons and electrons. Those with an excess of protons are positively charged and called cations. Ions with more electrons are negatively charged and called anions. Because they are charged, ions interact well with polar molecules like water but are repelled by the non-polar interior of a phospholipid bilayer. Therefore, ions cannot move between the cytoplasm of a cell and the extracellular fluid without the assistance of membrane transport proteins. Ion channels possess a hydrated interior that spans the membrane. Ions can diffuse through the channel in either direction without coming into contact with the hydrophobic tails of the phospholipids in the membrane, and the transported ions do not bind to or otherwise interact with the channel proteins. Two conditions determine the direction of net movement of the ions: their relative concentrations on either side of the membrane, and the voltage across the membrane. Each type of channel is specific for a particular ion, such as calcium (Ca^{++}) or chloride (Cl^{-}), or in some cases for a few kinds of ions. Ion channels play an essential role in signaling by the nervous system.

2- *Facilitated diffusion:* In this case, the net movement always occurs from areas of high concentration to low, just as it does in simple diffusion, but carriers, another class of membrane proteins, facilitate the transport process in between the cytoplasm and the extracellular medium. For this reason, this mechanism of transport is sometimes called facilitated diffusion. A typical example is the facilitated diffusion in red blood cells of ions in each direction: : Cl^{-} in one direction and bicarbonate ion (HCO_3^{-}) in the opposite direction via some red blood cell (RBC) carrier proteins. This carrier is important in transporting carbon dioxide in the blood. A second im-

portant facilitated diffusion carrier in RBCs is the glucose transporter. Red blood cells naturally keep their internal concentration of glucose low.

3- *Osmosis* occurs when Polar solutes interact with water and can affect the movement of water across semipermeable membranes. The cytoplasm of a cell contains ions and molecules, such as sugars and amino acids, dissolved in water. The mixture of these substances and water is called an aqueous solution. Water, the most common of the molecules in the mixture, is the solvent, and the substances dissolved in the water are solutes. The ability of water and solutes to diffuse across membranes has important consequences. It is keynote that osmosis is the diffusion of water, but not solutes,across a membrane.

Molecules Diffuse down a Concentration Gradient:

Both water and solutes diffuse from regions of high concentration to regions of low concentration; that is, they diffuse down their concentration gradients. When two regions are separated by a membrane, what happens depends on whether or not the solutes can pass freely through that membrane. Most solutes, including ions and sugars, are not lipid-soluble and, therefore, are unable to cross the lipid bilayer of the membrane. Even water molecules, which are very polar, cannot cross a lipid bilayer. Water flows through aquaporins, which are specialized channels for water. The concentration of all solutes in a solution determines the osmotic concentration of the solution. If two solutions have unequal osmotic concentrations, the solution with the higher concentration is hyperosmotic (Greek hyper, "more than"), and the solution with the lower concentration is hypoosmotic (Greek hypo, "less than"). If the osmotic concentrations of two solutions are equal, the solutions are isosmotic (Greek iso, "the same").

In cells, a plasma membrane separates two aqueous solutions, one inside the cell (the cytoplasm) and one outside (the extracellular fluid). The direction of the net diffusion of water across this membrane is determined by the osmotic concentrations of the solutions on either side (Fig. 6). For example, if the cytoplasm of a cell were hypoosmotic to the extracellular fluid, water would diffuse out of the cell, toward the solution with the higher concentration of solutes (and, therefore, the lower concentration of unbound water molecules). This loss of water from the cytoplasm would cause the cell to shrink until the osmotic concentrations of the cytoplasm and the extracellular fluid become equal.

Maintaining Osmotic Balance:

Organisms have developed many solutions to the osmotic dilemma posed by being hyperos-

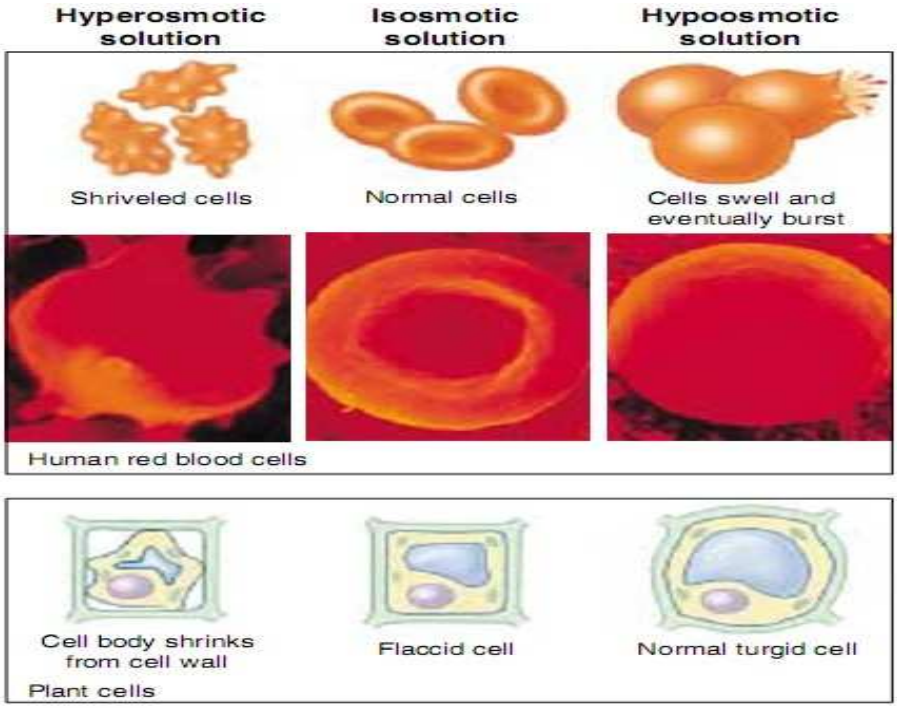

Figure 6: *Osmosis. In a hyperosmotic solution, water moves out of the cell toward the higher concentration of solutes, causing the cell to shrivel. In an isosmotic solution, the concentration of solutes on either side of the membrane is the same. Osmosis still occurs, but water diffuses into and out of the cell at the same rate, and the cell doesn't change size. In a hypoosmotic solution, the concentration of solutes is higher within the cell than without, so the net movement of water is into the cell.*

motic to their environment.

Extrusion: Some single-celled eukaryotes like the protest Paramecium use organelles called contractile vacuoles to remove water. Each vacuole collects water from various parts of the cytoplasm and transports it to the central part of the vacuole, near the cell surface. The vacuole possesses a small pore that opens to the outside of the cell. By contracting rhythmically, the vacuole pumps the water out of the cell through the pore.

Isosmotic Solutions: Some organisms that live in the ocean adjust their internal concentration of solutes to match that of the surrounding seawater. Isosmotic with respect to their environment, there is no net flow of water into or out of these cells. Many terrestrial animals solve the problem in a similar way, by circulating a fluid through their bodies that bathes cells in an isosmotic solution. The blood in your body, for example, contains a high concentration of the protein albumin, which elevates the solute concentration of the blood to match your cells.

Turgor: Most plant cells are hyperosmotic to their immediate environment, containing a high concentration of solutes in their central vacuoles. The resulting internal hydrostatic pressure, known as turgor pressure, presses the plasma membrane firmly against the interior of the cell wall, making the cell rigid. The newer, softer portions of trees and shrubs depend on turgor pressure to maintain their shape, and wilt when they lack sufficient water.

4- **Active transport across membranes is powered by energy from ATP:**

While diffusion, facilitated diffusion, and osmosis are passive transport processes that move materials down their concentration gradients, cells can also move substances across the membrane up their concentration gradients. This process requires the expenditure of energy, typically ATP, and is therefore called active transport. Like facilitated diffusion, active transport involves highly selective protein carriers within the membrane. These carriers bind to the transported substance, which could be an ion or a simple molecule like a sugar, an amino acid, or a nucleotide to be used in the synthesis of DNA. Active transport is one of the most important functions of any cell. It enables a cell to take up additional molecules of a substance that is already present in its cytoplasm in concentrations higher than in the extracellular fluid. Without active transport, for example, liver cells would be unable to accumulate glucose molecules from the blood plasma, as the glucose concentration is often higher inside the liver cells than it is in the plasma. Active transport also enables a cell to move substances from its cytoplasm to the extracellular fluid despite higher external concentrations.

I.5 Some relevant concepts on complex systems

I.5.1 Dynamical system

In this section, we look at equations of the following form:

$$\dot{x} = f(x,t;\mu) \text{ , and} \tag{1}$$

$$x \rightarrow g(x;\mu) \text{ ,} \tag{2}$$

with $x \in U \subset \mathbb{R}^n$, and $\mu \in V \subset \mathbb{R}^p$, where U and V are open sets in $\mathbb{R}^n$ and $\mathbb{R}^p$, respectively. The overdot in Eq. (24) means " $\frac{dx}{dt}$ ", and we view the variables μ as parameters. In the study of dynamical systems, the independent variable is often referred to as "time." We will often use this terminology. We refer to Eq. (24) as a vector field or ordinary differential equation and to Eq. (2) as a map or difference equation. Both will be termed dynamical systems. By a solution of Eq. (24), we mean a map, x, from some interval $I \subset \mathbb{R}^1$ into $\mathbb{R}^n$, which we represent as follows:

$$\begin{aligned} x : I &\rightarrow \mathbb{R}^n \text{ ,} \\ t &\rightarrow x(t) \text{ ,} \end{aligned} \tag{3}$$

such that $x(t)$ satisfies Eq. (24), that is:

$$\dot{x}(t) = f(x(t),t;\mu) \text{ .} \tag{4}$$

The map x has the geometrical interpretation of a curve in $\mathbb{R}^n$, and Eq. (24) gives the tangent vector at each point of the curve, hence the reason for referring to Eq. (24) as a vector field. We refer to the space of dependent variables of Eq. (24) (i.e., $\mathbb{R}^n$) as the phase space of Eq. (24),

and, abstractly, our goal is to understand the geometry of solution curves in phase space. We remark that in many applications, the structure of the phase space may be more general than $\mathbb{R}^n$; frequent examples are cylindrical, spherical, or toroidal phase spaces. However, we incur no loss of generality if we take the phase space of our maps and vector fields to be open sets in $\mathbb{R}^n$. The solutions of differential equations have different properties depending on whether or not the ordinary differential equation depends explicitly on time. Ordinary differential equations that depend explicitly on time (i.e., $\dot{x} = f(x, t; \mu)$) are referred to as non-autonomous or time-dependent ordinary differential equations, or vector fields; and ordinary differential equations that do not depend explicitly on time (i.e., $\dot{x} = f(x; \mu)$) are referred to as autonomous or time-independent ordinary differential equations, or vector fields.

I.5.2 Dependence on Initial Conditions

It may be useful to distinguish a solution curve by a particular point in phase space that it passes through at a specific time, i.e., for a solution $x(t)$, we have $x(t_0) = x_0$. We refer to this as specifying an initial condition. This is often included in the expression for a solution by writing $x(t, t_0, x_0)$. In some situations, explicitly displaying the initial condition may be unimportant, in which case we will denote the solution merely as $x(t)$. In still other situations, the initial time may be always understood to be a specific value, say $t_0 = 0$; in this case, we would denote the solution as $x(t, x_0)$.

I.5.3 Dependence on Parameters

Similarly, it may be useful to explicitly display the parametric dependence of solutions. In this case, we would write $x(t, t_0, x_0; \mu)$, or, if we weren't interested in the initial condition, $x(t; \mu)$. If parameters play no role in our arguments, we will often omit any specific parameter dependence from the notation. It is keynote that there are several different terms which are somewhat synonymous with the term solution of Eq. (24). $x(t, t_0, x_0)$ may also be referred to as the trajectory or phase curve passing through the point x_0 at $t = t_0$.

I.5.4 Nonlinearity and oscillations

Systems that oscillate in principle are usually called oscillators. But the systems we are interested in should be capable of demonstrating oscillations that are self-sustained, or self-oscillations.

The concept of self-oscillations was first proposed by Andronov, Khaikin and Vitt [86, 87, 88]. Self-oscillations form a special, but rather broad class of all oscillating processes and are characterized by the following features: o First and foremost, they do not damp, i.e., the repetitive motion of the system does not stop with the course of time, and does not show the tendency to stop. o Second and equally important, they oscillate "by themselves," i.e., not because they are repetitively kicked from outside. o The third feature is perhaps the most intriguing and fascinating: the shape, amplitude and time scale of these oscillations are chosen by the oscillating system alone. An outsider cannot easily change them, e.g., by setting different initial conditions. Nonlinearity is crucial in self-sustained systems since a self-sustained system must be nonlinear. Indeed, it is the interplay between the non-linear power supply and dissipation that makes self-oscillations possible. It is then important to know what nonlinearity is all about. Suppose we have a system about which we would like to find out whether it is linear or not. Apply some perturbation x_1 to it and record its response y_1. Then, apply another perturbation x_2 and record the response y_2 to that. Then, apply perturbation equal to $(x_1 + x_2)$ and calculate the response y_3. Then, calculate the sum $(y_1 + y_2)$ and compare the two quantities $(y_1 + y_2)$ and y_3. Are they equal for any chosen x_1 and x_2? If yes, then the system is linear. If they are not equal, the system is non-linear. Graphically, linearity can be illustrated as a straight line on the graph of response y as a function of input x. Anything different from a straight line would represent a nonlinear system. Examples of self-oscillators are a grandfather pendulum clock, a whistle, your throat when you sing a musical note, as well as many musical instruments, your heart and many other biological systems, a bottle of water with a narrow neck that is put vertically with its neck down (water will come out in pulses). In order to prevent possible confusion, we would like to give just one example of an oscillator which is not a self-sustained one. As counterexample, let us consider a bob pendulum consisting of a load on a rope, whose other end is fixed. If we give the load an initial kick, it will start to oscillate, but if we leave it alone, the oscillations will decay and eventually stop due to friction of the whole construction with air, and also at the point of the rope attachment. Of course, a repetitive kicking will resume the oscillations of the pendulum, but these will not be self -sustained because they would damp without the kicks. What if there were no friction in the system? Then the oscillations would not damp, but would that make them self-sustained? No, because the properties of these oscillations would be completely defined by the direction and strength of the initial kick made by an outsider who would wish

to launch them: the harder one kicks, the larger the swing will be. This would contradict the third feature of self-oscillations. Thus, for self-oscillations to occur, the oscillating system must be designed in a special way. The following three features of the self-oscillating systems are most essential: they must be non-linear systems, there must be dissipation in them, and there must be a source of power. It is noteworthy that dissipation is a mechanism due to which energy is being lost by the system while it changes its state, i.e., performs a motion. It has to be said that most macroscopic systems are dissipative anyway, since there is always some sort of friction in it. For example, mechanical systems lose energy because their details experience friction with other details or surrounding air. In electronic systems, elementary particles bump into other particles, the elements of the circuits heat and thus lose energy. This list can be continued, but the main idea is clear: dissipation is everywhere. It would be pertinent to emphasize again that the systems without (or almost without) dissipation are not self-oscillators. The study of physics has changed in character, mainly due to the passage from the analysis of linear systems to the analysis of nonlinear systems. Such a change began, it goes without saying, a long time ago but the qualitative change took place and boldly evolved after the understanding of the nature of chaos in nonlinear systems. The importance of these systems is due to the fact that the major part of physical reality is nonlinear. Linearity appears as a result of the simplification of real systems, and often, is hardly achievable during the experimental studies. Nonlinearity is closely related to chaos, which plays a constructive part in several physical phenomena.

I.5.5 Chaos in biological systems

A simplified and pragmatic explanation is frequently used to explain this phenomenon as follows: Dynamical chaos appears in nonlinear systems with trajectories utterly sensible to minor modifications of initial conditions. In that case, any person calculating a trajectory using a computer, observes that the small uncertainty (difference) of initial conditions engenders chaotic behavior (divergence). The universality of chaotic dynamics in mathematical and physical systems [89, 90, 91, 92] has prompted renewed interest in the application of nonlinear analysis to biological processes [4,5]. Attention has also focused on the physiological and medical implications of these concepts [92, 93, 94, 95, 96, 97]. The prevailing viewpoint is that the dynamics of health are ordered and regular and that a variety of pathologies represent a bifurcation to chaos [94, 96, 98]. For example, Smith and Cohen [96] advanced the hypothesis that ventricular fib-

rillation, the arrhythmia most commonly associated with sudden cardiac death, is a turbulent process (cardiac chaos) that may result from a subharmonic bifurcation (period-doubling) mechanism. Some authors [95, 99, 100, 101, 102] have proposed an alternative viewpoint, contrary to this notion of chaotic disease. In particular, they have suggested that chaos is useful in modelling the constrained randomness [103] inherent in the healthy function of physiological systems. Due to the importance of these phenomena in biological systems, a special interest will be given on the concept of chaos in our thesis.

I.5.6 Synchronization in biological systems

In most general terms, synchronization means that different systems adjust the time scales of their oscillations due to interactions, but there is a large variety of its manifestations and of the accompanying fascinating phenomena. An essential contribution to this concept has been made by Pikovsky, Rosenblum, and Kurths not long ago in their book [104], that has provided a contemporary view on synchronization as a universal phenomenon that manifests itself in the entrainment of rhythms of interacting self-sustained systems. It is a widespread phenomenon in biology, namely in cellular systems such as in cardiac cells and neuronal networks[105, 106, 107]. Cell synchronization means that cells at different stages of the cell cycle in a culture are brought to the same phase. Cell synchrony is required to study the progression of cells through the cell cycle. Due to the fact that this concept is crucial for a collective organization and efficient communication of cells, it will stand as a core aspect of our investigation.

I.5.7 Pattern formation

One of the most important aspects in complex systems is pattern formation. By pattern formation we mean that certain systems have the ability to self-organize into spatially structured states, from initially unstructured (or spatially homogenous) states. This behavior occurs all over the place around us, in several fields of science such as in physics, in chemistry, in biology, in social science, etc.

Examples of pattern forming in nature:

-In Physics: The most known example of spontaneous pattern formation in physics is probably Bénard convection. This happens when a liquid is heated from below at such a high rate that the heat cannot dissipate through the system fast enough. In this case convection rolls or cells

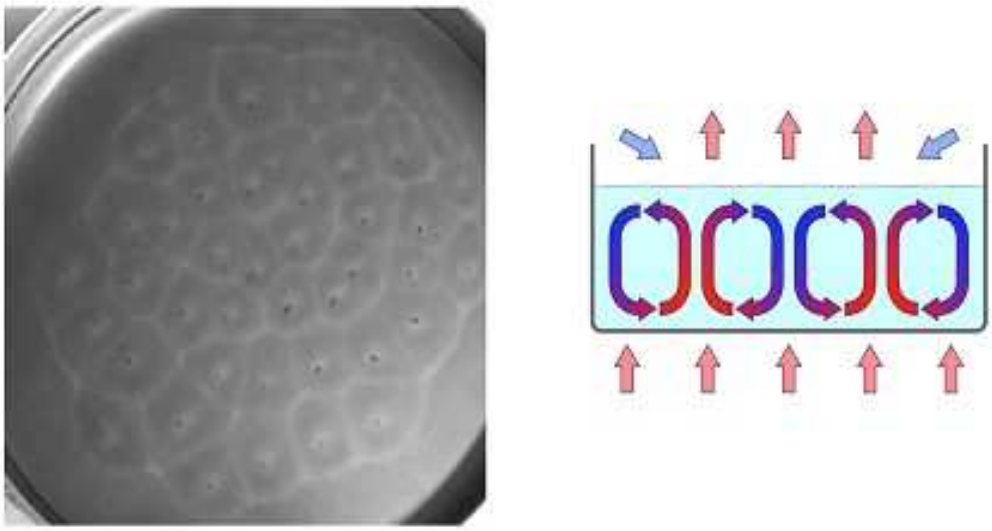

Figure 7: *Bénard Convection.*

emerge that transport the heat to the cooler regions of the liquid where heat is given off. The cooled liquid then gets pushed to the bottom to be reheated (See Fig. 7).

-Chemistry:

There is an abundance of chemical reactions that, if they occur in a not-well-stirred scenario, have the potential of generating patterns. One such reaction, the most famous one, is the Belousov-Zhabotinsky reaction. This reaction uses essentially five reactions, in which particular chemicals in it start oscillating in their concentration. If the reaction takes place in a petri dish, spiral and target wave form. This is because in its essence this reaction is an activator inhibitor system in which an autocatalytic reaction increases the abundance of a chemical which in turn increases the abundance of a chemical that turns this reaction off. Fig. 8 shows a snapshot of a pattern that the BZ reaction can generate.

Other notable pattern forming physical systems include hydrodynamical systems such as the Taylor-Couette flow which is analogous to Rayleigh-Bénard convection in that it also involves fluid moving in rolls; chemical reaction-diffusion systems such as those described by the complex Ginzburg-Landau equation which describes the dynamics of the amplitude of the global oscillatory modes that emerge from different local mechanisms, near a supercritical Hopf bifurcation. In general, the dynamics of all such models can be reduced to the complex Ginzburg-Landau equation (CGLE). A typical example is the FitzHugh-Nagumo (FHN) model which was

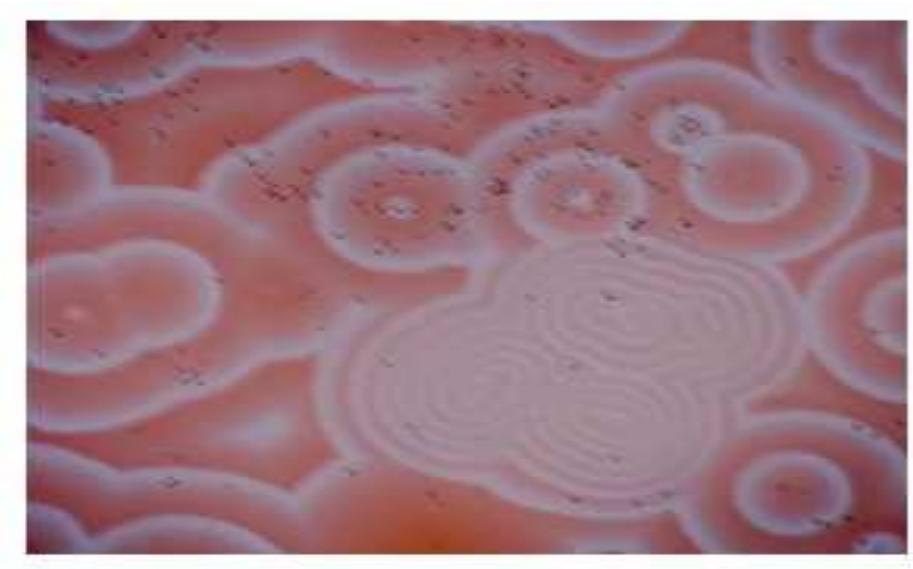

Figure 8: *Example of pattern generated by the Belousov-Zhabotinsky reaction.*

originally developed to describe the function of neural cells and the propagation of neural signals along axons [108].

-Biology:

Biology is full of pattern forming systems, such as in cAMP signaling in Dictyostelium discoideum, in the orientation maps in the visual cortex of primates and other higher mammals that have binocular vision, the case of patterns on sea shell(see Fig. 9), as well as patterns in animal fur(see Fig. 10). On Fig. 10, it is seen that some patterns are spotty, some consist of stripes of different wavelength. It turns out that with very few dynamic ingredients, one can devise a model that is capable of generating all these patterns at different parameter values.

The above patterns in animals are a special case of something a lot more fundamental called biological Morphogenesis, which focuses on the problem of how multicellular organisms with a great diversity of function and cell morphology can develop from a single, homogeneous fertilized egg. First, all cells in a multicellular organism have the same genome despite the variety in shape and function. This can be the case because these cells differ in what genes are expressed, i.e. active or repressed(inactive). On the way towards an adult organism, cells differentiate by a sequential switching off and on of genes. This mechanism is responsible for spontaneously introducing differences in embryos. For example in the drosophila melanogaster (fruit fly) embryo, different genes are expressed in different regions. The combination of expression levels

Figure 9: *Patterns on sea shell.*

Figure 10: *Patterns in animal fur.*

Figure 11: *Alan Turing*.

introduces different cell fates for the cells in specific locations which eventually governs the development of a full blown fly.

-Biological Morphogenesis and Turing instability

The scientist who first thought and published about the origins of spontaneous pattern formation was Alan Turing, who published a seminal paper called "The chemical basis of morphogenesis". In this paper, published only shortly before his death, Turing argued that an abundance of patterns observed in nature, many of the ones mentioned above, can be generated by the interaction of three different ingredients: activation, inhibition and diffusion. The basic idea being that essentially two types of agents (e.g. molecules, animals or other dynamical quantities) interact. An activator that does autocatalysis, which means this activator generates more of itself. Also, the activator triggers the generation of an inhibitor. The action of the inhibitor decreases the abundance of the activator. We have seen examples of such dynamical systems.

A Turing system consists of two or more coupled nonlinear partial differential equations (PDEs), which describe reactions and diffusion of chemicals or morphogens. The remarkable feature of the Turing mechanism is that it is capable of generating beautiful time-independent spatial patterns from any random initial configuration provided that particular conditions are satisfied [108]. The clue is that both activator and inhibitor can move in space diffusively during the Turing patterning process which is basically due to instabilities. Turing instability is a phenomenon that causes certain reaction-diffusion systems to spontaneously give rise to stationary patterns with a characteristic length scale from an arbitrary initial configuration. The

key factor in inducing the instability is diffusion and this is why Turing instability is often called diffusion-driven instability. A remarkable feature of Turing systems as compared to many other instabilities in systems out of equilibrium [109, 110] is that the characteristics of the resulting patterns are not determined by externally imposed length scales or constraints, but by the chemical reaction and diffusion rates that are intrinsic to the system. The spirals, target patterns and travelling waves generated by the Belousov-Zhabotinsky (BZ) reaction are not due to a Turing instability since they are not stationary and the diffusion rates of the chemicals involved in BZ reaction are usually more or less the same. The difference in the diffusion rates of the chemical substances is a necessary, but not a sufficient condition for the Turing instability [108]. These basic ideas developed by Turing are highly valuable because of their impact on science as a whole, and because it is still a topic of contemporary interest. This is the reason why the year 2012 has been dedicated to him by the scientific community in recognition of his immense contribution to science. A photographic representation of Alan Turing is shown in Fig. (11).

I.6 Literature review on cells with activator-inhibitor pathways

The most significant achievement of the reductionist approach of molecular biology has been the elucidation of almost all the biochemical reactions or pathways controlling different functions in the bacteria Eschericia-coli. Also known as E. coli, it is a gram-negative, facultatively anaerobic, rod-shaped, coliform bacterium of the genus Escherichia that is commonly found in the lower intestine of warm-blooded organisms (endotherms). These single-celled, often parasitic, microorganisms without distinct nuclei, or organized cells structures, are categorized into various species. Most E. coli strains are harmless, but some serotypes can cause serious food poisoning in their hosts, and are occasionally responsible for product recalls due to food contamination. The harmless strains are part of the normal flora of the gut, and can benefit their hosts by producing vitamin K2, and preventing colonization of the intestine with pathogenic bacteria. Therefore, they actively partake in processes such as decay, fermentation, nitrogen fixation, and many plants and animal diseases. E. coli is expelled into the environment within fecal matter. The bacterium grows massively in fresh fecal matter under aerobic conditions for 3 days, but its numbers decline slowly afterwards. E. coli and other facultative anaerobes constitute about 0.1 percent of gut flora, and fecal-oral transmission is the major route through which pathogenic strains of the bacterium cause disease.

Initially discovered by *Theodor Escherich* (1885) in goats fecal materials, this bacterium which can be grown and cultured easily and inexpensively in a laboratory setting, has been intensively investigated for over 60 years. E. coli is a chemoheterotroph whose chemically defined medium must include a source of carbon and energy. E. coli is the most widely studied prokaryotic model organism, and an important species in the fields of biotechnology and microbiology, where it has served as the host organism for the majority of work with recombinant DNA. Under favorable conditions, it takes only 20 minutes to reproduce.

As a fair approximation, a living cell can be considered as a collection of interacting biochemical pathways integrated into an overall reaction network [111, 112] through both enzymatic and genetic control elements (which are little more than molecules with conformational flexibility). It is known that when elements of a certain degree of complexity become organized into a totality of an entity belonging to a higher level of organization, the coherence of the higher level depends on properties which the isolated elements could not exhibit until they entered into certain relations with one another [113]. If this is true for living systems, this then tells us that the coherent behavior (or the property of coordinated activities) observed in the spatiotemporal organization seen in more complex systems (i.e. higher organisms) which have evolved from the simpler cells (which in turn are composed of basic biochemical elements) cannot always be understood by reducing it to its rudimentary elements; and it is helpful to study different levels of organizations to obtain valuable information about their functions and their interplay. Most of the molecular processes controlling different cellular functions are regulated by a few common phenomena, such as, sequential reactions with rate limiting steps, competition for common sites, allosteric changes, end-product inhibition or repression, etc. Hence it is useful to formulate general models of different levels of complexity incorporating the above mentioned common features and study their dynamical properties. Living systems seem to have taken advantage of the variability in functional dynamics emerging from a few common components by simply connecting them in different ways. Given the predominance of feedback processes and reaction pathways with low connectivity observed in both metabolic and transcriptional regulatory pathways in E.coli. [114, 115, 116], some authors have studied the canonical three-step single negative feedback system with end product inhibition and compared it to a structurally more complex system in terms of an additional positive feedback.

The aim of this section is to perform: on one hand, a relatively exhaustive review of the analy-

sis of the different topologies of feedback processes, previously conducted by many researchers, in isolation as well as when they are interacting with each other, and to highlight the types of dynamics attainable by these designs under various genetic and biochemical alterations of the pathway. We equally revisit the response of the pathway to perturbation in the end product concentration in order to judge the robustness of the dynamics in that particular topology. According to many investigators, this approach could be a possible way of studying regulation in cellular processes and arriving at a set of minimal designs adopted by nature. For this purpose, we will present the results of studies performed by several researchers, on two generalized biochemical control systems with: firstly, (a) a single negative feedback describing end-product repression, and secondly, (b) a coupled negative and positive feedback mechanism representing end-product inhibition and allosteric activation. On the other hand, at the multicellular level, we will briefly report the impacts of the local coupling strength and system size on the local and global dynamics in the pathway ensembles as specified in the literature, where interesting events of occurrence of synchronization and patterns generations have been reported by some investigators.

I.7 Model pathways: Presentation, description and cellular rhythms

A metabolic pathway consists of two interdependent flows: reaction pathways and control feedbacks. Reaction pathways are composed of systems of enzymes with tightly linked specificities for one another's products and substrates. In many cases, these pathways are forked, with more than one enzyme having specificity for a given product. As demonstrated by the citrate cycle, pathways may also feed back into themselves, producing an iterative structure. Control feedback may be positive or negative, internal to the pathway, or caused by external metabolic or signalling pathways. The citrate cycle for instance is regulated by substrates and products within the cycle. Glycolysis is regulated by hormones, notably insulin. The functions of pathways are either anabolic (constructive), catabolic (destructive), or amphibolic. Amphibolic pathways are both anabolic and catabolic, and often link anabolic and catabolic pathways. In this section, we present two different models pertaining in the description of the pathway rhythms in the E. coli.

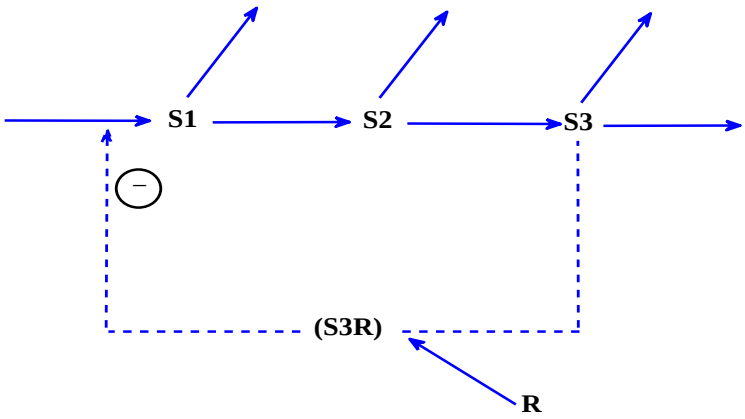

Figure 12: *Three-step biochemical pathway with end-product inhibition mediated by the formation of a complex by the end-product with a repressor R. The arrows from the substrates S_1, S_2, S_3 indicate the degradation of the substrates and utilization of the end-product.*

I.7.1 Model I

The abundance of negative feedback controls in biochemical reaction pathways helps maintaining homeostasis in cellular functions. The basic three-step reaction module (process) considered here (see Fig. 12) is a three step reaction involving the conversion of a substrate S_1 into a product S_3 via an intermediate substance S_2, where $S3$ inhibits the formation of S_1 through a cooperative process by combining with another molecule R [111]. This type of process is common in gene regulation and is known as repressor-mediated repression [117, 118, 119]. This activity is equally similar to the repressor-mediated repression of bacterial operons, where the end-product can repress the operon only after combining with the repressor molecule and these two interactions have very different specificities and dissociation constants. The time evolution of such a process can be written in non-dimensional form as:

$$\begin{aligned} \frac{dx}{dt} &= (\frac{\gamma}{1+\gamma})\frac{1}{1+(1+\gamma)^n} + \frac{1}{1+\gamma} - \alpha_1 x \ , \\ \frac{dy}{dt} &= x - \alpha_2 y \ , \\ \frac{dz}{dt} &= y - \alpha_3 z - g \ , \end{aligned} \tag{5}$$

where α_1, α_2, α_3 are the degradation rates of S_1, S_2 and S_3, whose dimensionless concentrations are given by x, y and z, respectively. g is related to the rate of utilization of the end-product (say, use of amino acids in protein synthesis in a cell), and γ is a parameter describing the strength of repression. Here, it is assuming the complex $[S_3 - R]$ interaction is of the Michaelis-Menten type with n as the cooperativity of repression. To study the above process, the tryptophan operon was taken as the model system for which the parameter values are known from experiments [119]. Numerical simulations and bifurcation analysis of the model pathways were carried out. The basal parameter values, taken from the normal (wild-type) tryptophan biosynthetic pathway in E.coli [118, 120, 121] are: $\gamma = 10$, $g = 4$, $n = 2$, $\alpha_1 = 1$, $\alpha_2 = 0.01$, $\alpha_3 = 0.01$, $\beta = 0.33$, and $k = 0.0173$.

Subsequent to a linear stability analysis of the steady states and some numerical simulation of the equations (5) near the steady states, Somdatta Sinha and Ramaswamy showed that the following behavioral pattern of the system was observed, when one of the parameter, namely the strength of the repression γ, was varied [111]:

STABLE → BISTABLE → PERIODIC.

To identify the minimal conditions under which the pathway may destabilize to induce oscillations, its behavior on varying γ is investigated [116]. The study shows that, at the basal parameter values, as γ is increased, the steady state concentration of the end product reduces drastically until it loses its stability through a subcritical Hopf bifurcation, and the pathway shows bistable behavior, that is, coexistence of a stable limit cycle and equilibrium dynamics. It is keynote to indicate that this phenomenon is known as *hard excitation* [14, 122].

In order to highlight the role of different parameters in the stability of the system, the authors

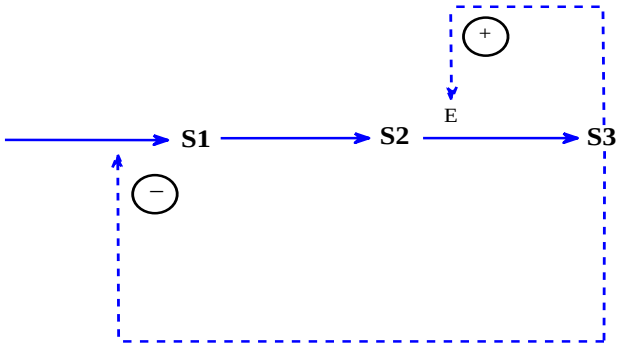

Figure 13: *The minimal biochemical reaction pathway: A three-step reaction sequence with the inhibition of S_1 by end-product S_3 and activation of the allosteric enzyme E by S_3.*

in [116] described the effect of altering the rates of degradation, α_1, α_2, α_3, with respect to the rate of utilization of end-product, g, on the dynamics of the system.

It is noteworthy that the biochemical pathways in cells are subjected to fluctuations both in the rates of various reactions and in the concentrations of the metabolites. To judge the robustness of the dynamics exhibited by the model pathway, the authors evaluated its dynamical response under the effect of sudden perturbations in the end-product concentration z. When the Model I pathway is at equilibrium or is oscillating(that is in the presence of only one stable attractor, outside of the range of values of γ suitable for hard excitation), instantaneous perturbation of z returns the pathway to its original dynamics. However, in the bistable region, the effect of the perturbation depends on the strength of the perturbation.

I.7.2 Model II

As discussed above, negative feedback processes are crucial in biochemical activities. Yet, Though less prevalent, positive feedback processes in both metabolic and genetic regulations are used for important activities through amplification of signals, rapid response pathways, switching activities, and in cellular processes that show periodic and complex dynamics, such as glycolytic oscillations in cells free extracts of yeast cells, peroxidase-oxidase reactions, insulin secretion in

pancreatic beta cells, calcium oscillations and amplification of $cAMP$ signal in the aggregation of cellular slime molds.

To describe a higher level of organization, we consider the biochemical pathway model shown in Fig. 13, which is a three-step reaction having substrates S_1, S_2 and end-product S_3, whose concentrations are regulated by a positive and a negative feedback process in terms of end-product inhibition of S_1 by S_3 and autocatalytic activation of the allosteric enzyme E, by S_3. Here, the S_2 to S_3 reaction is catalyzed by an allosteric enzyme E, which is assumed to be a dimer (that is a double molecule or a molecule made up of two simpler identical molecules), obeying the concerted transition model (Fig. 13) [76]. The generalized dimensionless form of the equations describing the above process is given as:

$$\begin{aligned} \frac{dx}{dt} &= F(z) - kx \ , \\ \frac{dy}{dt} &= a_3 x - G(y,z) \ , \\ \frac{dz}{dt} &= a_4 G(y,z) - qz \ , \end{aligned} \tag{6}$$

where $F(z)$ and $G(y,z)$ are given by:

$$F(z) = \frac{a_1}{a_2 + z^n} \quad \text{, and} \quad G(y,z) = \frac{Ty(1+y)(1+z)^2}{L + (1+y)^2(1+z)^2}$$

,

where a_1, a_2, a_3 and a_4 are parameters which are functions of the pseudo-Michaelis constants and dissociation constants of the reactions, k and q are the degradation rates of S_1 and S_3, which are assumed to be of first order [111]. L and T are the allosteric constant and maximum activity of the enzyme E. n denotes the cooperativity of repression. The values of the parameters can be chosen from existing literature on both hypothetical metabolic reactions and specific processes [15, 123, 124]. To reduce the dimensions of the parameter space to be explored, Somdatta Sinha and Ramaswamy have fixed the values of a_1, a_2, a_3, a_4, L, T and n.

The time evolution of the normalized substrates in this pathway model can be described by equation (6), where, x, y and z are the normalized concentration of the substrates, S_1, S_2 and S_3, respectively. The term $F(z)$ is a nonlinear function describing the inhibition of S_1 by the end-

product, S_3. We assume that this interaction follows cooperative kinetics and requires binding of n molecules of z for inhibition. The positive feedback term, $G(y, z)$, involves the allosteric enzyme E, obeying the concerted transition model. These nonlinear kinetic processes are common in mechanisms of biochemical regulation and are widespread in both genetic and metabolic reactions underlying cellular processes, such as the cell cycle, gene repression/induction, glycolysis, hormonal signalling, $cAMP$ oscillations in cellular slime moulds and calcium-induced-calcium-release [14]. Many authors have studied the system in model II using a combination of analytical and numerical methods. The values of the parameters were obtained from experimental systems with similar regulatory mechanisms [111]. The basal values of the parameters are given as $n = 4$, $T = 10$, $L = 10^6$, $k = 1.0$ and $q = 0.01$.

The authors in [107, 125, 126] have studied the behavior of the pathway by varying the rates of degradation, k and q of S_1 and S_3, since the net accumulation of the substrates depends critically on these parameters. They found that the pathway shows a variety of dynamics, starting from equilibrium to periodic, complex and chaotic oscillations with changing k and q.

A notable complex behavior of model II emerged in a new form of *bistability* known as *birhythmicity* [15], and denotes the coexistence between two simultaneously stable attractors.

Effect of Perturbation on model II and collective cells dynamics

The coexistence of two very dissimilar attractors, or birhythmicity, has interesting implications. The basins of attraction map of the two attractors, Type I attractor and Type II, is found to be fractal, having no well-defined boundary and so the asymptotic evolution of the pathway is unpredictable. The fractal nature of the basins of attraction is of particular interest in the presence of noise, since this means that the pathway dynamics are very sensitive to small variations in substrate concentrations in this birhythmic parameter regime. Since the concentrations of biomolecules within the cells can fluctuate considerably, these results imply that the pathway dynamics exhibited by individual cells within an isogenic population can show different oscillatory phenotypes even under the same environmental conditions.

At the collective level, cell-to-cell communication is a crucial prerequisite for the development and maintenance of structure and function of multicellular organisms. Nowadays, diverse mechanisms of intercellular exchange of information have been documented, and the variations in strength of communication have been found to be responsible of the changes in dynamical states leading to disease [127]. Biochemical pathways with activator-inhibitor reactions under-

lie many cellular functions and end-products of such pathways metabolically couple cells in populations and tissues in order to induce a collective behavior. We have reviewed the collective behavior of a one dimensional ring of cells, diffusively coupled to their nearest neighbors through the end product of a intracellular activator-inhibitor biochemical pathway. The individual cells, which are chaotic when uncoupled, were found to show multiple modes of synchronized spatiotemporal dynamics, chaos suppression, phase synchronization, travelling wave, and intermittent synchronization, for ranges of coupling strength. Along with suppression of chaos to P_4 oscillations, regular spatial patterns are also observed with cells in the lattice having phase synchronized dynamics but with different amplitudes. Unlike other systems, here synchronization does not persist for higher coupling after establishment. Phase synchronization observed in this model has certain important and distinct features. Most of the earlier investigations were concentrated on synchronization of either chaotic or limit cycle oscillators. Here, the phase entrainment is observed in a collection of oscillators whose intrinsic dynamics is a lower subharmonic state (period 4). Even when the pathways in individual cells continue to exhibit chaotic dynamics, travelling waves were observed in the lattice. Travelling waves have long been shown to underlie pattern formation in tissues [128].

I.8 Conclusion

In this chapter, we have reviewed and ascertained the high degree of complexity embedded in living cells. We found that it is possible for a simple system to elicit a wide variety of dynamical modes as seen in real biochemical reactions in cells. This type of variation in behavior for any change in the parameters is possible due to the inherent nonlinearity of the regulatory processes. The behavior ranges from equilibrium dynamics for a large range of parameters to more complex behaviors for smaller range.

The occurrences of *bistability* either in the form of *hard excitation* (in Model I) or *birhythmicity* (in Model II), show that it is possible for pathways with identical parameter values to exhibit widely varying dynamics. In the specific case of *birhythmicity*, the fractal nature of the basins of attraction in this region has interesting consequences for the system dynamics in presence of small fluctuations in the substrates. The pathway dynamics can be quite unpredictable and non-intuitive as it can continue in the same state, or switch between the two kinds of oscillations with different amplitudes and time periods, or even show long transients. We have shown that

the noise sensitivity is more prevalent in a restricted region of the phase space around the steady state, where the switching of dynamics occurs. Thus, this pathway (Model *II*) is highly sensitive to fluctuations in concentration, in contrast to the case of multiple steady states, which requires a minimum threshold perturbation for effecting a change in the dynamics. The noise sensitivity, therefore, can lead to "spontaneous" alteration in dynamics even under small fluctuations. In one-dimensional spatial lattices, these pathways are found to be able to cooperate and synchronize via the help of local interactions, with sometimes the emergence of interesting collective spatiotemporal dynamics.

These findings are extremely valuable in order to appreciate the natural complexity of biochemical processes taking place at the cellular scales. However, despite these huge contributions, several questions still remain unanswered. Cellular signallings involve more than just nearest neighbor interactions. Long range interactions and indirect links among their pathways are equally crucial in the processes pertaining in their functional activities aiming at preserving homeostasis. Assessing the impacts (both solely and simultaneously) of such connections on the local and collective rhythms of the pathways shall be one of our foremost concern in the next chapters.

Concomitantly, even though one-dimensional (ring-like) network models of cells with activator-inhibitor pathways display tremendous dynamical features, we believe that the cooperativity of the pathways in a two-dimensional spatial domain may exhibit more complex spatiotemporal organization than what has been observed so far in one-dimensional spatial lattices. Therefore, investigating the emergence of spatiotemporal conformations in the framework of diffusively connected two-dimensional spatial arrays of such pathways will be a key point of interest in the next parts of this piece of work.

In line with these objectives, and based on the massive background literature previously reviewed on cells with activator-inhibitor pathways, the next chapter will be dedicated to the presentation and description of models and methods, both analytical and numerical, that will be brought into play, in the course of our investigations of the aforementioned phenomena.

CHAPTER II

METHODOLOGY: MODELS DESCRIPTION, MATHEMATICAL AND NUMERICAL METHODS

II.1 Introduction

A wide array of cellular functions are performed by biochemical reactions within the cell. These reactions form a complex network of interconnected pathways, consisting of both genetic and metabolic reactions. These are controlled by variety of regulatory mechanisms. These pathways are too complex to be understood by intuition and informal models alone. Mathematical models have provided useful insights into the dynamics of these pathways. This chapter will concomitantly cover, the depiction of some scientifically sanctioned (approved) mathematical models pertaining in the description of the phenomenological features of biochemical pathways, the report of some analytical and numerical methods essential in their exploration, and a tender (suggestion) of how these methods can be used to understand and predict the properties of both these biochemical pathways and the behavior of cells.

II.2 Mathematical modelling of biochemical pathways: Incisive aims

Until recently, experimental approaches have sought to understand cellular functions by using a reductionist approach, breaking the system into modules and studying each module separately. However, in addition to being expensive, cumbersome and time consuming, this method posed problems when researchers attempted to put all the parts together into a coherent whole. With the advances in technology, faster and more powerful methods have been developed, which allow scientists to conduct studies at much larger scale. Some of these include the high throughput gene sequencing technologies, large-scale DNA microarrays, proteomics, metabolomics, etc. All

these methods have generated huge amounts of data. Computers and computer-based methods of storing, retrieving and analyzing the data have become indispensable in order to deal with this explosion of data. Nowadays, scientists attempt to get a picture of the whole system by taking the systems approach, which consists of taking inputs from more than one method and additionally using mathematical models.

Mathematical models have the advantage that they help us to understand the essential, qualitative features of any system. Methods used in engineering, physics, mathematics and other disciplines can be employed when we recognize that the basic features are similar. They help us understand the non-intuitive behavior of the system, which is not apparent or obvious from intuition alone. Using mathematics, we can make broad generalizations and organize disparate information to gain a coherent picture of the whole system. Mathematical methods help us think logically and clearly about the components and interactions that are important in a complex system. Since we can examine situations, which may not be accessible to experiments, we can uncover new strategies and answer complex "*what if*" questions, in order to predict possible outcome of perturbation (or change). We can build new hypotheses and reject false hypotheses, using such modelling approaches.

The most critical thing needed in modelling is to have a biological knowledge of the process we are trying to model. For example, if we want to model cell division, we must understand the different stages of the cell cycle, times scales, the pathways and the regulatory processes involved in the process, and so on. We must have some idea of the concentrations of substances, reaction mechanisms and rate constants, gene expression flux, protein turnover, degradation of substances and maybe the topology or structure of the network. In addition, we would need to know the environmental conditions such as temperature, pH, etc, which are required for the reactions to take place. In case of multicellular models, we would also need information about the kind of interactions that take place between the cells. With all this information in hand, one can look at formulating a mathematical model.

While mathematical methods convert large problems into manageable tasks, there are still inherent difficulties. The biggest challenge is the enormous complexity of biological systems. In addition, their behavior differs in vivo (in cells or organisms) and in vitro (in experiments). So, when we make generalizations based on models, we must be aware of the many pitfalls. The controlling processes in biological systems are manifold, coupled and nonlinear. Over and

above all this, these systems are constantly changing and adapting and often respond to change in counterintuitive ways. For all these reasons, we must make assumptions and simplifications in order to have a manageable model.

Noteworthily, expectations in terms of prediction from a model are diverse. They would vary from model to model and method to method. When we formulate the models, therefore, we also focus on what predictions and insights we are looking for. When we need simple predictions, it makes sense to use a simple model. A more detailed model is not necessarily a better model. More detailed models, or ones with higher level of complexity would obviously take longer to simulate and the mathematical analysis would be harder. The tools required for the analysis use mathematical and numerical approaches and there is a wide spectrum of these. We cannot cover all of them, but in what follows, we shall expound some of those which have pertinence in the current work.

II.3 Single cell and its dynamics

Since the 1980s, modelling has emerged as a novel tool to handle the rapidly growing information on the molecular parts list and the overwhelmingly complex interaction circuitry of signalling networks. Following this development, Sinha *et al* [1, 105, 111] proposed in 1987 a mathematical model of a biochemical system describing the dynamics of normalized concentration of the substrates in a single cell with activator-inhibitor pathways. Since then, many studies have been carried out on this model ranging from classical nonlinear dynamical analysis to synchronization of electrically coupled network formed by units of single cell described by this model [11, 34, 106, 107]. This cell, namely "the cell with activator-inhibitor pathway", has a biochemical pathway regulated by negative and positive feedback processes. Its model describes actually a three-step sequential reaction having two substrates, and one end product. Their concentrations are regulated by a positive and a negative feedback process respectively in terms of end product inhibition of the first substrate (i.e. when the concentration of the end product is large in the cell, the negative feedback induces an attenuation in the concentration of the substrate in the intracellular medium (see Refs. [1, 105, 111] for more details)) as shown on Fig. 14.

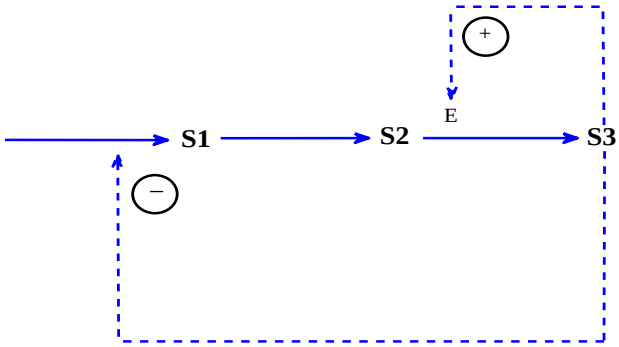

Figure 14: *A three-step reaction sequence in the single cell model with the inhibition of S_1 by end-product S_3 and activation of the allosteric enzyme E by S_3.*

The model is represented by the following set of ordinary differential equations:

$$\begin{aligned} \frac{dx}{dt} &= F(z) - kx \ , \\ \frac{dy}{dt} &= x - G(y,z) \ , \\ \frac{dz}{dt} &= G(y,z) - qz \ . \end{aligned} \tag{7}$$

The present model describes a three-step sequential reaction having successively two substrates and one end product whose normalized concentrations in the intracellular medium are respectively represented by x, y and z. Therefore, x is the normalized concentration of the first substrate, y is that of the second substrate, and z is the normalized concentration of the end product. The end product is the signal molecule intended to be diffused into the extracellular medium to other cells via the cells's plasma membrane. As reported previously, these concentrations are regulated by a negative feedback process in terms of the end product inhibition of the first substrate, as well as via an autocatalytic activation of the allosteric enzyme by the end product. The functions $F(z)$ and $G(y,z)$ representing the negative and positive feedback processes, are nonlinear processes designed following the concerted transition model described in [14, 15, 76] and are given by:

$$F(z) = \frac{1}{1+z^4} \quad \text{, and} \quad G(y,z) = \frac{Ty(1+y)(1+z)^2}{L+(1+y)^2(1+z)^2} \ . \tag{8}$$

The parameter "k", called the rate of degradation of the first substrate represents the speed at which the first product's normalized concentration decreases in time. The parameters T and L are respectively, the maximum velocity of the enzyme which determines the maximum rate at which the biochemical reaction transforming the second substrate into end product is performed; and the allosteric constant of the enzyme determining how the alterability in the protein's (i.e. enzyme) activity takes place after reception at its binding site of the signal from the cell through positive feedback, as one form of autocrine signaling. It is noteworthy that autocrine signaling takes place when a cell sends some signals back to itself in order to regulate internal cellular mechanisms vital for a good human body functional balance. q is the rate of degradation of the end product. It determines the speed at which z decreases over time, especially when z is sufficiently large in the intracellular medium of biological cells. Thus, the accumulations in first substrate and end product depends critically on the parameters k and q.

II.4 Coupled system: Synchronization

II.4.1 Collective dynamics of multicellular systems: Dynamics of electrically coupled cells

The two most important features of collective dynamics in any multicomponent, coupled system are synchrony and spatiotemporal patterns [104, 108]. Here, the dynamics exhibited by the "whole" ensemble can be quite different from the individual components' behavior [129]. Spatial patterns can also be set up in structured ensembles (e.g. embryos, cardiac tissue) whose length scale spans that of its several components [130]. The focus of this section is to present a model important for the study of the impact of nearest neighbor interactions and the role of scales of measurement in the faithful description of collective spatiotemporal patterns and processes in a multicellular ensemble.

The model single cells Eq. (6), are coupled with their two nearest neighbors by the dif-

fusion of the end product of their respective activator-inhibitor reaction pathways, on a one-dimensional lattice with periodic boundary conditions [11, 131, 132]. The coupled-cell model can be written as:

$$\begin{aligned} \frac{dx_i}{dt} &= F(z_i) - kx_i \ , \\ \frac{dy_i}{dt} &= x_i - G(y_i, z_i) \ , \\ \frac{dz_i}{dt} &= G(y_i, z_i) - qz_i - \varepsilon z_i + \frac{\varepsilon}{2}(z_{i-1} + z_{i+1}) \ , \end{aligned} \tag{9}$$

with $i = 1, N$, and

where $F(z)$ and $G(y, z)$ are given by:

$$F(z) = \frac{1}{1+z^4} \quad \text{, and} \quad G(y,z) = \frac{Ty(1+y)(1+z)^2}{L + (1+y)^2(1+z)^2} \ , \tag{10}$$

and where, ε is the diffusive coupling strength of the end product, and, i, the cell number that ranges from 1 to N, where N is the lattice size. For numerical simulations, the authors have used the fourth-order Runge-Kutta scheme. Simulations have been performed on lattices with varying number of cells, with random initial conditions uniformly distributed around the steady state z^*, that is, $z^* \mp 2$, with $z^* \approx 5.163$. Simulations have been performed for $t = 10^5$, and results were presented for the last 5000 time units.

For the multicellular ensemble in this context, we consider a simple model where the cells are assumed to form a closed ring-like lattice structure, as is observed in cells in a plant root section. Each cell in this one-dimensional lattice of N cells (Fig. 15 (b)) has the model biochemical pathway described by Eq. (7) (shown in Fig. 15 (a)), and interacts through the diffusion of the end-product z, from each cell (i) to its two neighboring cells ($i+1$ and $i-1$).

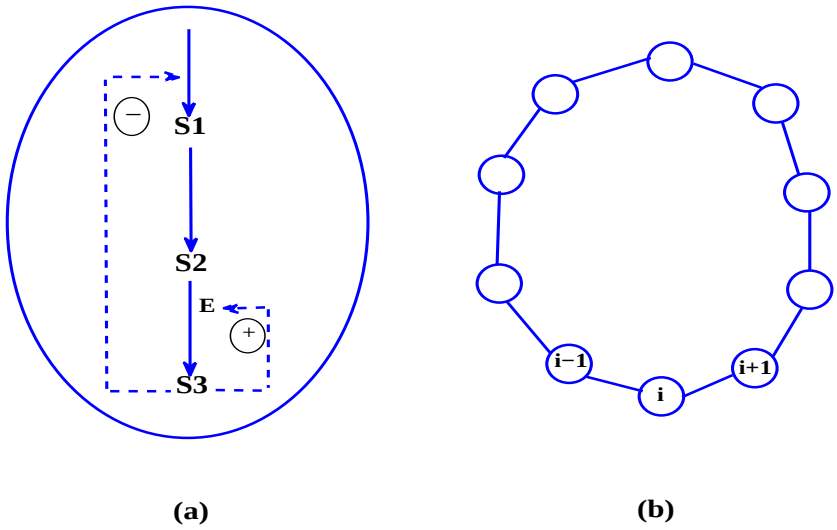

Figure 15: *The model multicellular ensemble: (a): A single cell incorporating a three-step biochemical pathway; (b): A model ring of cells, where each cell (node i, as shown in (a)) is diffusively coupled to its nearest neighboring cells(nodes $i-1$ and $i+1$).*

II.4.2 Chemically coupled cells

It is well known that the chemical synaptic coupling also considered as a fast threshold modulation has been extensively used to model chemically connected neurons [69, 70, 71]. However, this type of coupling can also be found in cells. In fact, there are two primary ways that cells communicate with neighbors. Many cells (e.g. muscles and cardiac cells) are connected to their immediate neighbors by gap junctions in the cell membrane that form a relatively nonselective, low resistance, pore through which electrical current or chemical species can flow. Hence, a gap junction is also called an "electrical synapse". The second means of communication is through a chemical synapse, in which the message is mediated by the release of a chemical from one cell and detected by receptors on its neighbors [75]. Examples of this are endocrine signaling and synaptic signaling [133]. Conscious of these facts, we proposed ourselves to use the sigmoidal function type employed to represent the chemical coupling in neural network to portray the chemical coupling among cells with activator-inhibitor pathways. We believe that it depicts the naturally modulated long range interactions between cells. This may be triggered by their difference in signal molecules concentration, and being representative of the physiological processes pertaining to a good cellular communication and functioning. For this purpose, we consider a

pulsatile function modelled as a static sigmoidal nonlinear input-output function with a threshold and a saturation parameter [69]. The equations describing the dynamics of the normalized concentrations of the substrates in their intracellular media is given by:

$$\begin{aligned} \frac{dx_i}{dt} &= F(z_i) - kx_i \ , \\ \frac{dy_i}{dt} &= x_i - G(y_i, z_i) \ , \\ \frac{dz_i}{dt} &= G(y_i, z_i) - qz_i + g_s(z_i - V_{inh}) \sum_{j=1}^{2} c_{ij} H(z_i, z_j) \ , \end{aligned} \tag{11}$$

$i, j = \overline{1,2}$, where the parameter g_s is the chemical coupling strength and the coupling function $H(z_i, z_j)$ reads $H(z_i, z_j) = H(z_j) = \Gamma(z_j) = \dfrac{1}{[1 + \exp\{-\lambda(z_j - \theta_s)\}]}$, and $c_{ii} = -1$ and $c_{ij} = 1$ if $i \neq j$. The parameter V_{inh} represents a control value for the concentration of the end-product in the cells, since the values of the concentrations of the chemical products must not be found out of a given range of values. Even though , cells with activator-inhibitor pathways regulate these concentrations naturally, it has been observed through numerical studies that this coupling scheme for some values of V_{inh} produces very large values of the concentration into the cells, for the end-product, which is to avoid. The values $V_{inh} = 2$ and $\theta_s = -0.25$ are chosen in order to always maintain the quantity $(z_i - V_{inh}) > 0$.

II.4.3 Electrically and chemically coupled cells

Even in clonal cell populations and under the most uniform experimental conditions, considerable variations are observed in the rates of development, morphology and the concentration of each molecular species in each cell. Organisms are biochemically dynamic and will be subjected to different type of interactions. These interactions between cells usually represent the coupling amongst them. Cells couple themselves in several ways: Adjacent cells can couple by direct contact, each of them sending signals across gap junctions. Nearby cells that are not touching can communicate through paracrine signals. In paracrine signaling, secretions from one cell have an effect only on cells in the immediate area. Two other systems mediate communication over longer distances: in endocrine signaling the blood carries hormones to distant cells, and in synaptic signaling nerve cells secrete neurotransmitters from long cellular extensions close to the responding cells [133].

The complementary roles of electrical and chemical couplings have been studied in many

biological systems [69, 71]. It was found that the chemical coupling is especially good at wiping out the effects of initial conditions but cannot deal with significant heterogeneity, no matter how strong it is. The electrical coupling acts to wipe the heterogeneity and foster synchronization in the system. Our concern in this section is to understand this phenomenon in the case of coupled cells with activator-inhibitor pathways. It is known that the electrical coupling between cells with activator-inhibitor pathways favors synchronization [11, 34]. We are therefore interested into investigating the contribution of chemical and electrical couplings to the global synchronization dynamics of the biochemical cells. Therefore, we expect that the presence of electrical coupling will reinforce the coupling between the cells. We then expect that the combination of both coupling types will lead to an improvement into the global synchronization dynamics of both cells.

Taking into account these two ways of coupling (electrical coupling and fast threshold coupling), the equations describing the dynamics of the coupled pathways are given by:

$$\begin{aligned} \frac{dx_i}{dt} &= F(z_i) - kx_i \ , \\ \frac{dy_i}{dt} &= x_i - G(y_i, z_i) \ , \\ \frac{dz_i}{dt} &= G(y_i, z_i) - qz_i - g_s(z_i - V_{inh}) \sum_{j=1}^{2} c_{ij}\Gamma(z_j) + g_l(z_j - z_i) \ , \end{aligned} \tag{12}$$

$i, j = \overline{1, 2}$, where the parameter g_l is the electrical coupling strength and g_s as previously defined.

II.4.4 Adaptively environment-mediated coupled cells

In the present study, we consider two chaotic cells with activator-inhibitor pathways, indirectly coupled through a common environment u, with feedback and adaptive control mechanism, according to the following set of differential equations:

$$\begin{aligned}
\frac{dx_i}{dt} &= F(z_i) - kx_i \ , \\
\frac{dy_i}{dt} &= x_i - G(y_i, z_i) \ , \\
\frac{dz_i}{dt} &= G(y_i, z_i) - qz_i - \epsilon_1 \beta_i u \ , \\
\frac{du}{dt} &= -\kappa u - \epsilon_2 \frac{(\beta_1 z_1 + \beta_2 z_2)}{2} \ , \\
\frac{d\kappa}{dt} &= \alpha(\beta_1 z_1 + \beta_2 z_2)^2 \ ,
\end{aligned} \tag{13}$$

$i = 1, 2$; with $\beta_1 = -\beta_2 = 1$ and $0 < \alpha \ll 1$.

$F(z)$ and $G(y, z)$ are given by:

$$F(z) = \frac{1}{1+z^4} \quad \text{, and} \quad G(y,z) = \frac{Ty(1+y)(1+z)^2}{L + (1+y)^2(1+z)^2} \ .$$

They stand for the negative and positive feedback processes present in the sequence of biochemical reactions that internally contribute to maintain homeostasis in cellular functions by suppressing stochastic variations [134] and regulating activities in cellular processes that show periodic and complex dynamics. This is the case of glycolytic oscillations in cell free extracts of yeast cells, peroxidase-oxidase reactions, calcium oscillations, etc. x_i, y_i and z_i represent the normalized concentrations of the substrates and end-product of these cells pathways. The parameters k and q are respectively the rate of degradation of the first substrate and the rate of degradation of the end product. T and L are related to the maximum velocity of the enzyme and the allosteric constant. The variable u stands for the concentration of various biochemical species in the exterior of the cells, thereby globally determining the intrinsic dynamics of the environment which decays with κ as its damping parameter. κ varies depending on the feedback from the systems, which in return enable the environment to sustain itself for extended periods of time. ϵ_1 is the strength of the feedback to the system and ϵ_2 that to the environment. Here, we assume that the biochemical components of the cells that take part in the coupling are the end-products, as they diffuse through the environment with their respective normalized concentrations z_i. The nature of the feedback from and to the environment is prescribed by the values of β_1 and β_2. In the present case, the coupling is of difference type, that is $(\beta_1, \beta_2) = (1, -1)$. A similar model has been used by Resmi and Ambika [135] to couple Rössler and Lorenz systems through

a common environment without adaptive feature. This coupling mechanism has the interesting property that the common environment does not alter the local chaotic dynamics of the systems as it attempts to synchronize them. In their synchronized regime, the systems preserve more or less the same phase space structure of the uncoupled system. Our idea consists in tuning the gain of a linear damping coefficient of the environmental coupling during the control procedure. We wish to update this gain with a proper adaptation law such that the proposed feedback control law can track and predetermine the optimal gain of the environmental controller.

Several references in the literature indicate that cells with activator-inhibitor pathways are complex systems capable of exhibiting complex dynamics ranging from simple limit cycle to chaotic behavior[11, 12, 34]. For their chaotic regime, the parameter values of their biochemical pathways carrying nonlinearities will be taken as: $q = 0.1$, $k = 0.003$, $L = 10^6$ and $T = 10$. It is noteworthy that cell signaling can occur in different forms. In the present work, we assume that signal molecules released by cells can diffuse through the extracellular fluid to other cells. If those molecules are taken up by neighboring cells, destroyed by extracellular enzymes or quickly removed from the extracellular fluid in some other way, their influence is restricted to cells in the immediate vicinity of the releasing cell. Such short-lived signals with local effects are called paracrine signals. They play crucial roles in the early development of the cell, coordinating the activities of clusters of cells. If a released signal molecule remains in the extracellular fluid, it may enter the organism's circulatory system and travel widely throughout the body. These longer-lived signal molecules which may affect cells very distant from the releasing cell, are called hormones and this type of intercellular communication is referred to as endocrine signaling. Both animals and plants use this signaling mechanism extensively.

It is worth mentioning that homeostasis is crucial for the survival of any living being. It refers to the maintenance of stable internal conditions in an organism living in a changing environment. The relevance of this importance lies on the fact that cells function best within a limited range of conditions. Therefore, for an active entity, temperature, blood sugar, acidity and other conditions must be controlled. Failure to regulate these parameters may elicit detrimental functional disorder within the cellular ensemble pertaining to illness. To prevent this scenario, cells constantly convey their needs to the extracellular space in terms of organic resources by releasing some chemical signals such as hormones across their plasma membrane in order to achieve their numerous tasks. Consequently, all cells regularly respond to their environment through

steady feedback reports about their states and needs. These reactions are systematic processes that help our bodies to uphold their metabolic equilibrium states. Incidentally, it is the duty of their common dynamic extracellular medium to cater for their consistent demands by providing the required chemical resources. The aptitude of the environment to wisely make provisions for these cells sets the pace that is paramount to instate a harmonious cooperation among their pathways, thereby avoiding competition among them. Careful attention should be given to the fact that rivalry within the cellular medium can be harmful for the smooth evolution and stability of the functional mechanisms involve in the developmental stages of the cells, aiming at maintaining homeostasis and perpetuating life.

Based on these facts, the steadiness of these cellular responses towards the environment in the course of time thereby enables us to assume in the present analysis that the strength of the feedbacks of the biochemical pathways to their living medium and vice-versa are constant all through, and that only the extracellular medium adjusts its parameter values in terms of available resources in order to care for the biochemical systems which there live as a community. To achieve this, only the damping parameter κ of the dynamic environment will exhibit this adaptive feature, enabling the environment to constantly look for the optimal level in terms of availability and allocation of resources. Let us note that this optimal level also clearly depends on the cellular demand, that is the strength of the feedbacks ϵ_1 and ϵ_2. This is the reason why the subsequent study will be concerned with looking for the suitable values of ϵ_1 and ϵ_2 vital(necessary) to achieve this goal. Nonetheless, in other circumstances, these couplings(feedbacks) strengths could equally be considered to be adaptive and assumed to be influenced by hormones from other distant cells, that bind to receptors on the target cell's membrane and trigger it to produce a needed chemical compound. However, this aspect of their operations shall not be taken into account in the present study. This may be the core of a later probe.

II.5 Coupled system: Pattern formation

The system of equations describing the sequence of biochemical reactions within such networks of cells with activator-inhibitor pathways is given by:

$$\begin{aligned} \frac{\partial U}{\partial \tau} &= F(W) - kU + D_u \nabla^2 U \ , \\ \frac{\partial V}{\partial \tau} &= U - G(V,W) + D_v \nabla^2 V \ , \\ \frac{\partial W}{\partial \tau} &= G(V,W) - qW + D_w \nabla^2 W \ , \end{aligned} \tag{14}$$

where τ denotes the time. U, V and W represent the normalized concentrations of the substrates and end-product of these cells pathways. The parameters D_u , D_v and D_w are the elements of the diagonal matrix of positive constant diffusion coefficients.

The functions $F(W)$ and $G(V,W)$ are given by:

$$F(W) = \frac{1}{1+W^4} \quad \text{, and} \quad G(V,W) = \frac{TV(1+V)(1+W)^2}{L+(1+V)^2(1+W)^2} \ .$$

They account for the negative and positive feedback processes present in the sequence of biochemical reactions that internally contribute to preserve homeostasis in cellular functions by suppressing stochastic variations [134] and regulating activities in cellular processes that show periodic and complex dynamics as it is the case for glycolytic oscillations in cell free extracts of yeast cells, peroxidase-oxidase reactions, calcium oscillations, etc. These functions determine the sequence of reactions occurring locally in each site of the space, that is at the level of each cell.

II.6 Analytical methods

II.6.1 Linear stability analysis for systems of ordinary differential equations

Consider the following two-dimensional system:

$$\begin{aligned} \frac{dx}{dt} &= f(x,y) \ , \\ \frac{dy}{dt} &= g(y,z) \ , \end{aligned} \tag{15}$$

and suppose that $(\overline{x}, \overline{y})$ is a steady state, that is, $f(\overline{x}, \overline{y}) = 0$ and $g(\overline{x}, \overline{y}) = 0$.

The question of interest is whether the steady state is stable or unstable. Consider a small

perturbation from the steady state by letting:

$$\begin{aligned} x &= \overline{x} + u \ , \\ y &= \overline{y} + v \ , \end{aligned} \tag{16}$$

where both u and v are understood to be small. The question of interest translates into the following: will u and v grow (so that x and y move away from the steady state), or will they decay to zero (so that x and y move towards the steady state)?

In the former case, we say that the steady state is unstable, in the latter it is stable. To see whether the perturbation grows or decays, we need to derive differential equations for u and v. We do so as follows:

$$\begin{aligned} \frac{du}{dt} &= \frac{dx}{dt} \ , \ (since \ \overline{x} \ is \ constant) \\ &= f(x,y) \ , \ (by \ definition) \\ &= f(\overline{x}+u, \overline{y}+v) \ , \ (by \ substitution) \\ &= f(\overline{x},\overline{y}) + \frac{\partial f}{\partial x}(\overline{x},\overline{y})u + \frac{\partial f}{\partial y}(\overline{x},\overline{y})v + ...(Taylor \ series \ expansion \ around \ the \ steady \ state) \\ &= \frac{\partial f}{\partial x}(\overline{x},\overline{y})u + \frac{\partial f}{\partial y}(\overline{x},\overline{y})v + ... \end{aligned} \tag{17}$$

Similarly:

$$\frac{dv}{dt} = \frac{\partial g}{\partial x}(\overline{x},\overline{y})u + \frac{\partial g}{\partial y}(\overline{x},\overline{y})v + ... \tag{18}$$

The ... denote higher order terms, involving u^2, v^2, uv, etc. Since u and v are assumed to be small, these higher order terms are extremely small. If we can safely neglect the higher order terms, we obtain the following linear system of equations governing the evolution of the perturbations u and v:

$$\frac{du}{dt} = \frac{\partial f}{\partial x}(\overline{x},\overline{y})u + \frac{\partial f}{\partial y}(\overline{x},\overline{y})v \ , \tag{19}$$

$$\frac{dv}{dt} = \frac{\partial g}{\partial x}(\overline{x},\overline{y})u + \frac{\partial g}{\partial y}(\overline{x},\overline{y})v \ . \tag{20}$$

We refer to the related matrix as the Jacobian matrix of the original system at the steady state $(\overline{x},\overline{y})$. The above linear system for u and v has the trivial steady state $(u,v) = (0,0)$, and the stability of this trivial steady state is determined by the eigenvalues of the matrix, as follows:

If the eigenvalues of the Jacobian matrix all have real parts less than zero, then the steady state is stable. If at least one of the eigenvalues of the Jacobian matrix has real part greater than zero, then the steady state is unstable. Otherwise, there is no conclusion (then, we have a borderline case between stability and instability; such cases require an investigation of the higher order terms we neglected, and this requires more sophisticated mathematical machinery discussed in advanced courses on ordinary differential equations).

Last but not least, there is a theorem (the Hartman- Grobman Theorem) that guarantees that the stability of the steady state $(\overline{x},\overline{y})$ of the original system is the same as the stability of the trivial steady state $(0,0)$ of the linearized system. Thus, the procedure to determine stability of $(\overline{x},\overline{y})$ is as follows:

1. Compute all partial derivatives of the right-hand- side of the original system of differential equations, and construct the Jacobian matrix.

2. Evaluate the Jacobian matrix at the steady state.

3. Compute eigenvalues.

4. Conclude stability or instability based on the real parts of the eigenvalues.

Let us note that the theorem and procedure apply to N- dimensional systems.

II.6.2 Master stability function approach for synchronized coupled systems

Considerable progress toward developing a general approach to the assessment of the stability of synchronization of identical coupled dynamical systems has been done lately [20]. The consequence of this is a master stability equation, which allows us to calculate the stability (as determined from a particular choice of stability measure, like Lyapunov or Floquet exponents).

Assuming that for N identical systems, there is an exactly synchronized solution for a cou-

pled system, the synchronization manifold is defined by $\mathcal{M}$=$\{x_1 = x_2 = ... = x_N = x_s\}$.

To study the stability of the manifold $\mathcal{M}$ of our coupled system, we make use of this function (master stability function). For N coupled dynamical units, each of them giving rise to the evolution of a 2-dimensional vector field x_i ruled by a local set of ordinary differential equations $\dot{x}_i = \mathbf{F}(x_i)$, the equation of motion read:

$$\dot{x}_i = \mathbf{F}(x_i) - K\sum_{j=1}^{N} G_{ij}\mathbf{H}(x_j) \ , \qquad i = 1, 2, ..., N, \tag{21}$$

where $\dot{x}_i = \mathbf{F}(x_i)$ governs the local dynamics of the i^{th} node. K is a coupling strength. The output function $\mathbf{H}(x_i)$ is a vectorial function defined as an arbitrary function of each nodes variables that is used in the coupling. $G(t)$ is a symmetric Laplacian matrix ($\sum_j G_{ij} = 0$) describing the networks connection.

The stability of the synchronization state can be determined from the variational equation obtained by considering an infinitesimal perturbation δx_i from the synchronous states, $x_i = \delta x_i + x_s$. The equation of motion for the perturbation δx_i can be straightforwardly obtained by means of Taylor series expansion of first order of the original coupled system around the synchronized state which gives:

$$\begin{aligned} \delta x_i &= D\mathbf{F}(x_s)\delta x_i - K\sum_{j=1}^{N} G_{ij} D\mathbf{H}(x_s)\delta x_i, \\ &= \sum_{j=1}^{N} [D\mathbf{F}(x_s)\delta_{ij} - KG_{ij}D\mathbf{H}(x_s)] \cdot \delta x_i \ , \\ i &= 1, 2, ..., N, \end{aligned} \tag{22}$$

where $D\mathbf{F}$ and $D\mathbf{H}$ are the Jacobians of the vector field and the output function.

Equation (22) is referred to as a variational equation and is often the staring point for stability determinations. This equation is rather complicated since, given an arbitrary coupling G, it can be quite high dimensional. However, we can simplified the problem by noticing that the arbitrary state δx_i can be written as $\delta x_i = \sum_{i=1}^{N} \mathbf{v}_i \bigotimes \xi_i(t)$, with $\xi_i(t) = (\xi_{1,i}, \xi_{2,i})$, where the $(\mathbf{v}_i)$ form the set of orthogonal eigenvectors of the matrix G, and which are associated to the real eigenvalues γ_i, respectively, such that $G\mathbf{v}_i = \gamma_i\mathbf{v}_i$ and $\mathbf{v}_i^T\mathbf{v}_i = \delta_{ij}$. By applying $\mathbf{v}_i^T(t)$ to the left side of each term in equation (8) one finally obtains a set of N blocks of equations for the

coefficients $\xi_i(t)$ ($2N$ equations as a total for this specific case example where each dynamical unit has two state variables). The first term with the Kronecker delta remain the same. This results in a variational equation in eigenmode form:

$$\begin{aligned} \dot{\xi}_k &= [D\mathbf{F}(x_s) + K\gamma_k D\mathbf{H}(x_s)]\,\xi_k \ , \\ & k = 0, 1, 2, ..., N-1 \end{aligned} \tag{23}$$

We recall that γ_k is the eigenvalue of G. Also, we note that each equation in (23) corresponds to a set of 2 conditional Lyapunov exponents λ_k^j (j=1,2) along the eigenmode corresponding to the specific eigenvalue γ_k. For $k = 0$, we have the variational equation for the synchronization manifold and its maximum Lyapunov exponent $\lambda_{max} = max(\lambda_0^1, \lambda_0^2)$ is that of the isolated dynamical unit.

The remaining variations ξ_k, k=1,2,...,N-1 are transverse to $\mathcal{M}$, and describe the system's response to small deviations from the synchronization manifold, and then control the stability of the synchronized state. Any deviation from the synchronization manifold will be reflected in the growth of one or more of these variations. We note that the stability of the synchronized state is ensured if arbitrary small transverse variations decay to zero. For $k \neq 0$, equations (23) enable us to calculate the maximum Lyapunov exponent λ_k^{max} of each mode k as the function of the coupling parameter K.

II.6.3 Lyapunov exponents

Here, we consider the Lyapunov exponents [152, 153, 154, 155], which has proven to be the most useful dynamical diagnostic for chaotic systems. Lyapunov exponents are the average exponential rates of divergence or convergence of nearby orbits in phase space. Since nearby orbits correspond to nearly identical states, exponential orbital divergence means that systems whose initial differences we may not be able to resolve will soon behave quite differently, consequently the predictive ability is rapidly lost. Any system containing at least one positive Lyapunov exponent is defined to be chaotic, with the magnitude of the exponent reflecting the time scale on which system dynamics become unpredictable [155].

The method for finding Lyapunov exponents for dynamical systems can be highlighted as follows. Here, we consider a two-dimensional dynamical system with state variables X_n and Y_n.

The linearization of its corresponding map can be written as:

$$\left[\begin{array}{cc} \delta X_{n+1}, & \delta Y_{n+1} \end{array} \right] = J_n \left[\begin{array}{cc} \delta X_n, & \delta Y_n \end{array} \right],$$

where $J_n = J_n(X_n, Y_n)$, is the Jacobi matrix, and X_n and Y_n are the $(n-1)^{st}$ iterates of an arbitrary initial condition (X_1, Y_1). An orthonormal frame of principal axis vectors such as $((0,1),(1,0))$ is evolved by applying the product Jacobian to each vector. For either vector, the operation may be written as the multiplication of the latest Jacobi matrix with each current axis vector, which is the initial vector multiplied by all previous Jacobi matrices. For example, for the vector $(0, l)$, by regrouping the terms, we have:

$$\left[\begin{array}{cc} \delta X_n, & \delta Y_n \end{array} \right] = J_{n-1} J_{n-2} ..... J_1 \left[\begin{array}{cc} 0, & 1 \end{array} \right].$$

The magnitude of each current axis vector diverges, and the angular separation between the two vectors goes to zero (decreases). We locate the nearest neighbor (in the Euclidean sense) of the evolving point with respect to the corresponding point on the fiducial trajectory and denote the distance between these two points by $L(t_o)$. At a later time t_1, the initial length will have evolved to length $L'(t_1)$. The length element is propagated through the attractor for a time short enough so that only small scale attractor structure is likely to be examined. If the evolution time is too large, we may see L' shrink as the two trajectories which define it pass through a folding region of the attractor. This would lead to an underestimation of λ_1 , the largest Lyapunov exponent. We now look for a new data point that satisfies two criteria reasonably well: its separation, $L(t_1)$, from the evolved fiducial point is small, and the angular separation between the evolved and replacement elements is small. If an adequate replacement point cannot be found, we retain the points that were being used. This procedure is repeated until the fiducial trajectory has evolved for a sufficiently large time, after which we estimate:

$$\lambda_1 \quad = \quad \frac{1}{t_M - t_o} \sum_{k=1}^{M} \log_2 \frac{L^{'}(t_k)}{L(t_{k-1})} \ , \tag{24}$$

where M is the total number of replacement steps. In the fixed evolution time procedure, the

time step $\Delta = t_{k+1} - t_k$ between replacements is held constant.

II.6.4 Conditional Lyapunov function approach

The Lyapunov stability method specialized for the linear time invariant systems has more theoretical importance than practical value and can be used to derive and prove other stability results. The calculation of the Lyapunov function for ordinary differential equations is usually very difficult to obtain. For the purpose of this work, we use the conditional Lyapunov function approach. It consists in looking for the Lyapunov function of the variational equations for synchronization stability. We define the Lyapunov function L as:

$$L = \varepsilon^2 + \eta^2 + \rho^2 \ , \tag{25}$$

computed from a mathematical model of the system dynamics in the synchronization manifold and the variational equations. The variables ε, η and ρ represent the dynamics transverse to the synchronization manifold. The function L is equal to the square of the distance between the trajectory and the synchronized state for small distances. Following the Lyapunov stability criterium, a sufficient condition that all perturbations decay to the manifold without any transient growth is given by $\frac{dL}{dt} \leq 0$. This condition can be used to quickly estimate the range of coupling strengths that result in high-quality, burst-free synchronization of coupled nonlinear systems. To do so, we define:

$$L_\varepsilon = 2\varepsilon\dot{\varepsilon} \ \ , \ \ L_\eta = 2\eta\dot{\eta} \ \ \text{, and} \ \ L_\rho = 2\rho\dot{\rho} \ , \tag{26}$$

characterizing the evaluation of the rate of change of the Lyapunov function along the principal directions of the phase space of the transverse dynamics. The time derivative of the Lyapunov function L is thus given by:

$$\frac{dL}{dt} = L_\varepsilon + L_\eta + L_\rho \ . \tag{27}$$

This parameter LT is evaluated as the coupling setting varies. The range of values of the coupling parameter corresponding to high quality synchronization, is obtained for LT strictly negative. The consequence being that the synchronization manifold is completely stable.

II.6.5 Pattern formation: System normalization

The condition to obtain Turing instability in our coupled system via linear stability analysis is to first of all normalize the system. Let us keep in mind that the dynamics observed at the level of one cell is called the local dynamics, provided by the local model (or single cell model). In this local model, all terms of motion, that is all terms of diffusion, are neglected; whereas, only terms describing the cells dynamics in a point of the spatial domain are taken into account [65]. Next, assuming the existence of an equilibrium state with positive values for each substrate in the local model, namely (U_s, V_s, W_s), and considering periodic boundary conditions for equations (14), then the spatially constant function:

$$U(\overrightarrow{z}) = U_s \quad , \quad V(\overrightarrow{z}) = V_s \quad , \quad W(\overrightarrow{z}) = W_s \quad ,$$

(where $\overrightarrow{z}$ represents a spatial location or position) constitutes an equilibrium state for the system. Making use of this steady state, we can perform a normalization of variables as:

$$\begin{aligned} u(\overrightarrow{z},\tau) &= \frac{U(\overrightarrow{z},\tau)}{U_s} \ , \\ v(\overrightarrow{z},\tau) &= \frac{V(\overrightarrow{z},\tau)}{V_s} \ , \\ w(\overrightarrow{z},\tau) &= \frac{W(\overrightarrow{z},\tau)}{W_s} \ , \end{aligned} \tag{28}$$

and the normalized functions are given by:

$$\begin{aligned} f(w) &= \frac{F(W_s w)}{F(W_s)} \ , \\ g(v,w) &= \frac{G(V_s v, W_s w)}{G(V_s, W_s)} \ . \end{aligned} \tag{29}$$

Substituting the sets of formulae (28) and (29) into equations (14), and making use of the fact

that:

$$F(W_s) = kU_s \ , \ G(V_s, W_s) = U_s \ , \text{and} \ G(V_s, W_s) = qW_s \ , \tag{30}$$

conditions which hold in the spatially homogeneous steady state, we get:

$$\begin{aligned} \frac{\partial u}{\partial \tau} &= k(f(w) - u) + D_u \nabla^2 u \ , \\ \frac{\partial v}{\partial \tau} &= \alpha_v (u - g(v, w)) + D_v \nabla^2 v \ , \\ \frac{\partial w}{\partial \tau} &= q(g(v, w) - w) + D_w \nabla^2 w \ , \end{aligned} \tag{31}$$

where $\alpha_v = \frac{G(V_s, W_s)}{V_s}$.

Subsequently, by the means of time and space normalization, we get from the set of equations (31), the transformation $(\tau, \overrightarrow{z}) \rightarrow (t, \overrightarrow{X})$, yielding the normalized system:

$$\begin{aligned} \frac{\partial u}{\partial t} &= f(w) - u + \nabla^2 u \ , \\ \frac{\partial v}{\partial t} &= \rho_{rv} (u - g(v, w)) + \rho_{dv} \nabla^2 v \ , \\ \frac{\partial w}{\partial t} &= \rho_{rw} (g(v, w) - w) + \rho_{dw} \nabla^2 w \ , \end{aligned} \tag{32}$$

where $t = k\tau$, $\overrightarrow{X} = \sqrt{\frac{k}{D_u}} \overrightarrow{z}$, $\rho_{rv} = \frac{\alpha_v}{k}$, $\rho_{dv} = \frac{D_v}{D_u}$, $\rho_{rw} = \frac{q}{k}$ and $\rho_{dw} = \frac{D_w}{D_u}$.

$\overrightarrow{X} = (x, y)$ is the two-dimensional position of a cell with spatial coordinates x and y.

Thus, following this transformation, the system of equations (32) is a normalized set which admits the spatially homogeneous state:

$$u_s(x,y) = 1 \ \ , \ \ v_s(x,y) = 1 \ \ , \ \ w_s(x,y) = 1 \ , \tag{33}$$

as its equilibrium state.

II.7 Numerical methods

II.7.1 Fourth-order Runge-Kutta scheme

Initially designed by Runge in 1894, then improved by Kutta in 1901, it is a computational method of integration based on Trapeze and Simpson integration scheme.

Assuming a first order ordinary differential equation of the form:

$$\frac{dy}{dx} \ = \ f(x,y) \ . \tag{34}$$

The aim is to find the exact value $\overline{y}$ of y that corresponds to $x = x_0 + h$, assuming we know the value $y = y_0$ at x_0, and where h is a discretization (mesh or grid) step in the domain of existence of the variable x. In some cases, such an issue can be addressed by means of analytical and classical methods such as the method of separation of variables, the integrating factor, Laplace transforms, to name just a few. When no analytical method can enable us to calculate the general solution of the equation, there is then a need to use numerical methods in order to estimate the desired solution.

Integrating equation (34), we get:

$$\overline{y} \ = \ y_0 + \int_{x_0}^{x} f(x,y)dx \ . \tag{35}$$

We then get:

$$\overline{y} \;=\; y_0 + \int_{x_0}^{x_0+h} f(x,y)dx \;. \tag{36}$$

It is at this stage that the fourth-order Runge-Kutta ($RK4$) scheme intervene in order to assess numerically the value of the above integral. Its iterative scheme reads:

$$y_{k+1} \;=\; y_k + \frac{1}{6}(L_1 + 2L_2 + 2L_3 + L_4) \;, \tag{37}$$

with:

$$\begin{aligned} L_1 &= hf(x_k, y_k) \;; \\ L_2 &= hf(x_k + \frac{h}{2}, y_k + \frac{L_1}{2}) \;; \\ L_3 &= hf(x_k + \frac{h}{2}, y_k + \frac{L_2}{2}) \;; \\ L_4 &= hf(x_k + h, y_k + L_3) \;. \end{aligned} \tag{38}$$

Several other Runge-Kutta schemes exist but the fourth-order Runge-Kutta scheme is the most popular of all.

II.7.2 Newton-Raphson scheme (or tangent method)

Even though this method has been given by Raphson in 1698, Newton formulated a similar method some months before him. A unified scheme has then been elaborated in 1960 under the name Newton-Raphson method for the resolution of nonlinear algebraic equations of the form:

$$f(x) \;=\; 0 \;.$$

It consists in taking first a coarsely chosen solution x_0, referred to as the zeroth order approximation of the solution. In the eventuality of a physical problem, such a solution may be suggested by the physical meaning of the issue at hand, or by a suggesting curve. Generally, we

define an interval $[a, b]$, such that x_0 lies in it. If $\overline{x} = x_0 + h$ is the sought solution, then, based on the Taylor series expansion of $f(x)$ in the vicinity of x_0, we can obtain a first order approximation of the solution $\overline{x}$, by means of the Newton-Raphson scheme as:

$$\begin{aligned} \overline{x} &= x_1 \ , \\ &= x_0 - \frac{f(x_0)}{f^{'}(x_0)} \ . \end{aligned} \tag{39}$$

For successive approximations, the general scheme reads:

$$x_{n+1} = x_n - \frac{f(x_n)}{f^{'}(x_n)} \ , \tag{40}$$

where $f^{'}(x)$ is the derivative of the function $f(x)$ with respect to x.

It is keynote that when $f(x_0)f^{''}(x_0) > 0$, then, the sequence in equation (40) is monotonous, bounded and converges towards the exact solution $\overline{x}$. In case there is no convergence, it is advised to change the initial guess value x_0 of the solution.

II.7.3 Dichotomy scheme or bisection method

This is an alternative method for the resolution of nonlinear algebraic equations. Let us assume that $f(a) < 0 < f(b)$, and $f(x)$ is strictly increasing on the interval $[a, b]$.

The solution x_0 of the equation $f(x) = 0$, belongs to $[a, b]$. The middle of the interval is $d = \frac{a+b}{2}$. If $f(a)$ and $f(d)$ have opposite signs, then $x_0 \epsilon [a, d]$. If instead $f(b)$ and $f(d)$ have opposite signs, then $x_0 \epsilon [d, b]$. In either case, the size of the interval reduces by half of its initial size. A new bisection is then performed on the new interval containing the bisecting element, and so on. Thus, after n steps, if the interval size which is now $\frac{b-a}{2^n}$ has become small enough, we can then capture the sought solution with a given degree of accuracy.

II.8 Conclusion

In this chapter, we have presented and described some mathematical models, alongside with some analytical and numerical methods used in the survey of the dynamics, both local and collective, of cells with activator-inhibitor pathways. The described analytical methods include the variational approach and the linear stability analysis. We have shown that the variational approach allows us to construct a master stability function for synchronized coupled systems, providing a stability criterion for the synchronous solutions. The linear stability analysis presented here helps in investigating the stability of the equilibrium states of the systems, both coupled and uncoupled. The results obtained with the analytical methods need to be compared to those found through numerical simulations of the original equations. Numerical solutions can be constructed by means of different computational schemes. We have outlined some numerical methods for ordinary differential equations and nonlinear algebraic equations. They include the fourth-order Runge-Kutta, Newton-Raphson and dichotomy schemes.

In the following, we will apply the aforesaid methods in order to examine some relevant phenomena such as the advent of synchronized dynamics and patterns generation settings in pathway networks, in response to the different previously highlighted signalling schemes and network topologies, crucial for cells communication and pertaining in the smooth development of biological organisms.

CHAPTER III

RESULTS AND DISCUSSION

III.1 Introduction

There is a remarkable diversity as well as similarity in functions, behavior and processes across all species of life. All biological systems are composed of the same type of molecules and have similar organizations at the cellular level. Although biologists still rely on experiments to make sense of the way cells function and evolve, they now recognize that mathematical and theoretical methods can provide powerful tools for systems wide studies. In the previous chapter, we have expounded some of these techniques, both analytically-wise and computationally-wise, and ascertained their relevance in the present context. Indeed, their importance can't be overstated. Therefore, this chapter is fully dedicated to the presentation and discussion of the main outcomes of our inquiries, by means of the applications of the aforementioned methods in probing the spatiotemporal dynamical features of arrays of cells with activator-inhibitor pathways. Synchronization and patterns generation in metabolic ensembles are crucial for cellular communication and tissues development. Hence, investigating the requirements for the occurrences of such physical phenomena in biochemical pathway arrays is then the hub of this research work.

III.2 Single cell and its dynamics

III.2.1 Fixed points and their stability

In order to analyze the linear stability of the system, we start by finding the fixed points of the system (7). The fixed points are obtained by setting $\frac{dx}{dt} = \frac{dy}{dt} = \frac{dz}{dt} = 0$. These conditions can be rewritten as

$$\begin{cases} z^5 + z - \frac{1}{kq} = 0, \\ x = qz, \\ x[L + (1+y)^2(1+z)^2] - Ty(1+y)(1+z)^2 = 0. \end{cases} \tag{41}$$

From the following, the fixed points are obtained whenever the three equations in (41) are satisfied. However, it is not possible to obtain analytical solution for this system. We thus proceed by solving numerically the first equation of the system using the Newton Raphson's algorithm. Substituting this solution into the two other one, we obtain the fixed point solution (x_0, y_0, z_0). A plot of the solutions z_0 with respect to the parameter k and T is presented in figure (16).

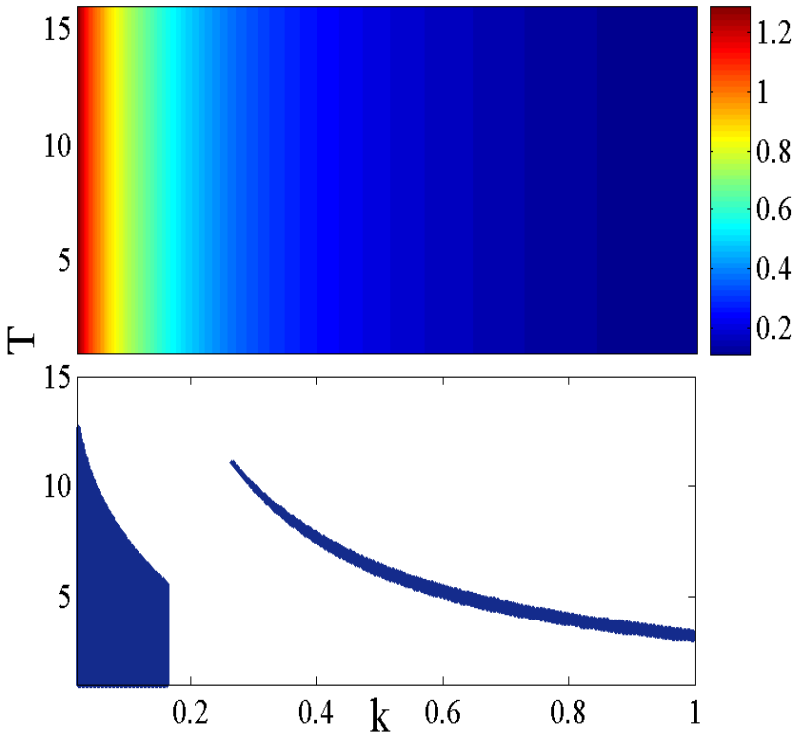

Figure 16: *Fixed points obtained as a function of the rate of degradation of the first substrate k. The other parameters are as in figure for $T = 10$.*

It is seen from this figure that the larger value of the concentration of the end product are obtained for very low value of the rate of degradation of the first substrate k. Meanwhile the maximum velocity of the enzyme plays a little role.

We wish now to study the stability of the fixed points that are inherent in the dynamics of the cell. To investigate for the stability of the cell's dynamics in these fixed states defined by the normalized concentrations of the end-product z_0. In the vicinity of the solution (x_0, y_0, z_0), we perform a first order Taylor expansion of equations (7) making use of the transformation $x = x_0 + u$, $y = y_0 + v$ and $z = z_0 + w$, where u, v and w are small perturbations produced on the fixed states. These states are stable if and only if the variables u, v and w remain bounded as

time goes on. The linear analysis approach performed on this study case leads to an eigenvalue problem whose characteristic equation is given by:

$$\begin{aligned} &\lambda^3 + (k + q - G_{y_0} - G_{z_0})\lambda^2 \\ &+[k(q - G_{y_0} - G_{z_0}) - qG_{y_0}]\lambda \\ &-G_{y_0}(kq - F_{z_0}) \quad = \quad 0. \end{aligned} \tag{42}$$

The fixed points are stable when all the eigenvalues obtained from the characteristic equation are of negative real part, that is according to the Routh-Hurwitz conditions:

$$\begin{cases} -G_{y_0}(kq - F_{z_0}) > 0, \\ (k + q - G_{y_0} - G_{z_0}) > 0, \\ (k + q - G_{y_0} - G_{z_0})[k(q - G_{y_0} - G_{z_0}) - qG_{y_0}] - G_{y_0}(kq - F_{z_0}) > 0. \end{cases} \tag{43}$$

The stability maps is depicted in Figure (16.b). The darker regions correspond to the stable domains. One can particularly notice that when the maximum velocity of the enzyme T is greater than 12.6, no fixed point is stable, this, irrespective of the value of the rate of degradation of the first substrate k. It is also notice that the lower values of k favor the existence of more stable fixed points to the system.

III.2.2 Complex chaotic dynamics

Deterministic chaos has attracted widespread interest in the physical and biological sciences over the past two decades. It represents one of the three fundamental classes of dynamical behavior (stationary, periodic, and chaotic) and, hence, is of central importance in characterizing dynamical systems. The variety of behavior exhibited by this system, under different conditions, were explored in [11, 34, 107]. They includes steady state, simple limit cycle oscillations, complex oscillations and period bifurcations leading to random oscillations or chaos. The system also shows the existence of two distinct limit cycles (bi-rhythmicity), as well as chaotic regimes under the variation of a single parameter.

Although chaos is usually studied in biochemical systems, several recent investigations have demonstrated that transient chaos may occur in closed biochemical systems, where the changing

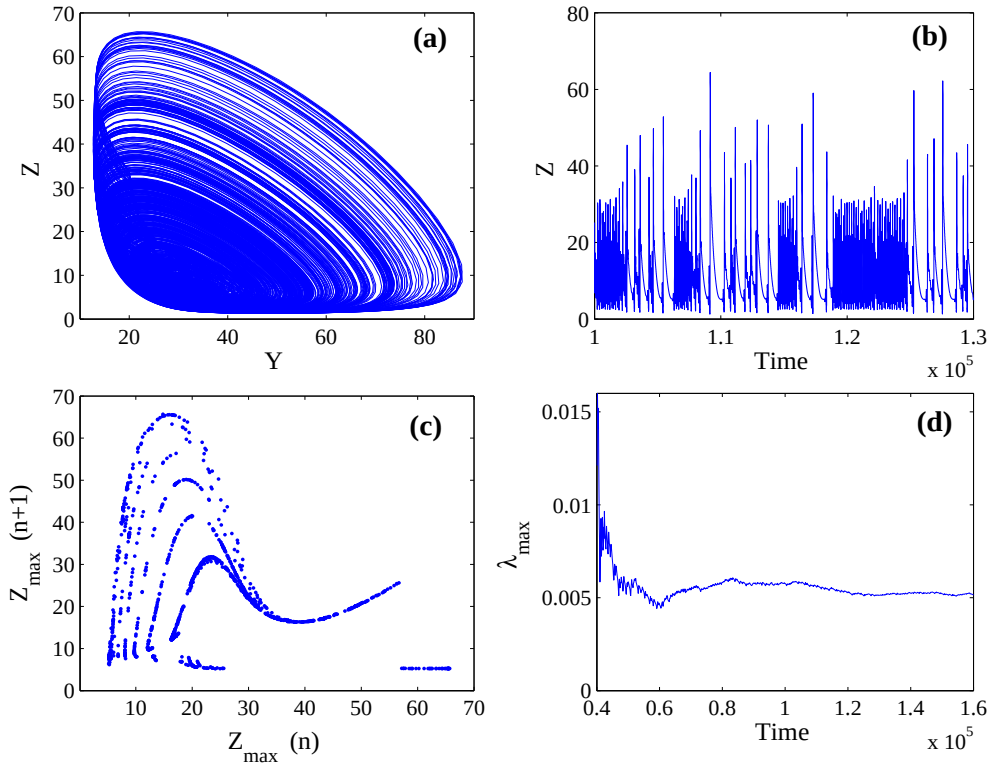

Figure 17: *Single cell dynamics: (a): (y,z) phase portrait, (b): time series, (c): return map and (d): maximum Lyapunov exponent.*

composition of the system, as reactants are consumed, serves as the bifurcation parameter [14, 15, 136]. Following these results, this section focus on chaos and associated complex periodic oscillations found in the biochemical systems as the rate of degradation of the first substrate and the maximum velocity of the enzyme change.

For parameters $k = 0.003$, $q = 0.1$, the pathway exhibits chaotic oscillations. Fig. 17 shows various aspects of the chaotic behavior in a single cell.

The $(y - z)$ phase portrait in Fig. 17 (a), and the time series of z in Fig. 17 (b) clearly show that the oscillations of multiple time scales are associated with the chaotic state of the cell. Earlier studies [107] have shown that there are more than one overlapping attractors that exhibit period-doubling to chaos in this system. The multilayered structure of the return map in Fig. 17 (c), constructed from the successive maxima of z, shows evidence of homoclinic chaos [163]. The Lyapunov exponent in Fig. 17 (d) constructed from the time series of z shows divergence between initially infinitesimally close orbits, symptomatic of sensitivity to initial conditions. At this stage, we have ascertained the complex biochemical rhythms exhibited by the aforementioned

pathway under different biochemical assumptions based on simple models.

The dynamical behavior of nonlinear systems can be quantified by the Lyapunov exponents spectrum, since the exponent values measure the divergence (or convergence) rates of trajectories in the directions of the flow. For our continuous-time three-dimensional nonlinear systems, for example, the Lyapunov exponents spectrum has three values, and the dynamical behavior can be described analyzing the exponent signs. In general, with one positive exponent, one null, and the third negative the system's behavior is chaotic. With the largest exponent of the Lyapunov exponent spectrum, we have constructed a colorful Lyapunov exponent diagram, varying simultaneously two parameters of the system and keeping fixed the other parameters, to study its complex behavior. The corresponding diagram is shown in Fig. 18. One notices the abundance of chaotic dynamics in the system for low value of k and as the values of k increase, periodicity regions increase. Larger values of T favor the presence of chaotic motion in the system. In order to gain more insight into the dynamics of the system, we will examine two bifurcation diagrams following this parameter space. The first one using the maximum velocity of the enzyme T as the bifurcation parameter and the second using k.

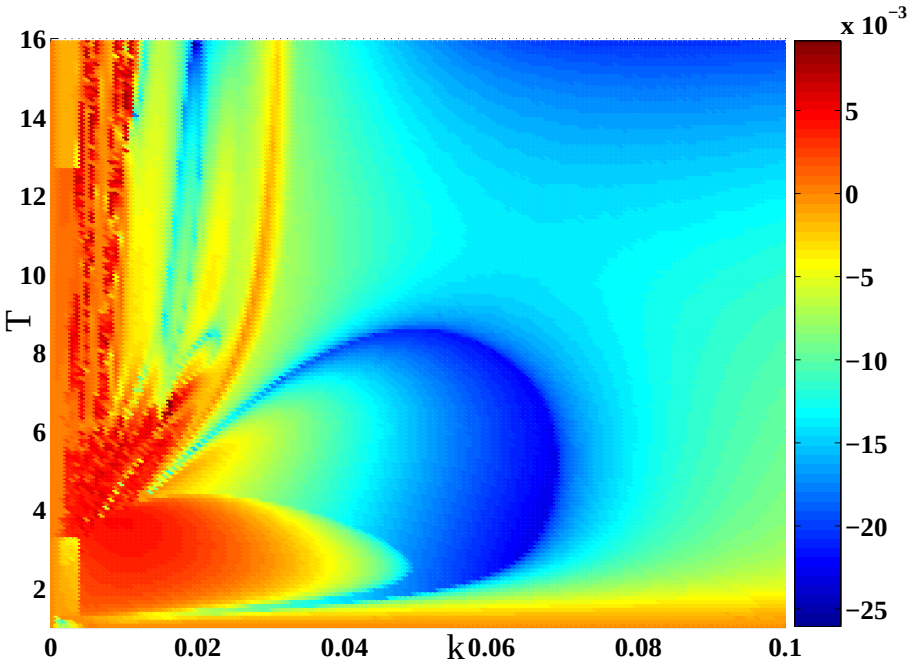

Figure 18: *The Lyapunov diagrams of system (7), showing periodic regions in black (blue) and chaotic region gray (red) as functions of the maximum velocity of the enzyme T and the rate of degradation of the first substrate k. The other parameter been fixed as $L = 10^6$ and $q = 0.1$.*

The bifurcation diagram of Fig. 19 (a) presents the evolution of the concentration of the

substrate as a function of the maximum velocity of the enzyme. z_{max} stands for the maximal amplitude of oscillation attained by the normalized concentration in end-product dynamics in the single cell. The first observation is that the maximum velocity of the enzyme should be greater than 1, in order to observe oscillations in the biochemical system. This has never been discussed before concerning this biochemical system. The phenomenon observed here, common in biological systems, is similar to the one observed in biological neuron, where a minimum initial excitation current of $I \approx 1.37$ is required to set the Hindmarsh-Rose neuron into an active state [69]. As T increases beyond 1, the system reaches periodic oscillations and remains periodic although the oscillations can exhibit several bursts in their time series over a period. Further increase of the maximum velocity of the enzyme T abruptly takes the system to a chaotic domain at $T \approx 3.3$. Furthermore, one observes bands of chaotic and periodic motions succeeding to each other alternatively. Most importantly, the system falls into two different attractors when T reaches the value of 8.26, one chaotic and the other periodic. At this level, one can guess that the presence of these two attractors will be determined with the initial condition of the system. This could also explain the bi-stability between two oscillatory states, a phenomenon that is often seen in systems of coupled oscillators. Many forms of multi-stability occurring in biochemical systems have been reported earlier [34, 136, 137]. Beyond the value $T \approx 11.2$, follows an inverse period doubling cascade, interrupted by a small chaotic window, and leading to a sequence of periodic orbits. This result is supported by the Lyapunov exponent curve shown in Fig. 19 (b), right below the bifurcation diagram.

The bifurcation diagram of Fig. (20) is plotted as the rate of the degradation of the first substrate (k) changes. It is observed from the bifurcation diagram and the corresponding Largest Lyapunov exponent in Fig. 20 (a) and Fig. 20 (b), respectively, that the system follows a backward bifurcation to move from pronounced chaotic dynamics to periodic dynamics as k increases. We should remind ourselves that the rate of degradation of the first substrate has been found to play an important role in the existence of chaotic and bi-rhythmic behavior in the model of cells with activator-inhibitor pathways [34]. We should also recall that bi-rhythmicity is a situation where for the same parameter value, the system possesses two types of rhythmic behavior different significantly in period and amplitude and taking place around different mean substrate levels. Each stable limit cycle possesses its own basin of attraction, defined as the set of initial conditions from which the system evolves to the particular periodic solution [14].

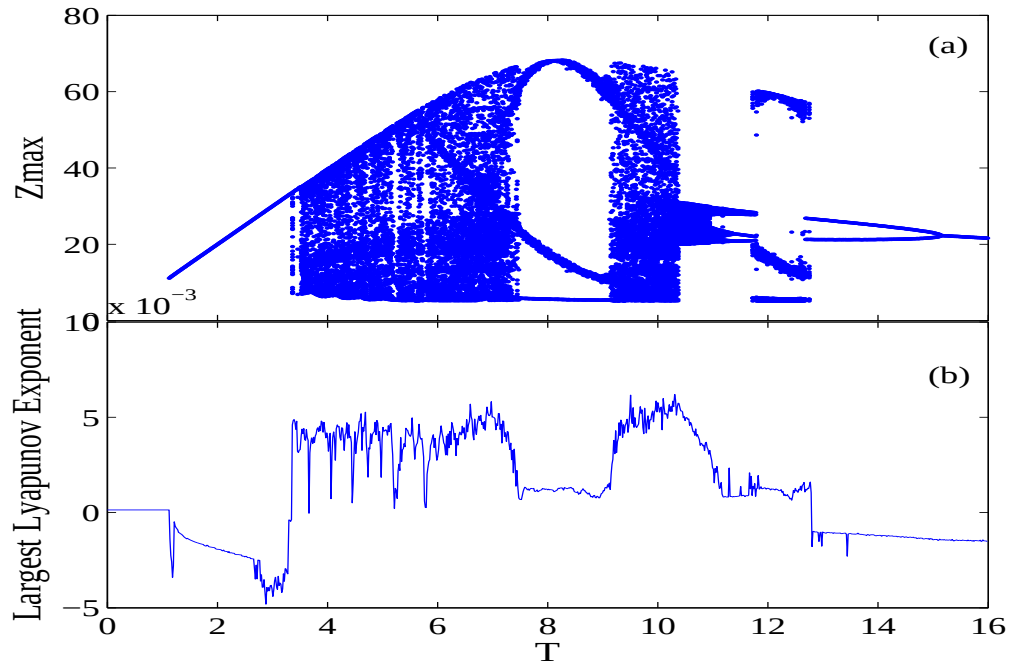

Figure 19: *Bifurcation diagram (a) and Largest Lyapunov exponent (b) describing the dynamics of the system as a function of the maximum velocity of the enzyme T for $k = 0.003$, $L = 10^6$ and $q = 0.1$.*

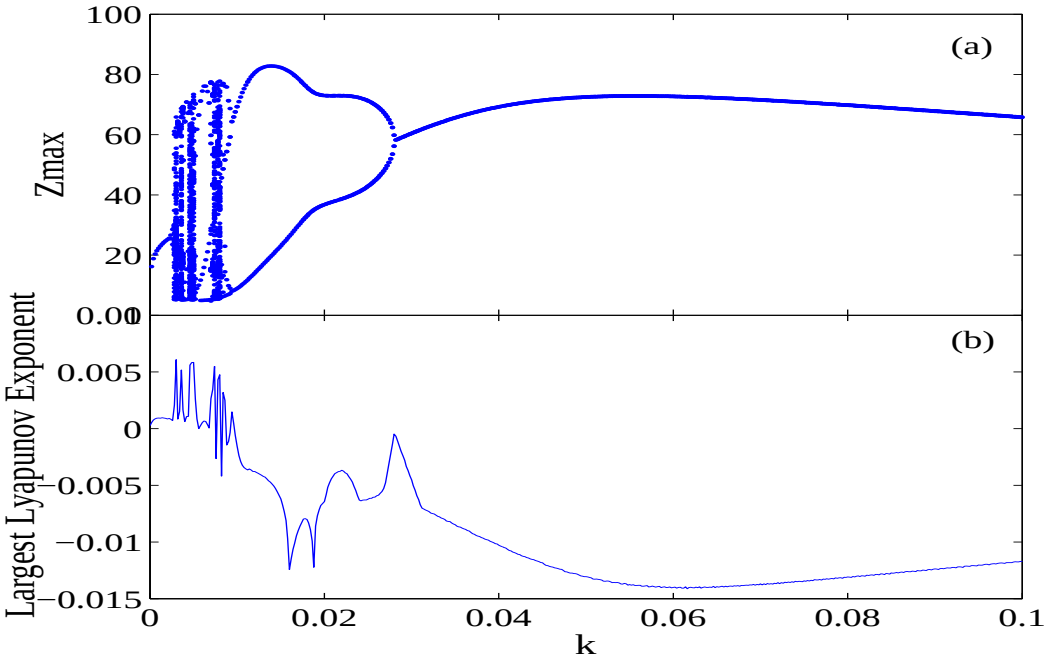

Figure 20: *Bifurcation diagram (a) and Largest Lyapunov exponent (b) describing the dynamics of the system as a function of the rate of degradation of the first substrate k. The other parameters are as in Fig. 16 for $T = 10$.*

III.3 Chemically coupled cells: Synchronization

III.3.1 Stability of the synchronous cells

The stability analysis of the synchronization manifold can predict whether there exists a synchronized solution. In principle, the behavior of the Largest Lyapunov exponent fully determines the linear stability of the synchronized solutions. However, the Lyapunov exponent spectrum evaluation for high dimensional systems is time consuming. More recently, the Master Stability Function (MSF) based on the transverse Lyapunov exponent has been established to be a necessary condition to detect synchronization, enabling us to reduce the dimensionality of the coupled system [20, 21]. The MSF measures the exponential rate at which an infinitesimal perturbation of the synchronization manifold grows. In the present context of dynamical systems, the MSF is the maximum transverse Lyapunov exponent of the synchronization manifold. A necessary condition for stable synchronization in the network is the negativity of the MSF. The MSF approach is appealing because it allows the properties of the local system to be separated from the coupling matrix characterizing the network topology. That is, the MSF can be obtained independent of the network topology even for networks containing a very large number of biochemical systems [20, 21, 22, 23, 24].

The starting point on the study of the synchronization and its stability is the determination of the synchronization manifold, representing the common state of the coupled systems when synchronization is achieved. In this case, the synchronous solution on the synchronization manifold takes the form:

$$\begin{aligned} \frac{dx}{dt} &= F(z) - kx, \\ \frac{dy}{dt} &= x - G(y,z), \\ \frac{dz}{dt} &= G(y,z) - qz - g_s(z - V_{inh})\Gamma(z), \end{aligned} \tag{44}$$

where $F(z)$ and $G(y,z)$ are defined as in Eq. (7). It is observed here that the dynamics of the system changes on the synchronization manifold as the coupling parameter also changes. This is due to the fact that the threshold modulation form of the coupling scheme remains present in the system even when completely synchronized [69, 70, 71].

In order to gain more insight into the dynamics of the system in the synchronization mani-

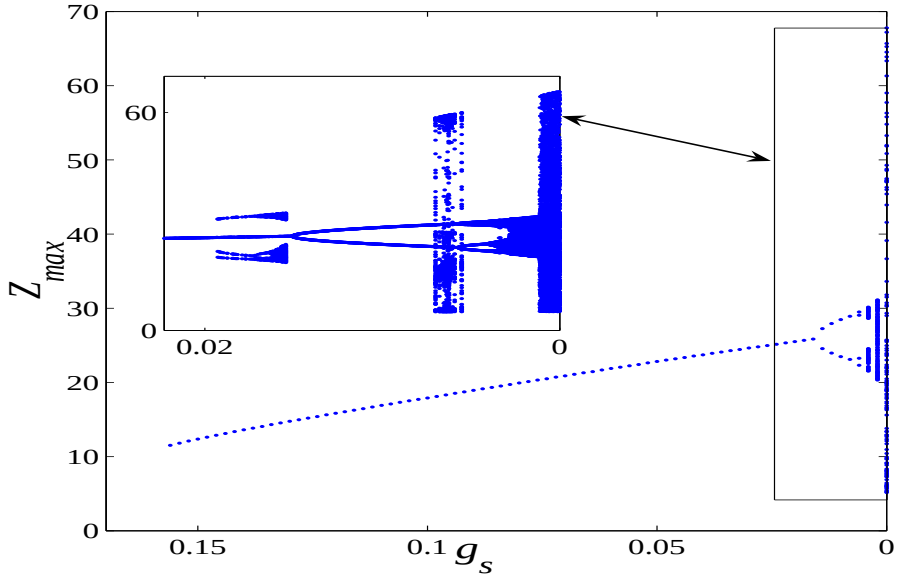

Figure 21: *Reverse bifurcation diagram describing the dynamics of the synchronous solutions of the coupled system as a function of the fast threshold coupling strength g_s, and in the box, a zoom on the bifurcation showing how the system moves from periodic oscillations to pronounced chaotic dynamics, and to periodic regimes through the sequence of period doubling bifurcations as g_s decreases. The parameters are the same as in Fig. 19 for $T = 10$.*

fold, we plotted the bifurcation diagram of the synchronous solutions as the coupling strength changes and it is depicted in Fig. 21, where z_{max} refers to the peaks in amplitude for the oscillations of the normalized concentrations in end-product in each of the cell when they are in a completely synchronized regime. It presents a rich variety of dynamical behaviors ranging from chaotic to periodic dynamics as shown in the figure. This is an interesting feature of the synchronous regime produced by the chemical coupling scheme. We plot a backward bifurcation diagram starting from large values of g_s to smaller values. The road from initially periodic motion to chaotic motion involves successive bifurcations, each undergoing period doubling bifurcation. Each bifurcation occurs increasingly close to a chaotic explosion in the system dynamics, until a point is reached where through another explosive bifurcation, the system undergoes chaotic motion and hence the oscillation is chaotic. This backward bifurcation diagram enables us to recover a classical period doubling scenario observed in most of the dynamical systems. In addition to periodicity obtained for large g_s, we should remind ourselves that the system has lost its extreme sensibility to initial conditions, hence favorable for synchronization.

It is then clear from the bifurcation diagram that the synaptic coupling strength g_s plays a control role over the dynamics of the synchronous state of the cells. As the coupling increases,

the dynamics of the synchronization manifold moves from pronounced chaotic dynamics to a sudden drop in the degree of chaos and then to a periodic state. It is noteworthy that fixed points appear for $g_s > 0.157$.

Assuming the coupled systems in the Master-Slave configuration, further analysis of the stability of the synchronization, is obtained by defining the directions transverse to the synchronization manifold, as: $\varepsilon = x_1 - x_2$, $\eta = y_1 - y_2$, $\rho = z_1 - z_2$. Substituting this into the coupled system Eq. (11), the dynamics of the transverse perturbations to the synchronization manifold of the system are described by:

$$\begin{aligned} \dot{\varepsilon} &= F_z(z)\rho - k\varepsilon, \\ \dot{\eta} &= G_y(y,z)\eta - G_z(y,z)\rho, \\ \dot{\rho} &= G_y(y,z)\eta + G_z(y,z)\rho - q\rho \\ &\quad -g_s\Gamma(x)\rho + g_s(V_{inh} - z)\Gamma_z(z)\rho, \end{aligned} \tag{45}$$

where the functions $F_z(z)$, $G_y(y,z)$and $G_z(y,z)$ and $\Gamma_z(z)$ are given in the Appendix due to their complex form. The complete transverse Lyapunov spectrum related to the above variational equations and characterizing the dynamics transverse to the synchronization manifold, are plotted as a function of the chemical coupling strength, and are depicted in Fig. 22.

Surprisingly, the largest transverse Lyapunov exponent (Fig. 22 (a)) is never negative, implying the absence of complete synchronization in the coupled cells. From the graph, we can see that increasing the strength of the chemical coupling does not decrease the heterogeneity in the coupled cells. However, as the coupling increases, the second transverse Lyapunov exponent crosses completely from positive to negative values (Fig. 22 (b)) showing convergence towards a state of phase synchronization in the coupled biochemical systems. Therefore, even though the complete synchronous regime remains unstable, as the coupling strength increases, both systems progressively stepped into a state of stable phase synchronization at $g_s = 0.0442$.

In conclusion, the inhibitory chemical coupling type used in this work has a pronounced role on the control of the concentration of the biochemical system than facilitating complete synchronization regime into the system. However, the phase synchronization is abundant in the coupled cells with inhibitor - activator pathways. At this stage, we need to stress out the importance of this lastly named type of synchronization, observed among these cells with activator-inhibitor

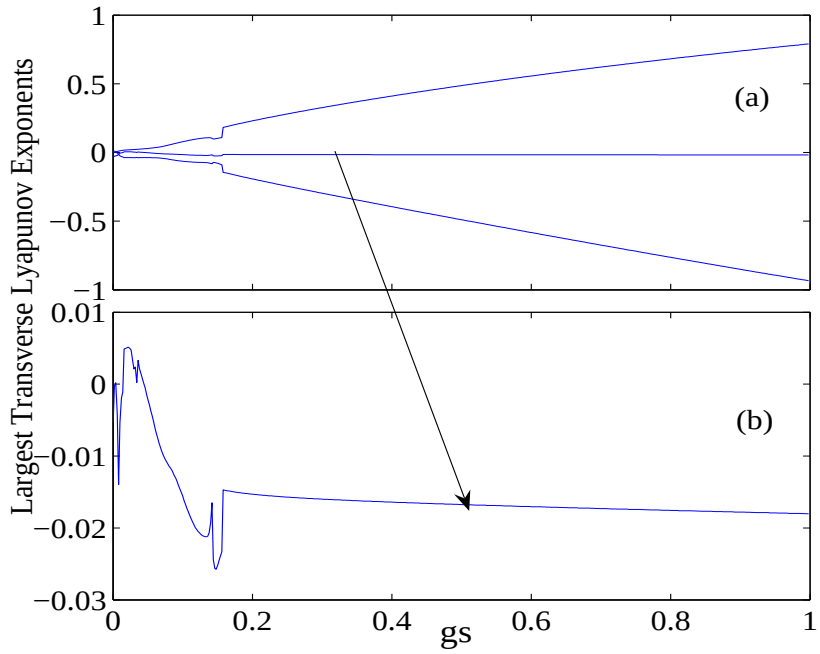

Figure 22: *(a): Master Stability Function based on the Transverse Lyapunov Exponents with respect to the coupling strength* (g_s)*, (b): Second Largest Transverse Lyapunov Exponent. The other parameters are as in Fig. 21.*

pathways, when coupled chemically. The phase synchronization phenomena can be summarized in general as describing coupled systems whose phase difference is bounded, despite the fact that their amplitudes are chaotic. It differs from all other types of synchronization by the remarkable property that it is the first type of synchronization that appears as one increases the coupling strength from zero to a small value different from zero. This has never been considered in the case of cells with activator-inhibitor pathways and will be the subject of the next section.

III.3.2 Phase synchronization

Phase synchronization is the process by which two or more cyclic signals tend to oscillate with a repeating sequence of relative phase angles. Many examples of biological phase synchronization, some of them quite startling, have been documented in the literature, but currently, theoretical understanding of the phenomena lags behind experimental and field-studies. In the present section, phase synchronization is investigated in the context of biochemical systems. Note that phase coherence guarantees that the populations oscillate at almost constant frequency which is characterized by a predominant peak in the power spectrum [138]. The motivation of this comes from the fact that in the preceding section, it has not been possible to observe com-

plete synchronization into the chemically coupled biochemical system studied here. However, from Fig. 22, the weaker kind of synchronization, the phase synchronization was suggested to take place. The approach to detect phase synchronization in this section consists in defining maps, which are a natural extension of the stroboscopic map, to coupled chaotic oscillators, in which the oscillators are observed at special times. Phase synchronization implies the existence of maps of the attractor that appear as localized structures in the accessible phase space. The fact that phase synchronization produces subsets of the attractor that are localized structures, by particular observations was previously used as a way to detect phase synchronization in chaotic oscillators ([139, 138] and references therein). In order to observe the phase synchronization in our case, we used the Poincaré section by defining the stroboscopic map as $z = 10$, with the constrain $\dot{z} > 0$. This is motivated by the extension of the approach of localized map by Pereira *et al.* [139], by demonstrating that localized sets can be constructed while in phase synchronization by means of any typical physical observation.

We illustrate this behavior of localized structure in Fig. 23. For $g_s = 0.00125$, the set is not localized over the attractor of the chemically coupled cells on Fig. 23(a). The set of points which are obtained on the second cell's attractor through the poincaré section of the first cell's attractor spread out over the attractor. Recall that the Poincaré section is defined at $z = 10$, with the constrain $\dot{z} > 0$. Therefore, there is no phase synchronization, i.e., the time series of the phase difference show divergence. The phase difference is not bounded it diverges . Indeed, on Fig.23 (b), the calculation shows that the phase difference increases up to 4000. As we increase the coupling, Phase Synchronization appears. In particular, for $g_s = 0.0025$ and $g_s = 0.005$, the sets of points are localized [on Fig.23 (c) and on Fig.23 (e), respectively]. Hence, the phase difference are bounded [on Fig.23 (d) and on Fig.23(f), respectively]. A close look at the curve of the second largest transverse Lyapunov exponent in Fig. 22 allows us to identify three different parameter regions where phase synchronized dynamics occur. These intervals of values of g_s are: $[1.3\times10^{-4}; 2.6\times10^{-3}]$, $[4.9\times10^{-3}; 1.4\times10^{-2}]$ and $[4.6\times10^{-2}; 1]$. Besides the phase synchronization of the coupled cells with activator-inhibitor pathways, the coupling controls the dynamics of the system as described earlier in the bifurcation diagram of the synchronous solutions. As an illustrative relevant importance to phase synchronization investigated here, it confers positive functional advantages to the organism, including temporal organization, spatial organization, and efficiency for communication between them.

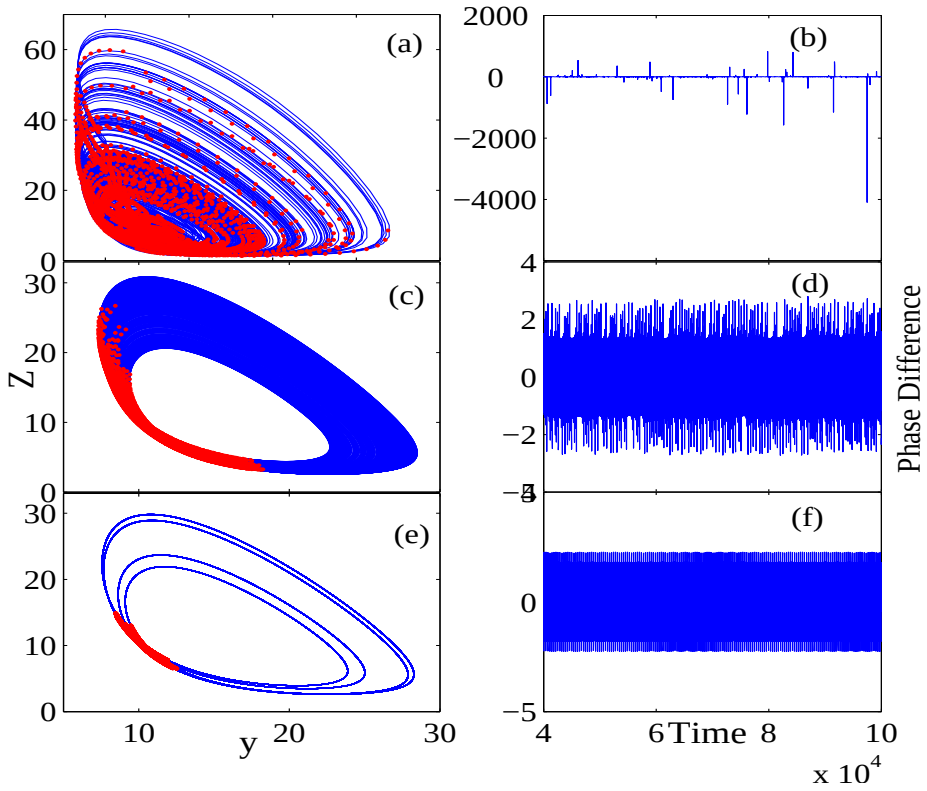

Figure 23: *Onset of phase synchronization in two coupled cells with activator-inhibitor pathways coupled through fast threshold. Figures (a), (c), (e) are the plots of the attractor of the first cell (continue line) and the stroboscopic projection of the attractor of the second cell on the cross section of the first cell (dots), for different values of the coupling strength [the points are localized as the coupling increases, indicating the onset of phase synchronization in the system]. Figures (b), (d), (f) are Time series of the phase difference of the two coupled cells for different values of the coupling. As the coupling increases, the phase difference is bounded, confirming the onset of phase synchronization in the biochemical system.*

III.3.3 Electrically and chemically coupled cells

Following the analysis of the preceding section, it is found that the synchronization manifold is also defined by Eq. (44). On the contrary of the analysis done in that section, electrical coupling does not affect the dynamics of the synchronous solutions.

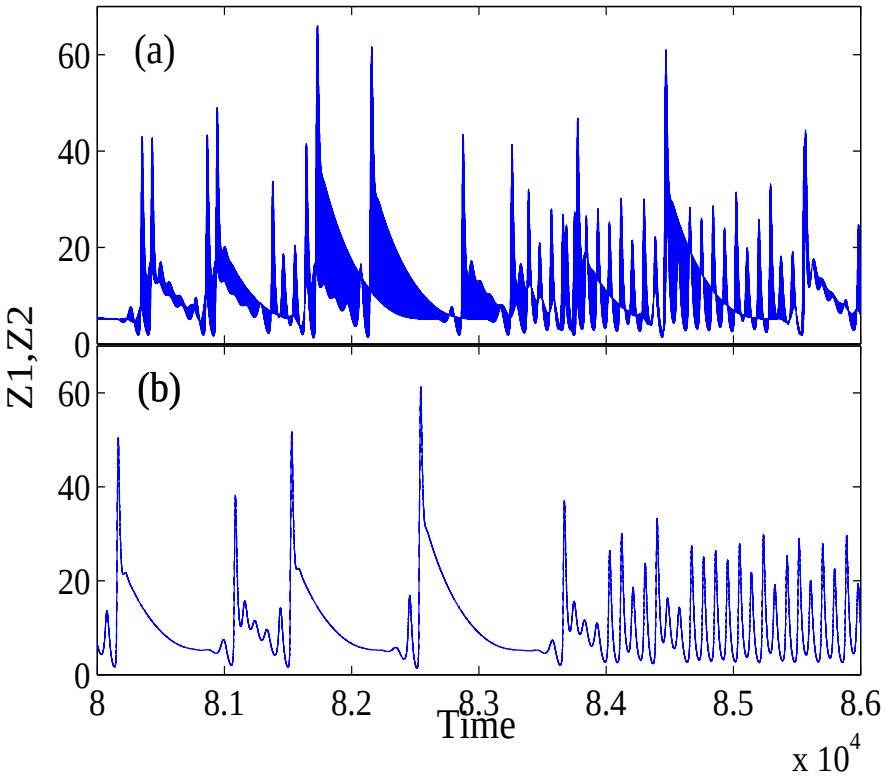

Figure 24: *Time series superposition of the trajectories of the two biochemical systems for* $g_s = 0.0005$*; (a):* $g_l = 0$ *and (b):* $g_l = 0.72$*. When the electrical coupling* g_l *is turned on* 0.72*, the biochemical system behaves in synchrony as a unique entity.*

The dynamics of the system in the synchronous state remains the same as described in the preceding section. However, when we take $g_l = 0.72$, the two coupled cells are always completely synchronized. The time series superposition, of the coupled cells for different values of g_l, and for $g_s = 0.0005$ presented in Fig. 24(a) and Fig. 24(b) attest for that. Following the different dynamical regimes observed on Figure 5 for the bifurcation diagram of the synchronization manifold with respect to g_s, we can reliably display a summary of the different synchronization regimes observed by changing the value of g_s, keeping $g_l = 0.72$, as summarized in Table 1.

The same observations can also be made for smaller value of the electrical coupling strength.

Table 1: *Different synchronization regime after the combine effect of electrical and chemical coupling for* $g_l = 0.72$

$values\ of\ g_s$	$synchronized\ \ dynamics$
$0 \rightarrow 0.004$	chaos
$0.004 \rightarrow 0.007$	period - 4
$0.007 \rightarrow 0.008$	chaos
$0.008 \rightarrow 0.0165$	period - 2
$0.0165 \rightarrow 0.017$	quasi-periodicity
$0.017 \rightarrow 0.0185$	period - 4
$0.0185 \rightarrow 0.157$	period - 1
$0.157 \rightarrow 1$	quiescent state

In the next section, we will perform numerical simulation on the model to gain more information about the role played by each of the two types of coupling. For example, intact yeast cells can synchronize their oscillations with each other. When two equally large populations of yeast cells that oscillate with opposite phases are mixed, they at first seem to extinguish each other. However, in the course of some periods, the amplitude grows again, and eventually, the autonomous oscillation with constant amplitude is reestablished [140]. As reported earlier, this suggests that some oscillating metabolite in coupled cells chain is able to permeate cellular membranes and affects the coupled cells kinetics of neighboring cells. Somehow, chemical and electrical coupling are able to affect the dynamics of the autonomous oscillations of the concentration of the cells, such that eventually all cells oscillate in phase again and on the same limit cycles.

III.3.4 Numerical simulations of the electrically and chemically coupled cells.

The stability of the synchronous solution is checked by plotting the largest transverse Lyapunov exponent (MSF), as function of coupling parameters g_s and g_l. It is seen from the graphs that the largest transverse Lyapunov exponent is negative for some values of the coupling strength, confirming the fact that the cells can completely synchronized. It is therefore clear that the presence of the electrical coupling increases greatly the degree of synchronization even when the synaptic strength is large. For this analysis, we have chosen two values for the maximum velocity of the enzyme, $T = 3.1$ and $T = 10$, respectively, corresponding to the cases of periodic and chaotic dynamics of the single cell pathways. For $T = 3.1$, Fig. 25(a), parameter space indicates that for $g_l > 0.23$, a stable synchronization dynamics is established among the cells since from this value, the $MSF < 0$ for all values of g_s. The simulations are made with the values of g_l and

g_s varying between 0 and 1. Nevertheless, for the values of $g_l < 0.23$, one can have $MSF < 0$, for low values of the chemical coupling g_s, that is between 0.005 and 0.1 only.

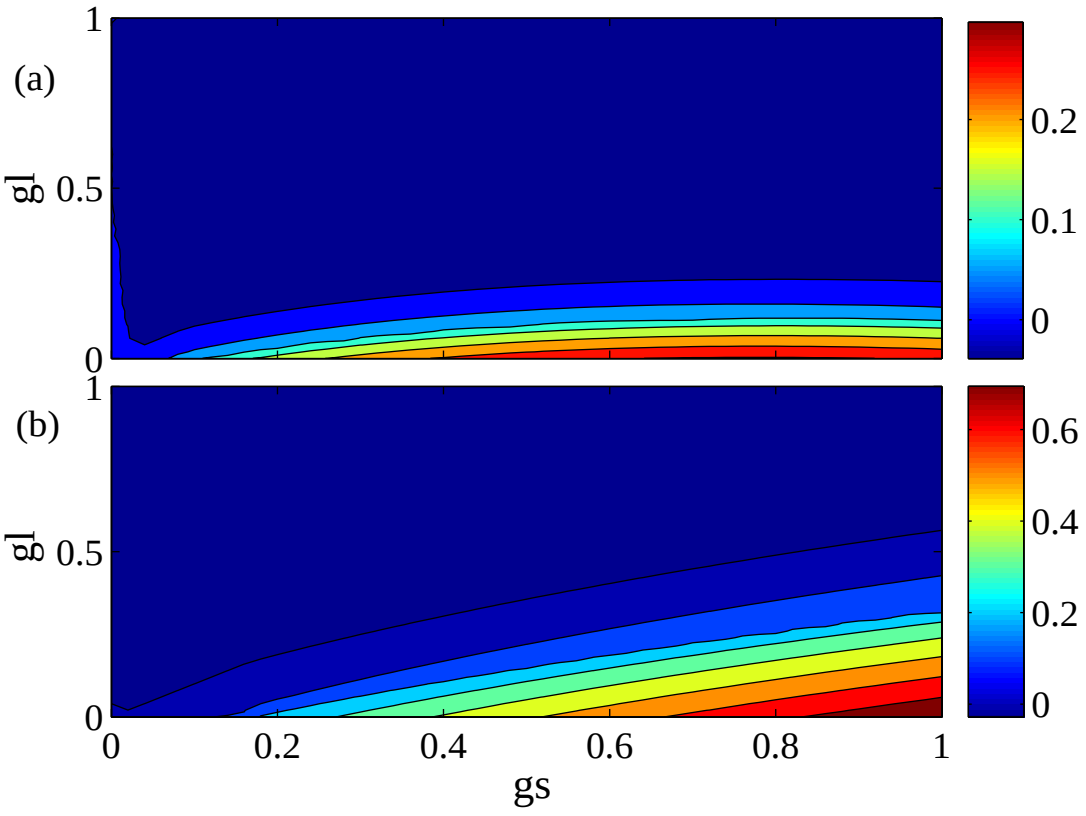

Figure 25: *Two dimensional contour plot of the Master stability function defined by the Largest Lyapunov Exponent as a function of the fast threshold coupling strength g_s and the electrical coupling strength g_l. The parameters are as in Fig. 22 and for two different values of the maximum velocity of the enzyme (a): $T = 3.1$, and (b): $T = 10$.*

On Fig. 25(b), obtained for $T = 10$, we observe the same phenomenon. However, due to the nature of the system at $T = 10$ (chaotic), the value of the electrical coupling should be larger ($g_l > 0.55$) in order to obtain $MSF < 0$ for all g_s, i.e. a stable synchronous regime fostered among the cells. The region of stable synchronous solution is more smaller in this case. Specifically, when $0.1 < g_l < 0.55$, as g_s increases, we move from a region where $MSF < 0$ to a region where $MSF > 0$, showing that in these coupling conditions, when the chemical coupling strength becomes strong enough, it destroys the stability of the manifold. It then requires a large amount of electrical coupling to fully establish a stable synchronization manifold for all the values of g_s. On the contrary of what was observed in Fig. 25(a) for $T = 3.1$ we see that as g_s increases, the region of stable synchronization reduces. In other words, there exists an optimal value of g_l for

each value of g_s, which is the characteristic signature of complete synchronization. Note that the peak position of g_l is shifted to a large value of the coupling strength when g_s is increased. The mechanism can be understood as follows. When the chemical coupling between cells is increased, each cell may be excited by the other even though it may be unable to respond to the external stimulus. They then behave like uncoupled cells with common impute leading to larger dispersions. As a whole, the coherence of the motion in the coupled system is enhanced by the introduction of the electrical coupling between them and if the electrical coupling is stronger, the excited cells become synchronized and behave as a single element. So the larger the chemical coupling strength is the larger the electrical coupling strength needed to be to achieve complete synchronization. The cells with activator inhibitor pathway become completely synchronous to either a limit cycle for large chemical coupling strength or to a chaotic attractor for small chemical coupling strength.

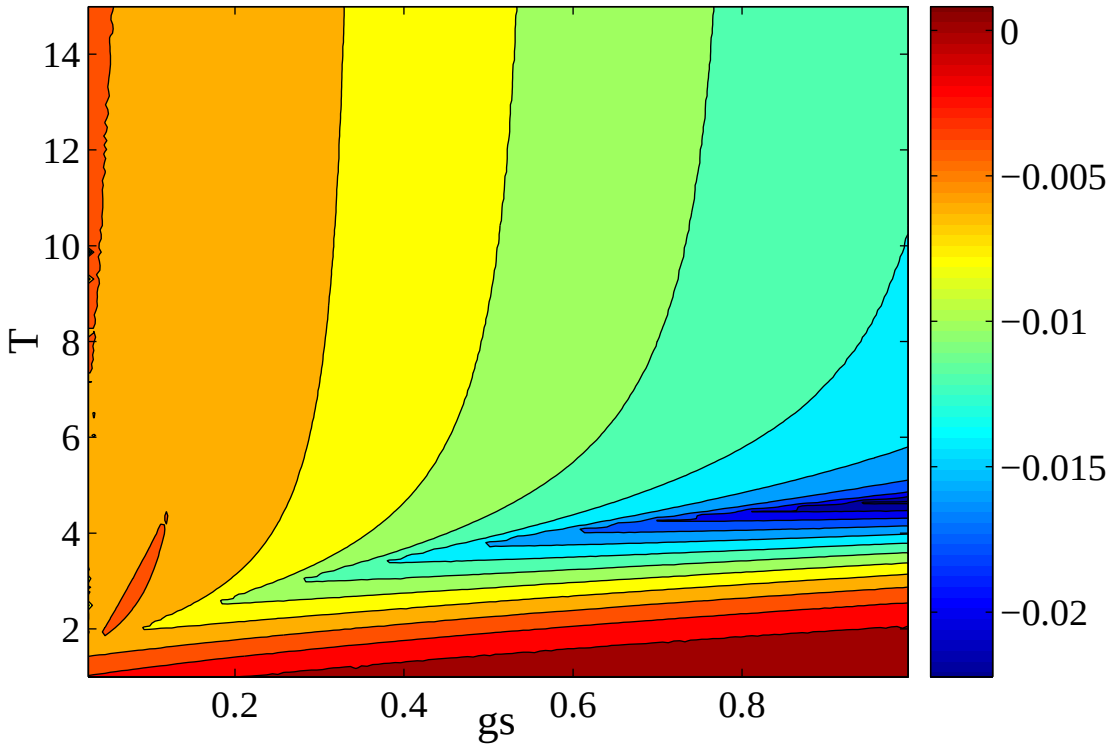

Figure 26: *Two dimensional contour plot of the Master stability function defined by the Largest Lyapunov Exponent as a function of the fast threshold coupling strength g_s and the maximum velocity of the enzyme T. The parameters are as in Fig. 22 and for $g_l = 0.72$.*

The synchronous dynamics of the concentration of the cells with activator-inhibitor path-

ways may strongly depend on the maximum velocity of the enzyme T and the amount of the external chemical input g_s. Therefore, it is important to evaluate the threshold of synchronization for these two parameters and for fixed value of the electrical coupling g_l. The synchronization regions as functions of T and g_s for electrical coupling coefficient fixed at $g_l = 0.72$ is shown in Fig. 26. The system exhibits synchronization in a wide region of the parameter space, as shown in Fig 26. However, for a relatively smaller value of chemical coupling and smaller value of the maximum velocity of the enzyme, the synchronization regimes are not found into the coupled cells. Meanwhile, large value of the two parameters foster synchronization in the coupled cells. Note that large values of the fast threshold coupling type control the dynamics of the system by wiping out effect of heterogeneity created by initial conditions in the coupled system hence favorable for synchronization. Furthermore, the more the amount of the chemical coupling input is, the smaller the range of the maximum velocity of the enzyme for which synchronization can be found.

In summary, two cells with activator-inhibitor pathways do not easily synchronize their dynamics when they are coupled chemically only. However, the interplay of the chemical and electrical couplings tremendously fosters the establishment of the stability and robustness of the synchronization dynamics of both cells. This could be of capital importance in biochemical systems since in metabolic pathway, the fluxes and the concentrations generally depend on the activities and kinetic properties of all of the involved enzymes simultaneously ([140]and references therein).

III.3.5 Detecting coupling range for high quality synchronization

From the previous section, it has been seen that the complete synchronous solution was stable under the combined effect of chemical and electrical coupling. Using the Runge Kutta integration algorithm, we integrate equation (44) and (45) over a very large interval of time, after discarding the transient time, we compute the mean value of the rate of change of the Lyapunov function L and defined by $LT = \left\langle \frac{dL}{dt} \right\rangle$. This parameter LT is evaluated as the coupling strength changes. The range of values of the coupling parameter corresponding to high quality synchronization, are obtain for LT strictly negative. The consequence being that the synchronization manifold is completely stable. The plots of LT with respect to the coupling strength are displayed in the figures Fig. 27 and Fig. 28. In these figures, LT is plotted in the parameters

space, (g_s, g_l) and (g_s, T) to localize the regions for high quality synchronization dynamics of the coupled cells.

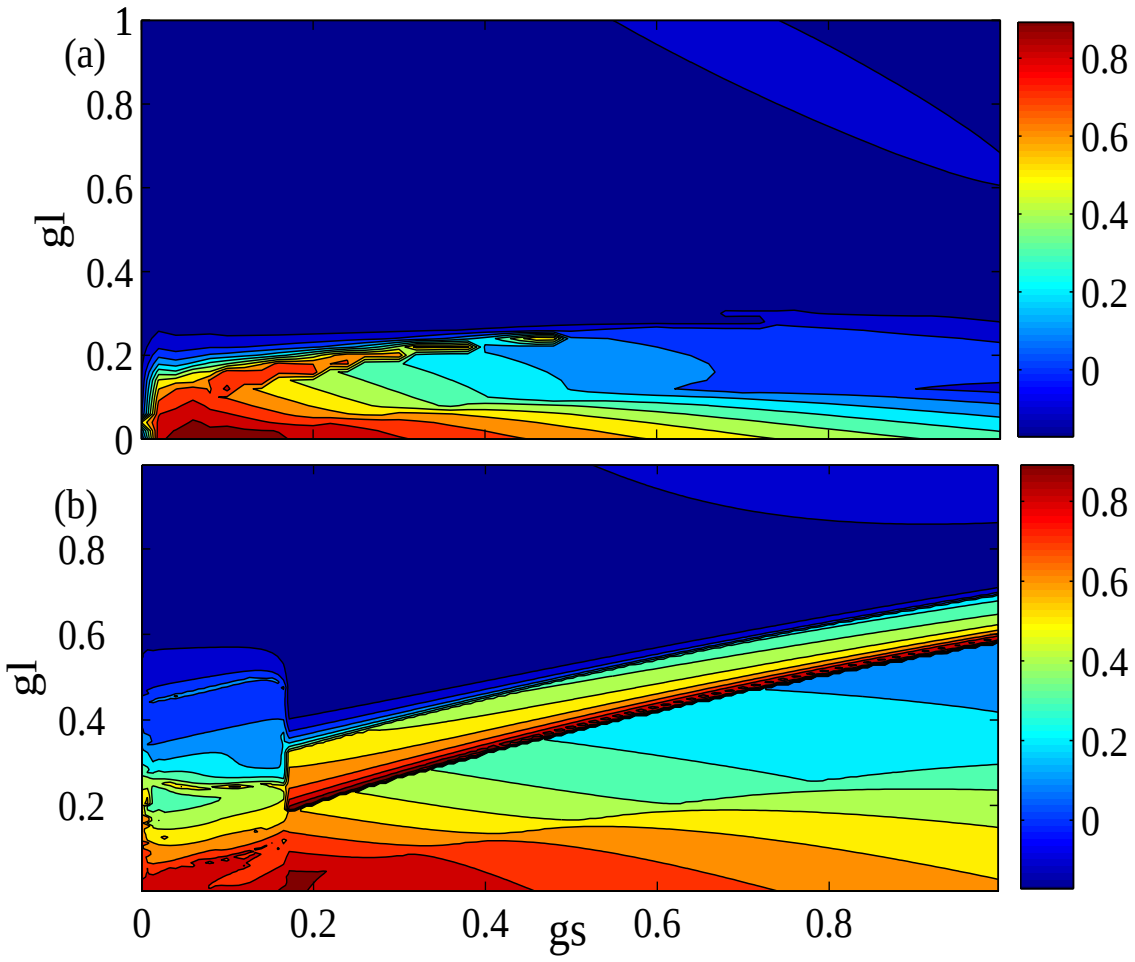

Figure 27: *Stability region for high quality synchronization obtained from numerical simulation of the mean value LT of the rate of change of the Lyapunov function in the parameter space (g_s, g_l) for two different values of the maximum velocity of the enzyme (a): $T = 3.1$ and (b): $T = 10$. The parameter values are the same as that of Fig. 25. The values of the parameters for high quality synchronization are in black (blue).*

The plot of Figs. 27 are reflecting different dynamical regions with the occurrence of robust synchronization in the cells in the parameter space of the two types of coupling (g_s, g_l). The analysis are done for two different values of the maximum velocity of the enzyme T. For $T = 3.1$ (the system is periodic), in Fig. 27(a), the region for high quality synchronization is obtained for any value of g_s when $g_l \geq 0.26$. So, the stable synchronization dynamics detected by the MSF in the preceding section (see Fig. 25) for $g_l > 0.23$ becomes robust when $g_l > 0.26$ for all g_s. So, in the region between $0.23 < g_l < 0.26$, the synchronous dynamics is of low quality and

the error dynamics could just be bounded. A similar observation is made when the maximum velocity of enzyme is $T = 10$. However, the region of robust synchronization is reduced due to the chaotic nature of the system as shown in Fig. 27(b). Also, as g_s increases, the parameter region for the robustness of the stability of the manifold is reduced meanwhile in the previous case, the increase of the coupling g_s was accompanied by an increase of the region for robust synchronization.

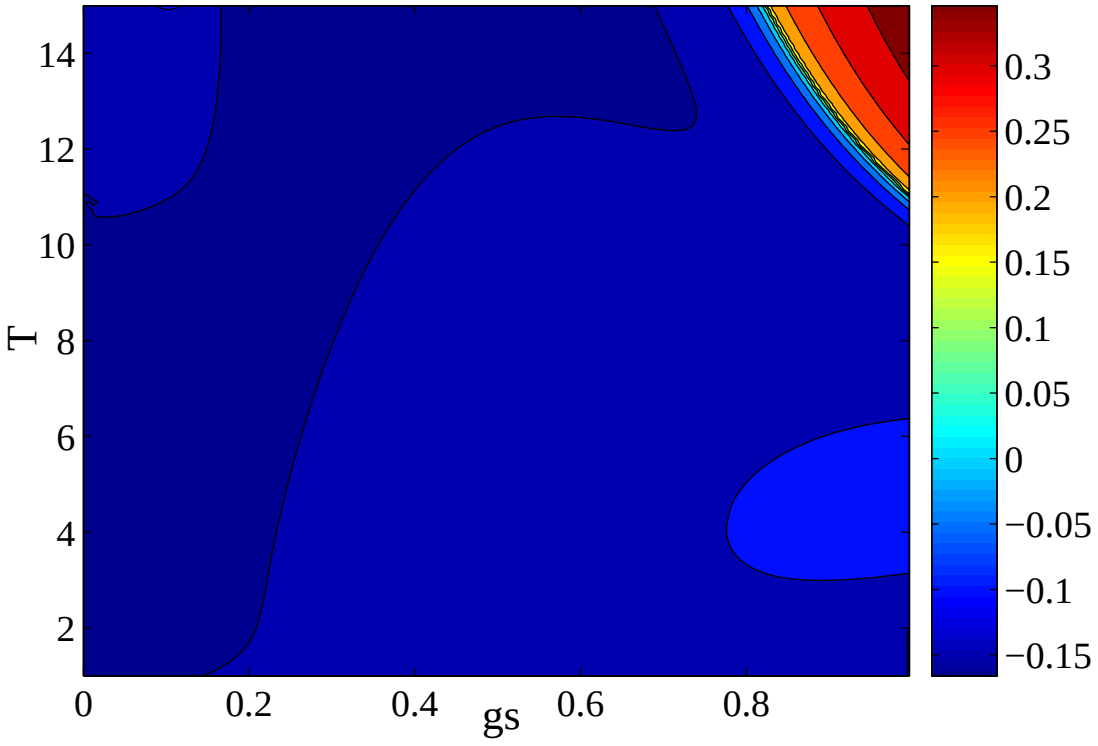

Figure 28: *Stability regions for high quality synchronization as functions of the maximum velocity of the enzyme T and the chemical coupling coefficient g_s. The system exhibits high quality synchronization in a wide region of the parameter space for low values of the coupling parameter. In the present simulation, g_l is fixed at* 0.72.

A look at the result of the investigation done in the parameter space (T, g_s) for $g_l = 0.72$ shows the same result as in the case of the master stability. The region of onset of robust synchronization based on the mean value on the rate of change of the Lyapunov function LT, on Fig. 28, indicates that even though there is a large parameter region where the robustness of the synchronization is achieved, for $0.81 < g_s < 1$ and $11 < T < 15$, the value of $LT > 0$, showing that the synchronization dynamics of both cells loose their robustness as observed for larger

values of T and g_s.

With the result highlighted here, it is clear that the existence of elaborate control mechanisms for the various biochemical processes inside and within living cells is responsible for the coherent behavior observed in its spatio-temporal organization. Stability and sensitivity are both necessary properties of living systems and these are achieved through negative and positive feedback loops as in other control systems. From a general point of view external forcing of cellular processes is important in many application areas ranging from bioengineering to biomedicine. At the specific level of biochemical systems, the problem is to supply specific input coefficient to the coupling of the cells such that the biochemical processes of the cell achieve robust synchronization objectives.

III.4 Adaptively environment-mediated coupled cells: Synchronization

In coupled systems, synchronization refers to an adjustment of the time scales of their oscillations due to interaction between the oscillating processes. It is the most fundamental phenomenon that occurs in oscillating processes. At this stage, we wish to investigate the simultaneous existence and stability of a complete synchronous regime. In order to achieve this, we need to remind ourselves about the fact that the complete synchronized state lies on the synchronization manifold where the cells have exactly identical biochemical pathways, that is $x_1 = x_2$, $y_1 = y_2$ and $z_1 = z_2$.

III.4.1 Stability of the Complete Synchronous solution: Linear stability analysis of the coupled adaptive systems

Here, we investigate the stability of the synchronous state of two systems coupled via the scheme of equation (13). Let ξ_1, ξ_2, v and η be the deviations from the synchronized state of the two coupled systems, the environment and the damping parameter, respectively, which are all dynamic. Their dynamics is governed by the linearized equations obtained from equation (13) which in matrix form can be written as:

$$\begin{aligned}
\frac{dX_1}{dt} &= f(X_1) + \epsilon_1\gamma\beta_1 u, \\
\frac{dX_2}{dt} &= f(X_2) + \epsilon_1\gamma\beta_2 u, \\
\frac{du}{dt} &= -\kappa u - \frac{\epsilon_2}{2}\gamma^T(\beta_1 X_1 + \beta_2 X_2), \\
\frac{d\kappa}{dt} &= \alpha[\gamma^T(\beta_1 X_1 + \beta_2 X_2)]^2,
\end{aligned} \tag{46}$$

where X_1, X_2, u and κ have dimension 3, 3, 1 and 1, respectively. γ is a column matrix (3×1) with elements zero or one and it decides the components of X_i that take part in the coupling. We then get:

$$\begin{aligned}
\frac{d\xi_1}{dt} &= f^{'}(X_1)\xi_1 + \epsilon_1\gamma\beta_1 v, \\
\frac{d\xi_2}{dt} &= f^{'}(X_2)\xi_2 + \epsilon_1\gamma\beta_2 v, \\
\frac{dv}{dt} &= -\kappa v - \frac{\epsilon_2}{2}\gamma^T(\beta_1\xi_1 + \beta_2\xi_2) - v\eta, \\
\frac{d\eta}{dt} &= 2\alpha[\gamma^T(\beta_1 X_1 + \beta_2 X_2)]\gamma^T(\beta_1\xi_1 + \beta_2\xi_2).
\end{aligned} \tag{47}$$

For a completely synchronized regime, that is $X_1 = X_2$, equation (47) can be reduced by defining:

$$\xi_0 = \beta_1\xi_1 + \beta_2\xi_2. \tag{48}$$

Then equation (47) reads:

$$\begin{aligned}
\frac{d\xi_0}{dt} &= f^{'}(X_1)\xi_0 + \epsilon_1(\beta_1^2 + \beta_2^2)\gamma v, \\
\frac{dv}{dt} &= -\kappa v - v\eta - \frac{\epsilon_2}{2}\gamma^T\xi_0, \\
\frac{d\eta}{dt} &= 2\alpha\gamma^T(\beta_1 X_1 + \beta_2 X_2)\gamma^T\xi_0.
\end{aligned} \tag{49}$$

The fixed point $(0, 0, 0)$ of Equation (49) corresponding to the synchronized state will be stable if all the Lyapunov exponents derived from Equation (47) are negative. A significant development can be made if we assume that the time average values of $f^{'}(X_1)$ and $f^{'}(X_2)$ are approximately the same and can be replaced by an effective constant value μ [135]. Similarly, $\beta_1 X_1 + \beta_2 X_2$ can be replaced by its time average constant value ω. In this approximation, we treat ξ_1 and ξ_2 as scalars. This type of approximation has been employed in reference [156], and it was observed that it describes the overall features of the phase diagram judiciously well. Thus using ξ_0 defined by Equation (48), Equation (47) can be written as:

$$\frac{d\xi_0}{dt} = \mu\xi_0 + 2\epsilon_1 v, \tag{50}$$

$$\frac{dv}{dt} = -\kappa v - v\eta - \frac{\epsilon_2}{2}\xi_0, \tag{51}$$

$$\frac{d\eta}{dt} = 2\alpha\omega\xi_0, \tag{52}$$

where we have $\beta_1^2 + \beta_2^2 = 2$.

Differentiating Equation (50) with respect to time and eliminating v from equation (50) and equation (48), we derive an equation for ξ_0 given as:

$$\ddot{\xi_0} = (\mu - \kappa - \eta)\dot{\xi_0} + [\mu(\kappa + \eta) - \epsilon_1\epsilon_2]\xi_0. \tag{53}$$

After differentiating again Equation (53) with respect to time and discarding all the deviation terms of order two(namely $\xi_0\dot{\xi_0}$, ξ_0^2, $\ddot{\xi_0}\eta$ and $\eta\dot{\xi_0}$), we find the equation:

$$\frac{d^3\xi_0}{dt^3} + (\kappa - \mu)\ddot{\xi_0} + [\epsilon_1\epsilon_2 + \alpha\omega^2 - \mu\kappa]\dot{\xi_0} - \mu\alpha\omega^2\xi_0 = 0. \tag{54}$$

Assuming a solution of the form $\xi_0 = Ae^{mt}$, we obtain the eigenvalue equation:

$$m^3 + (\kappa - \mu)m^2 + [\epsilon_1\epsilon_2 + \alpha\omega^2 - \mu\kappa]m - \mu\alpha\omega^2 = 0. \tag{55}$$

The parameter values of μ and ω can be obtained numerically from the time series of the coupled system as the temporal averaging values of the functions $\dot{z}_i$ and $\beta_1 z_1 + \beta_2 z_2$ over a long period of time (because the coupling scheme is implemented via the third variable, that is the end-product concentration) when weak perturbations are performed on the synchronization manifold. In this regard, the values of $\mu \approx 0.00612611845$ and $\omega \approx 1.0$ are found. For the sake of simplicity, we will choose the value $\kappa = 1.0$ in order to ensure that the value of the damping parameter be greater than all of the optimal values of κ observed numerically (depending on the initial conditions). This is necessary to obtain a synchronous solution, when the coupling strength is suitable to instate a synchronized regime in the coupled system. We take $\alpha = 3.5001 \times 10^{-9}$.

Based on the above considerations and on the assumption that $\epsilon_1 = \epsilon_2 = \epsilon$, we solve equation (55) for the eigenvalues of our system making use of the dichotomy scheme, for different values of ϵ. The solutions obtained are depicted on Fig. (29a) and it is observed that all the eigenvalues m (orange online) are always less than or equal to zero provided that the coupling strength $\epsilon > 0.0771$. This indicates that for this range of values of the coupling the synchronous state is stable. This is in close agreement with the previous result observed numerically on Fig. (30) through the plot of the evolution of the Lyapunov spectrum as a function of ϵ, where a similar trend was noticed for $\epsilon > 0.07$. To ascertain this fact, an enlargement of the region $\epsilon < 0.0771$ indicated by the rectangular box in Fig. (29a) is shown in Fig. (29b). This figure clearly suggests that for $\epsilon \leq 0.0771$, there exists at least one eigenvalue which visibly exceeds zero and which will contribute to the generation of an unstable synchronization manifold. As inference, we can say that both numerical and analytical tools advocate for the suitable interval of value of $\epsilon > 0.0771$, for which the synchronized regime attained through our adaptive feedback-control scheme of two environmentally coupled cells with activator-inhibitor pathways is stable.

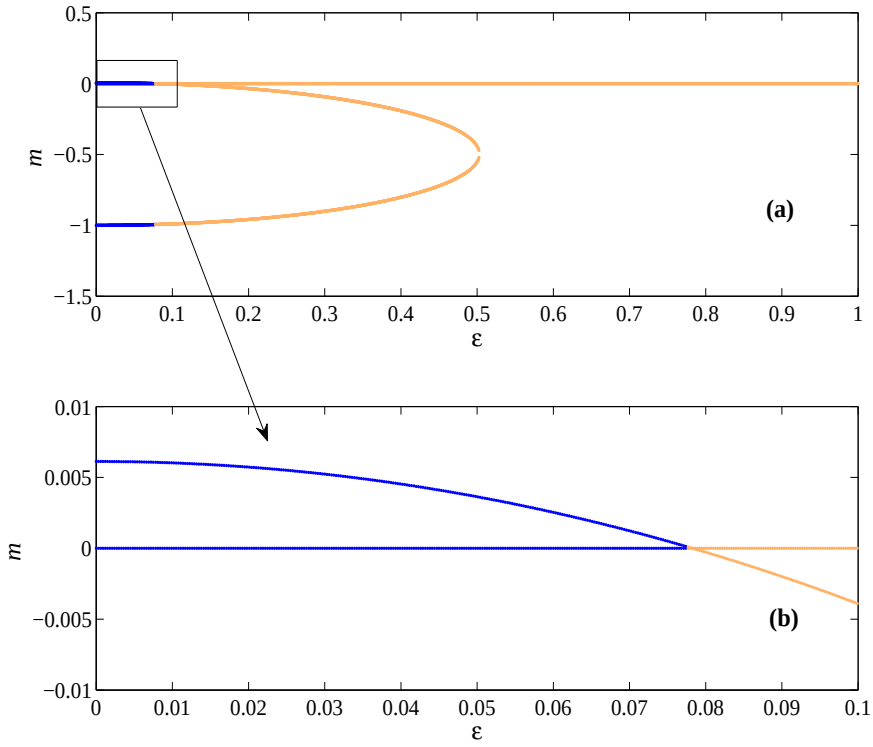

Figure 29: *The spectrum of eigenvalues as a function of ϵ: (a): Eigenvalue spectrum for which the synchronized state is unstable, $\epsilon \leq 0.0771$ in dark line (blue online); Eigenvalue spectrum for which the synchronized state is stable, $\epsilon > 0.0771$ in gray line (orange online). (b): Zoom of the small box in (a) as an evidence of the existence of at least one eigenvalue which exceeds zero, thereby yielding an unstable synchronization manifold, when $\epsilon \leq 0.0771$. The parameter values are $\mu = 0.00612611845$, $\omega = 1.0$, $\kappa = 1.0$ and $\alpha = 3.5001 \times 10^{-9}$.*

III.4.2 Numerical simulations of the Lyapunov Spectrum

Our study of the stability of this manifold will be based on the calculation of the Lyapunov spectrum of the coupled system. Lyapunov exponents are known to assess the fast exponential divergence of two trajectories of the same dynamical system, which started from almost indistinguishably close initial conditions in the phase space and with the course of time. In the actual case study, when the coupled systems are completely synchronized, they act as one unique entity on the synchronization manifold, thereby making the dimension of the coupled cells to settle from 8 to 4. In the event where perturbations are produced on the manifold in directions transverse to it, that dimension unfold again in phase space and grows above 4, leaving the system unsynchronized. A survey of how these perturbations grow in the phase space over a long period of time can be perceived through the calculation of the whole spectrum of Lyapunov ex-

ponents corresponding to the coupled system for a given value of the coupling strength. The technique for the obtention of this spectrum is described in reference[141]. It produces 8 Lyapunov exponents. First and foremost, the largest of them, λ_1, is an indicator of whether there is a chaotic dynamics on at least one of the coupled systems. In our case, because of the chaotic dynamics of the cells, λ_1 is always strictly positive for all the values of ϵ. Secondly and extremely important, the second largest exponent λ_2 of our coupled system detects whenever a fully stable synchronized regime is instated among the cells by the coupling. This occurs when λ_2 becomes strictly negative. Finally and not the least, the third Lyapunov exponent λ_3 provides information about the presence of a phase synchronized dynamics among the cells.

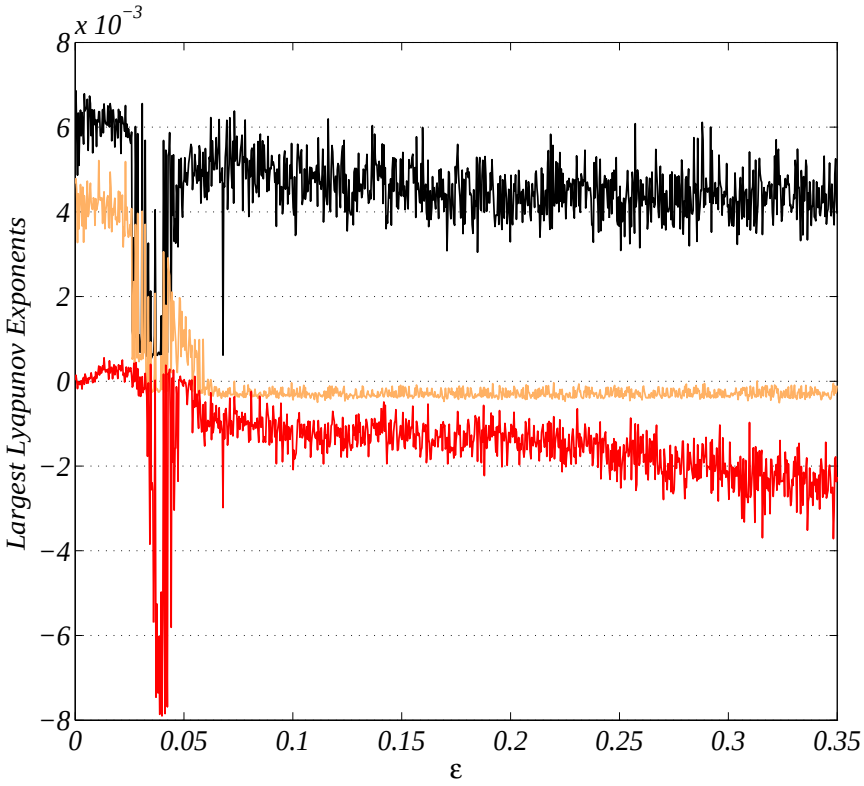

Figure 30: *The three Largest Lyapunov Exponent of the coupled system as a function of the coupling strength ϵ. The parameter values are $q = 0.1$, $k = 0.003$, $L = 10^6$, $T = 10$.*

Before closing this discussion, we support the previous relevant comments made on the ability of this feedback-control adaptive environmental coupling to preserve the local intrinsic chaotic behavior of cells while synchronizing them, by plotting the three largest Lyapunov exponents of our 8-dimensional coupled system as a function of the environmental coupling scheme. This is presented in Fig. (30) where it is observed that the largest Lyapunov exponent is always

strictly positive irrespective of the value of ϵ, showing that the global dynamics of the coupled system is always chaotic. Also, we observe that the third largest Lyapunov exponent definitely becomes negative when $\epsilon > 0.066$, indicating the onset of phase synchronization. In addition, when $\epsilon > 0.07$, the second largest Lyapunov exponent becomes steadily negative, indicating in its turns the onset of complete chaotic synchronization for the coupled cells. These results are in agreement with our previous observations.

Therefore, in order to enquire about the existence and stability of the synchronous solution, we will rely on the observations made on the evolution of λ_2 as we vary the strength of the coupling among the cells. Figure (31a) depicts the domains of stability of the synchronized state in the (ϵ, k) parameter space based on λ_2. It is observed that cells find it easy to synchronize for most of the couple of values (ϵ, k) of the coupling strength and the rate of degradation of the first substrate, except mainly when $(\epsilon, k) \in [0.028, 0.055] \times [0, 0.18]$; and for some few isolated points spread in the lower region of the parameter space. Figure (31b) shows the same analysis performed in the (ϵ, T) parameter space, where we see that the domain of stability is still large. But, the stable synchronized state is not accessible when the maximum velocity of the enzyme is such that $T \in [1, 3.8]$, and mostly when $(\epsilon, T) \in [0, 0.065] \times ([1, 7.5] \cup [9.1, 11.2])$.

Evidence of these observations are portrayed in Fig. (32) where we plot both the time series superpositions of the cells and their phase portrait correlations for two different values of ϵ. The parameter values are still those for the chaotic dynamics of the pathways. When $\epsilon = 0$, Fig. (32a) shows that the cells are not synchronized and their phase portrait correlation graph shows that they are uncorrelated as seen on Fig. (32c). However, when $\epsilon = 0.15$, Fig. (32b) and Fig. (32d) show that the cells have their biochemical pathways perfectly synchronized and correlated via their end-product normalized concentration.

It then becomes obvious that the proposed adaptive environmental coupling scheme is capable of producing a robust synchrony among the coupled cells with activator-inhibitor pathways. The adaptation and learning skills of this coupling involve dynamical processes that tend to reinforce themselves through long-term repeated experience of encoding, assimilating and decoding of information produced both endogenously and exogenously. Figure (33) portrays the adaptive character of this indirect coupling scheme with feedback control, where it is observed that for the value of the coupling $\epsilon = 0$, the damping parameter κ of the environment continuously grows with time, indicating that the coupled system cannot reach a stable synchronized dynamics. But,

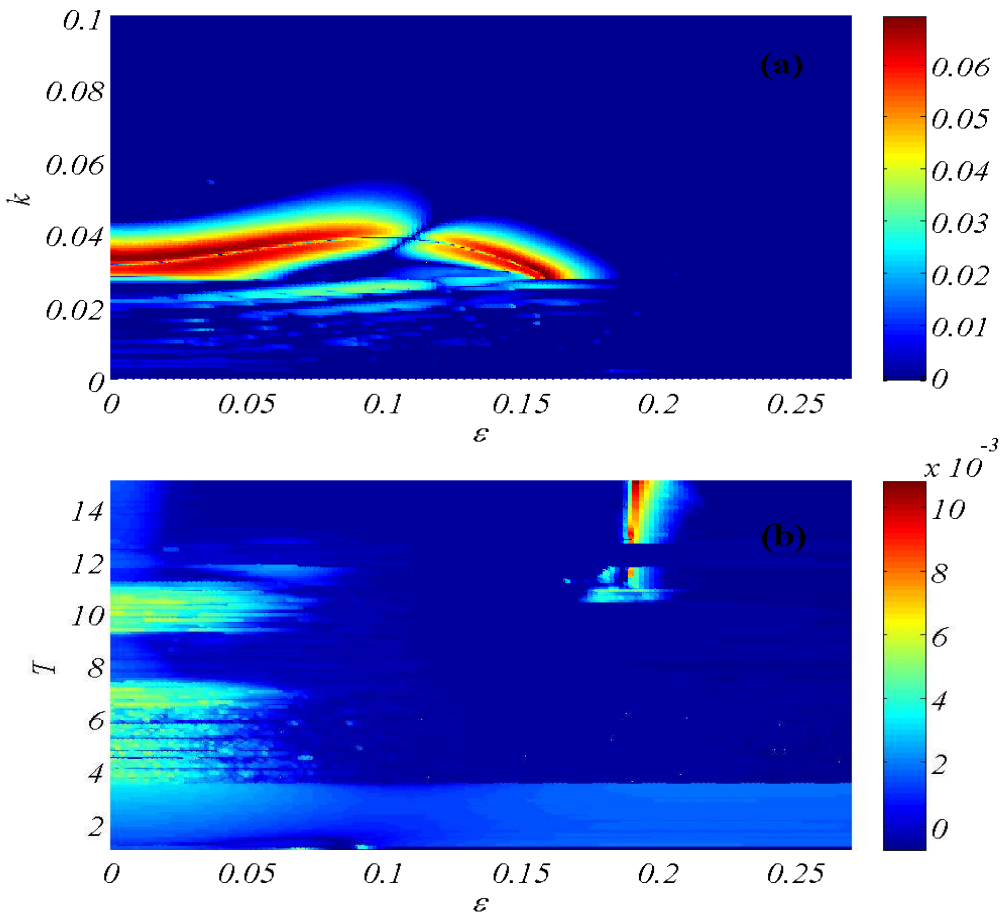

Figure 31: *The Lyapunov diagrams of the coupled system (13), defined by the Second Largest Lyapunov exponent of the spectrum, showing domains of stability of the synchronization manifold as functions of the coupling strength ϵ and: (a): the rate of degradation of the first substrate k, (b): the maximum velocity of the enzyme T. The other parameters being fixed as $L = 10^6$ and $q = 0.1$.*

for a suitable value of the coupling, κ increases and rapidly attains a constant value, corresponding to its optimal value when synchronization is established among the cells.

III.4.3 Phase Synchronization

When seeking procedures to assess to degree of synchronization between two oscillators, sufficient attention must be given to their respective "stages" of oscillations, that is their positions inside the specified cycle of oscillations; namely the beginning, the first quarter, the middle, the third quarter, the end, etc. The quantity responsible of characterizing the stage of oscillations of each oscillator at any instant of time is called the phase of that oscillator$(\phi(t))$. For harmonic

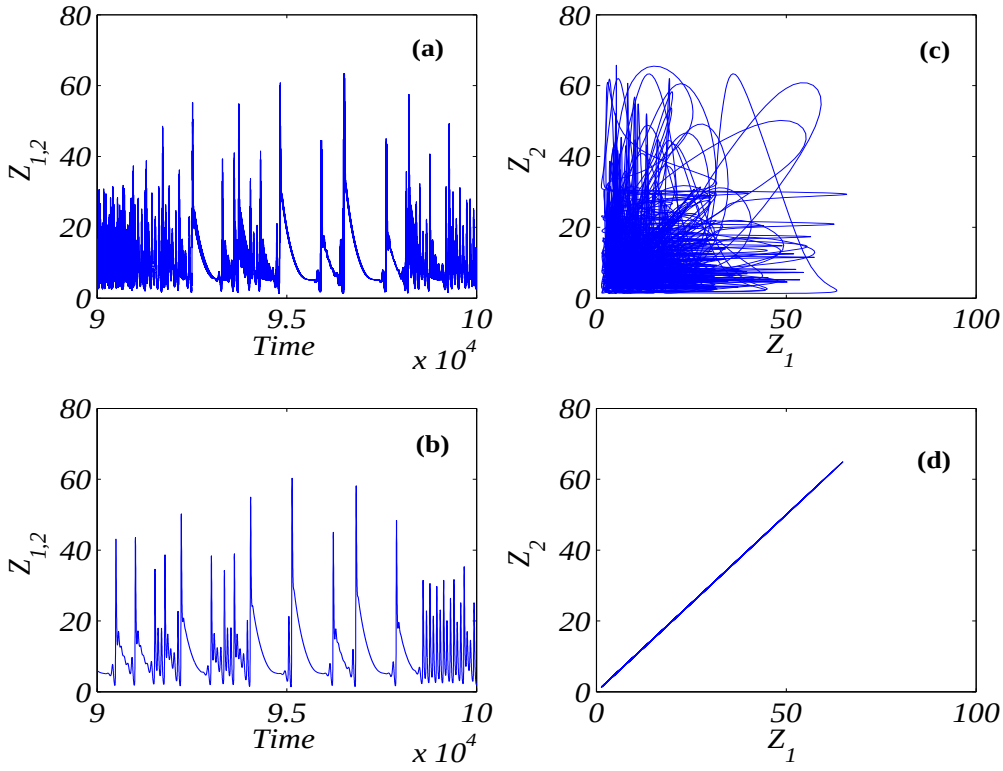

Figure 32: *Complete synchronization in two indirectly coupled cells with activator-inhibitor pathways coupled through an adaptive environment with feedback control mechanism. Figures (a):* $\epsilon = 0$*: no synchronization, (b):* $\epsilon = 0.15$*: synchronization; are the plots of the superposition of the time series of the two coupled cells. Figures (c):* $\epsilon = 0$*: no synchronization, (d):* $\epsilon = 0.15$*: are the correlation graphs for different values of the coupling. For a suitable coupling strength, a complete synchronized dynamics is obtained.*

oscillations, the phase is a linear function of time, while for more complex dynamics such as quasi-harmonic and chaotic oscillations, it has a more complex shape. Accordingly, the concept of phase is intimately associated with the phenomenon of synchronization. Phase therefore represents a convenient tool for the detection of whether two oscillators are synchronized or not. Specifically, considering the phase difference between oscillators, if the phase difference happens to be a constant or to slightly swing around a constant, this would typically suggest that the oscillators are $1:1$ synchronized. In this case, there is the appearance of frequency locking mechanisms due to the effect of suitable coupling scheme and strength, forcing the oscillators to vibrate "in phase". Alternatively, if the phase difference grows in time, there is no $1:1$ synchronization.

As well as in nature it is hard to find two exactly identical systems, complete synchroniza-

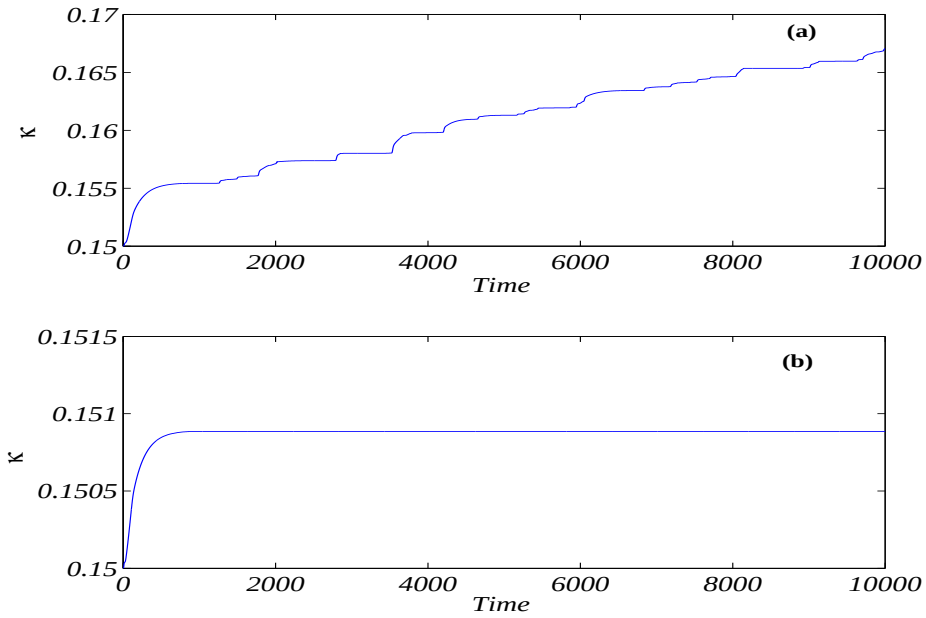

Figure 33: *Time series of the damping parameter of the environment κ for: (a): $\epsilon = 0$, (b): $\epsilon = 0.15$*

tion is more challenging to find compared to phase synchronization. Mindful of this fact, phase synchronization therefore occurs more naturally in coupled biological systems. It is the weakest form of synchronization and is usually obtained when the strength of interactions is low. As the coupling strengths become large, more ordered levels of synchronization regimes appear such as lag synchronization, followed by the strongest synchronized dynamics: the complete synchronization [11]. The intermittency in the phase synchronized dynamics usually takes place at the values of the coupling strength where transitions between these different types of synchronized regimes are obtained. This intermittency is characterized by intervals of loss of synchronization disconnecting epochs of synchronization.

In coupled dynamical systems, several indicators of the presence of a phase synchronized dynamics can be used such as the average phase difference between two systems, the stroboscopic poincaré maps, the Lyapunov exponents, the phase space diffusion and correlation parameters, namely the Kuramoto parameter to name just a few. First, it is noteworthy that a strong evidence of the existence of phase synchronization in coupled chaotic oscillators is the localization of conditional sets obtained from the observations of the position of one cell's trajectory at the time another cell makes any physical event [142]. This concept is an extension of the approach of localized map by Pereira et al. [139] who demonstrated that localized sets can be constructed

while in phase synchronization by means of any physical observation. In the present study, we define our physical event based on the Poincaré section of the attractor of the first cell through the plane defined by $z = 10$, with the constrain that $\dot{z} > 0$. In this manner, based on the repeated realizations in the phase space of the defined event by the trajectory of the first cell, a stroboscopic map is derived for the second cell through observations of its positions at the times the event takes place. A set of points is therefore constructed in phase space for the second cell for a given value of the coupling strength. For the sake of simplicity, we assume that $\epsilon_1 = \epsilon_2 = \epsilon$ as in the preceding analysis.

To have a clear picture of when phase synchronization might appear between the two coupled chaotic cells, we show in Fig. (34a) the plot of the quantity:

$$\chi = \frac{max(z_2^j) - min(z_2^j)}{max[z_2(t)] - min[z_2(t)]}, \tag{56}$$

where z_2^j represents the value of z_2 at the instant the trajectory of the first cell makes the j^{th} event. Thus χ is related to how broad the conditional observations spread over the whole attractor [17]. Figure (34b) depicts the captured values of z_2^j on the attractor of the second cell in phase space at the times the event occurs, for different values of ϵ. It appears from both figures that when $\epsilon > 0.066$, phase synchronization takes place, as the conditional observations obtained for the second cell when the first one makes the event always produce a localized set of points. Alongside this analysis, we carry out a temporal survey of the data using the parameter:

$$R = \frac{\sqrt{(\sum_{i=1}^{2} \sin(\phi_i))^2 + (\sum_{i=1}^{2} \cos(\phi_i))^2}}{2}, \tag{57}$$

defined by Kuramoto in 1984 as a rigorous quantity for the assessment of mutual phase entrainment and synchronization among coupled phase oscillators [143]. ϕ_i stands for the phase of the i^{th} cell. For a given set of parameters, we compute the temporal average $< R >$ of R and its amplitude $\delta R = max_t(R) - min_t(R)$. For full(complete) synchronization to be established, we consider that the following conditions must be fulfilled:

$< R >$ is strictly greater than $< R >_{threshold} = 0.98$, and that $\delta R < \delta R_{threshold} = 0.001$

Both $< R >_{threshold}$ and $\delta R_{threshold}$ have values chosen arbitrarily. Figures (34c) and (34d)

show the evolutions of $< R >$ and δR, respectively, obtained over a long period of time, as the environmental coupling ϵ varies. As previously indicated in the case of the generation of conditional sets, it is observed that when $\epsilon > 0.066$, phase synchronization takes place, immediately followed by the emergence of a high quality full synchronization.

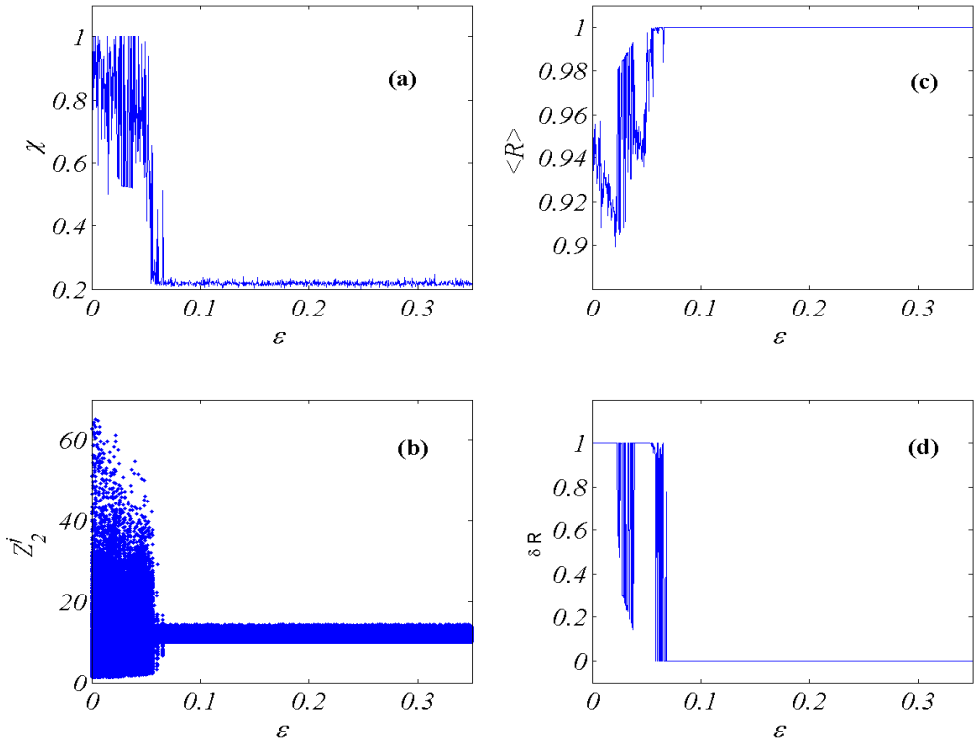

Figure 34: *Onset of phase synchronization in two indirectly coupled cells with activator-inhibitor pathways coupled through an adaptive environment with feedback control mechanism. Figures (a): Occupation of the conditional observations with respect to the attractor, χ; (b): End-product Normalized concentration z_2^j of the second cell when the first cell makes the j^{th} crossing with the section $z = 10$, for $\dot{z} > 0$; (c): Mean value of the Kuramoto parameter $< R >$; (d): The Kuramoto amplitude δR; as a function of the coupling strength $\epsilon_1 = \epsilon_2 = \epsilon$, detecting the emergence of phase synchronization in the coupled biochemical system. The parameter values are $q = 0.1$, $k = 0.003$, $L = 10^6$, $T = 10$.*

As illustrative evidences of the above remarks, we present respectively in figures (35a) and (35c) the set of points obtained in dark dots (blue online) from the second cell's attractor through the poincaré section of the first cell's attractor at the times the defined event takes place, and the time series of the phase difference between the cells, when $\epsilon = 0$. It is observed that the set of points are not localized and the time series of the phase difference show divergence as it is not bounded. The calculations indeed show in Fig. (35c) that the phase difference goes up to

4×10^4. For a larger value of the environmental coupling, namely $\epsilon = 0.15$, the set of points become localized as seen on Fig. (35b). Hence, the corresponding phase difference between the biochemical pathways on Fig. (35d) becomes perfectly zero due to the fact that they are completely synchronized for the given value of the environmental coupling.

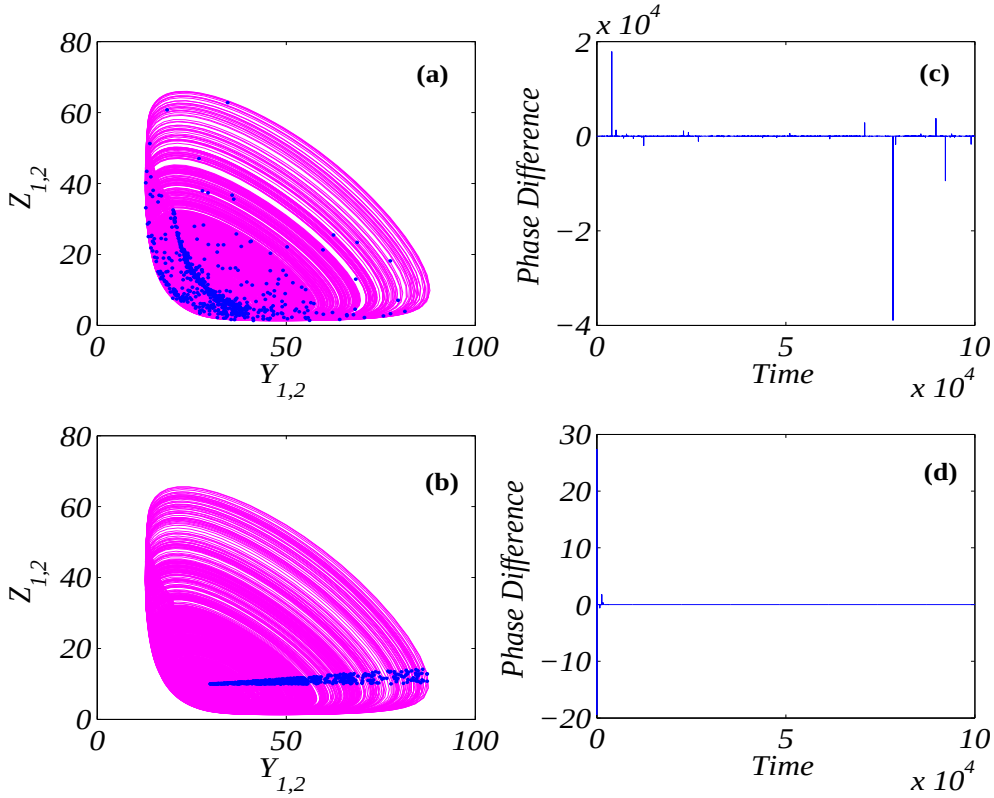

Figure 35: *Onset of phase synchronization in two indirectly coupled cells with activator-inhibitor pathways coupled through an adaptive environment with feedback control mechanism. Figures (a):* $\epsilon = 0$, *(b):* $\epsilon = 0.15$*: are the plots of the attractor of the first cell in gray lines (pink online) and the stroboscopic projection of the attractor of the second cell in dark dots (blue online) on the cross section of the first cell, for different values of the coupling strength [the points are localized as the coupling increases, indicating the onset of phase synchronization in the system]. Figures (c):* $\epsilon = 0$, *(d):* $\epsilon = 0.15$*: are Time series of the phase difference of the two coupled cells for different values of the coupling. As the coupling increases, the phase difference is bounded, confirming the onset of phase synchronization in the biochemical system. The parameter values are the same as that of Fig. (34) .*

We finalize our study on the appearance of phase synchronization in the coupled system by investigating in the parameter spaces (ϵ, k) and (ϵ, T) suitable requirements for the emergence of this synchronized regime, based on the mean value of the Kuramoto parameter. On both parameter space diagrams, the domains of phase synchronization are depicted in black (blue). From Fig. (36a), it appears that a phase synchronized regime is almost always present in the coupled

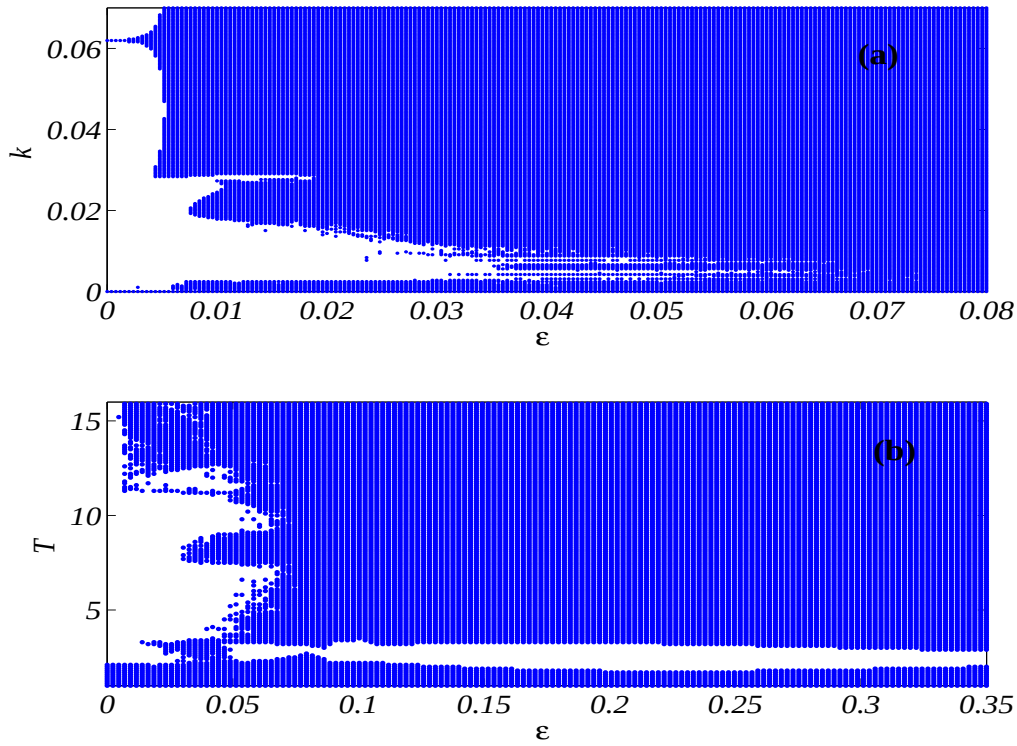

Figure 36: *The Kuramoto diagrams of the coupled system (13), based on the mean value of the Kuramoto parameter, showing phase synchronization regions in black (blue) and regions of unsynchronized dynamics white (white) as functions of the coupling strength ϵ and: (a): the rate of degradation of the first substrate k, (b): the maximum velocity of the enzyme T. The other parameters being fixed as $L = 10^6$ and $q = 0.1$.*

system as soon as $\epsilon > 0.066$, except in general for $k \in [0.0028, 0.029]$ where the synchronized dynamics is more or less reluctant to appear for a large range of values of ϵ. Exception made of that, the domain of existence of phase synchronization in the parameter space (ϵ, k) is very large. Thus the coupled cells are more inclined to synchronize their biochemical pathways for a wide range of parameter points (ϵ, k). Figure (36b) equally shows that in the parameter space (ϵ, T) there is a narrow band of points for which the maximum velocity of the enzyme $T \in [1.7, 3.4]$ and the coupling strength $\epsilon \in [0, 0.07233]$, where the coupled system defies synchronization. But exception made of these regions, a wide part of the parameter space (ϵ, T) is greatly in favor of the emergence of a phase synchronized dynamics. The above analysis performed on the concept of phase synchronization in coupled systems is particularly important since it determines immensely the spatiotemporal organization of coupled biological systems and the efficiency with which information is transferred from one cell to another.

III.5 Diffusively coupled system: Pattern formation

III.5.1 One-dimensional spatially heterogeneous networks: Suppression of chaos and spatial pattern formation

Since homogeneity in both neighborhood and behavioral parameters among the sub-populations in a meta-population does not capture the patchiness of the real world, the primary concern of this section is to address the role of realistic biochemical and behavioral features such as, pattern formation, in the spatiotemporal dynamics of rings of cells with activator inhibitor pathways, both in the presence and absence of local and global chaotic features. Sub-populations of organisms in different habitat patches may differ from each other in biotic (for instance inherent growth rate and interaction strength) and abiotic (such as climatic and landscape pattern) components. In reality, a population of cells can have different parameters due to intrinsic and extrinsic noise that permeates its environment. Such heterogeneity can influence the mode and extent of dispersal of individuals among these sub-populations, which, in turn, may regulate their spatiotemporal dynamics. Thus, as far as in real life situation, it is almost impossible to have perfectly identical systems, even in clonal populations, the pathways in the cells can be assumed to differ from one another to some extent(though marginally), in their intrinsic biochemical parameter conditions. In order to model such heterogeneous networks with weak parameter mismatch with respect to the rate of degradation of the first substrate, the values of k in each pathway are initially randomly distributed around the value k=0.003, so as to literally preserve a local chaotic dynamics in all the cells. Thus, a numerical treatment of the one-dimension model prescribed by Equation (9) yields the following outcomes.

A- Spatial pattern formation

Figures 16a and 16b compare the long-term spatial distribution of the maxima z_max of all cells for the uncoupled, and coupled ($\varepsilon = 0.138$) cells in a lattice of $N = 50$ for 4000 time units.

It shows the inherent chaotic dynamics of each uncoupled cell, as the peak values are distributed in an irregular manner in Fig. 37 (a). A similar plot in Fig. 37 (b) for the coupled cells, showing regular standing wavelike spatial pattern in the lattice which emerge as two horizontal "8" structures closed with boundary points. The pattern in the periodic lattice remains constant,

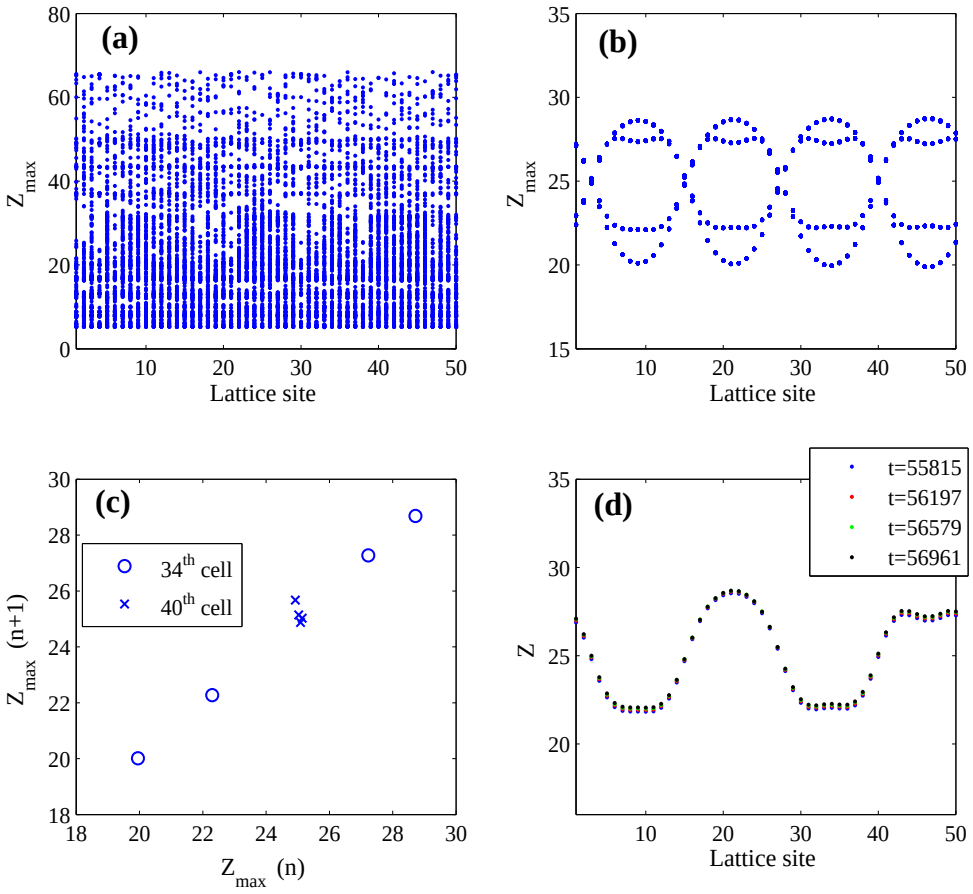

Figure 37: *Profile of the peaks of (a): uncoupled cells; (b): coupled cells showing spatial pattern; (c): return maps of the* 34^{th} *and* 40^{th} *cells in the lattice; and (d): snapshots of the cells' profile at intervals of* 382 *time units.* $N = 50$, $\varepsilon = 0.138$.

except for a phase shift, for any other initial condition. A closer look shows that each cell's local dynamics corresponds to a period 4 (P_4) oscillation although with different amplitudes. This is shown in Fig. 37 (c) by the return maps of two representative cells belonging to two different parts of the wave pattern: the boundary cell (40^{th} cell) and a cell with maximum z_{max}, (34^{th} cell). The boundary cells show P_4 dynamics but with minimum separation of amplitude, whereas the 32^{nd} cell shows P_4 dynamics with large deviation in the maxima. All other cells have P_4 dynamics with comparatively smaller deviations among the four peaks. To show that the spatial wave, once established, repeats about every 382 time units, snapshots of the lattice were plotted every 382 time units in Fig. 37 (d). This spatial pattern is indicative of standing wave where concentrations of z in some cells in space vary much more widely compared to others. Such patterns have been shown to occur in other model systems [144], and have been implicated in pattern formation in biological tissues [145].

B- Phase relationship of the cells

The phase synchronization with suppression of chaos and the spatial pattern shown by the coupled cells has important and distinct features. Firstly, the inherent chaotic dynamics in each cell is suppressed to a lower periodic state (P_4) having four local maxima of different amplitudes, which, when arranged in the descending order of heights, are ordered as $(1, 4, 2, 3)$. Secondly, there is phase entrainment with a phase slip among the cells that lead to the spatial pattern in Fig. 37 (b), and a unique global temporal pattern of "two high peaks followed by two smaller peaks" in the maxima of z. To show the distribution of phases that underlies the spatiotemporal pattern in the lattice, we plot the time series of three cells from the lattice in Fig. 38. They are perfectly synchronized (PS). As also seen in Fig. 37 (c), the peaks of the oscillations of the boundary cell (40^{th} in solid line) are very similar. The temporal behavior of z in two cells (34^{th} and 46^{th} cells) belonging to the opposite phases of the spatial wave are shown by dashed and dotted lines. It can be seen that the two cells are phase synchronized, but the amplitude maxima are temporally arranged as $(1, 4, 2, 3)$ (for 34^{th} cell) and $(3, 1, 4, 2)$ (for 46^{th} cell) leading to a phase lag by one-fourth of the period of the P_4 cycle due to the fixed phase slip. All cells on the two sides of the boundaries show the same phase slip. This leads to the shift of the highest peak of all the 50 cells such that the overlapped time series consists of "two high peaks followed by two smaller peaks"

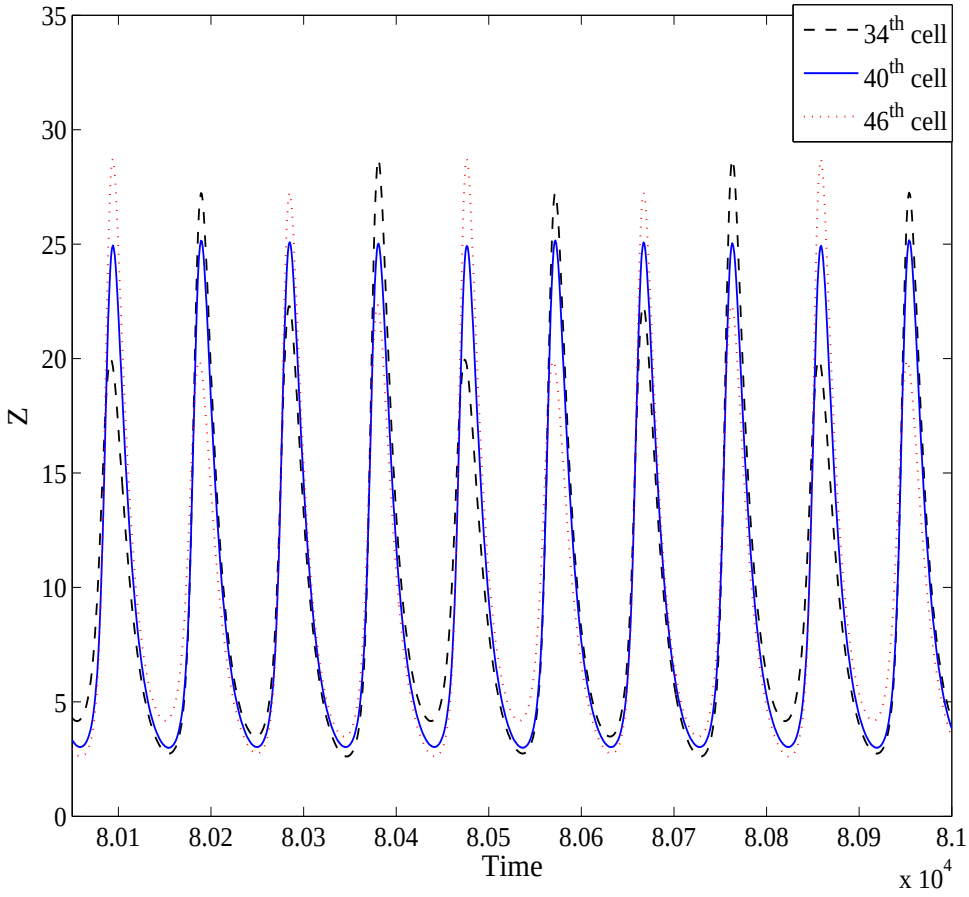

Figure 38: *Superposition of the time series showing the* $\frac{T}{4}$ *phase slip. A boundary cell* 40^{th} *in solid line, and two cells at opposite phases of the spatial wave* 34^{th} *and* 46^{th} *in dashed and dotted line, respectively.* $N = 50$, $\varepsilon = 0.138$.

in the time series of the $N = 50$ cells are superimposed. This phase synchronization with phase slip behavior underlies the spatiotemporal pattern in the lattice of coupled cells.

C- Incidental events of interplay between chaos and patterning

Numerous other structurally different spatiotemporal organizations could be retrieved from further investigations. Highlights of these remarkable structures as they emerge for increasing values of ε are provided in what follows. The emerging structures can be sorted in three main categories: (a) the case of pattern formation in the presence of chaos, (b) the case of pattern formation with suppression of chaos, and (c) the case of suppression of chaos without patterning.

Firstly, It is noteworthy that beyond the usual typical case of pattern generation via suppression of chaos previously encountered in the case of homogeneous lattices of such biochemical pathways, novel scenarios of patterning in the presence of chaos could be ascertained, both at low and moderate coupling strengths. Such structures can be spotted on Figs. 39 (a) and (c), on Fig. 40 (a), on Figs. 41 (a) and (c), where they usually arise as a sequence(succession) of chaotic bubbles spreading all over the closed spatial domain. In some cases, the chaotic bubbles distribute themselves along a bi-layered structure (Fig. 41 (a) and (c)). The corresponding spatial profiles of the lattice is provided besides each of them. These snapshots show the states of the lattice at some given points of their temporal evolutions. Amid these profiles, some interesting events of capture of multiple-humps structures are noticed (Fig. 39 (b), 39 (d), and on Fig. 41 (b), 41 (d)). These chaotic patterns are symptomatic of the fact that the degree of variability of the rhythms of end-product concentrations differ tremendously from one cell to another. While some pathways exhibit relatively moderate variations (bubbles' boundaries), some others (with several peaks of amplitudes embedded in the chaotic bubbles) experience large fluctuations in the course of their metabolism. This unevenness in their biochemical activities is the core of the emergence of these remarkable spatial patterns. Besides, on Fig. 41 (a)and (c), we notice that the local dynamics within the lattice is variable, with some pathways exhibiting local chaotic dynamics while others exhibit periodic rhythms.

Secondly, archetypal phenomena of pattern generation with suppression of chaos are incidentally observed. We can sometimes detect them with slight increments in ε from the values at which chaotic bubbles were observed. From there, the chaotic character of the patterns often tends to disappear, with the elimination due to the effect of the coupling, of some few unstable cycles in the attractors of the cells, thereby fostering the emergence of patterns with local periodic rhythms. Figs. 40 (c)and Figs. 42 (a) display examples of such cases.

Equally, another structurally different spatiotemporal setting with suppression of chaos can be noticed in Figs. 42 (a), which depict scenarios whereby suppression of chaos occurs without emergence of notable spatial patterns along the lattice. They are indicative of the existence of evenly(uniformly) distributed P8 and P5 local dynamics along the cellular ensembles. The $N = 50$ pathways remain phase synchronized, with P8 and P5 oscillatory regimes for $\varepsilon = 0.36$ and $\varepsilon = 0.37$ respectively. Therefore, it appears that the interplay between the heterogeneity of the

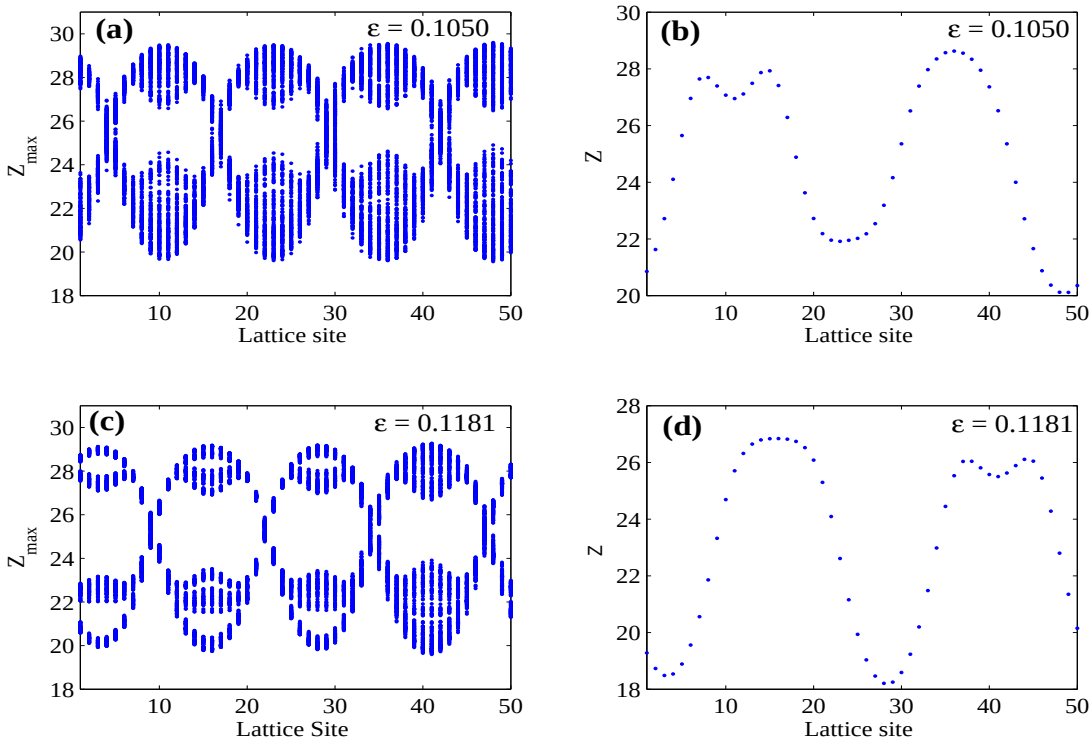

Figure 39: *Coupled cells showing spatial pattern.* $\varepsilon = 0.1050$*: (a): Profile of the peaks ; (b): snapshots of the cells' profile at an arbitrary time after discarding transients ;* $\varepsilon = 0.1181$*: (c): Profile of the peaks ; (d): snapshots of the cells' profile at an arbitrary time after discarding transients.*

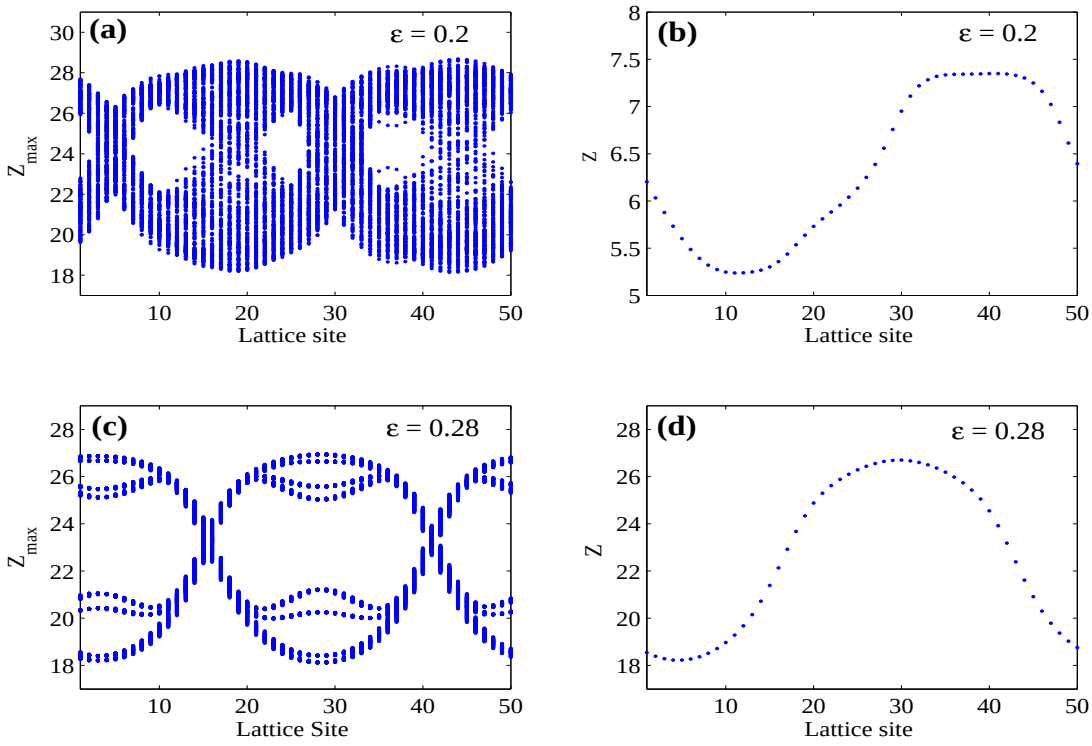

Figure 40: *Coupled cells showing spatial pattern.* $\varepsilon = 0.20$*: (a): Profile of the peaks ; (b): snapshots of the cells' profile at an arbitrary time after discarding transients ;* $\varepsilon = 0.28$*: (c): Profile of the peaks ; (d): snapshots of the cells' profile at an arbitrary time after discarding transients.*

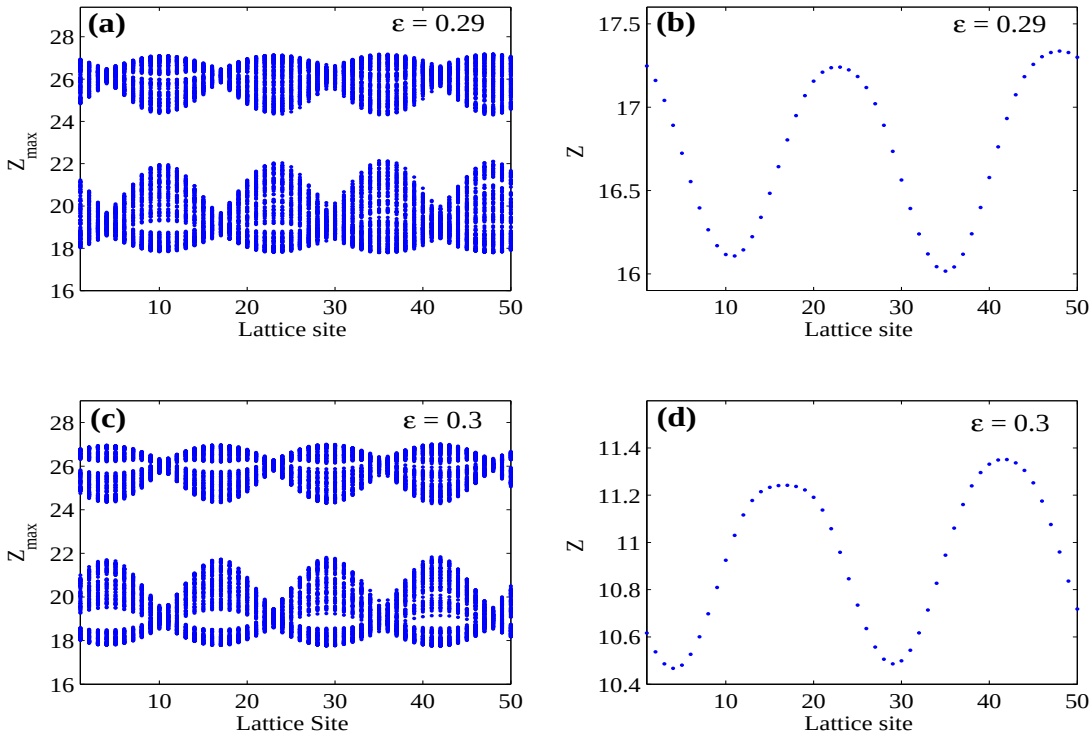

Figure 41: *Coupled cells showing spatial pattern.* $\varepsilon = 0.29$*: (a): Profile of the peaks ; (b): snapshots of the cells' profile at an arbitrary time after discarding transients ;* $\varepsilon = 0.30$*: (c): Profile of the peaks ; (d): snapshots of the cells' profile at an arbitrary time after discarding transients.*

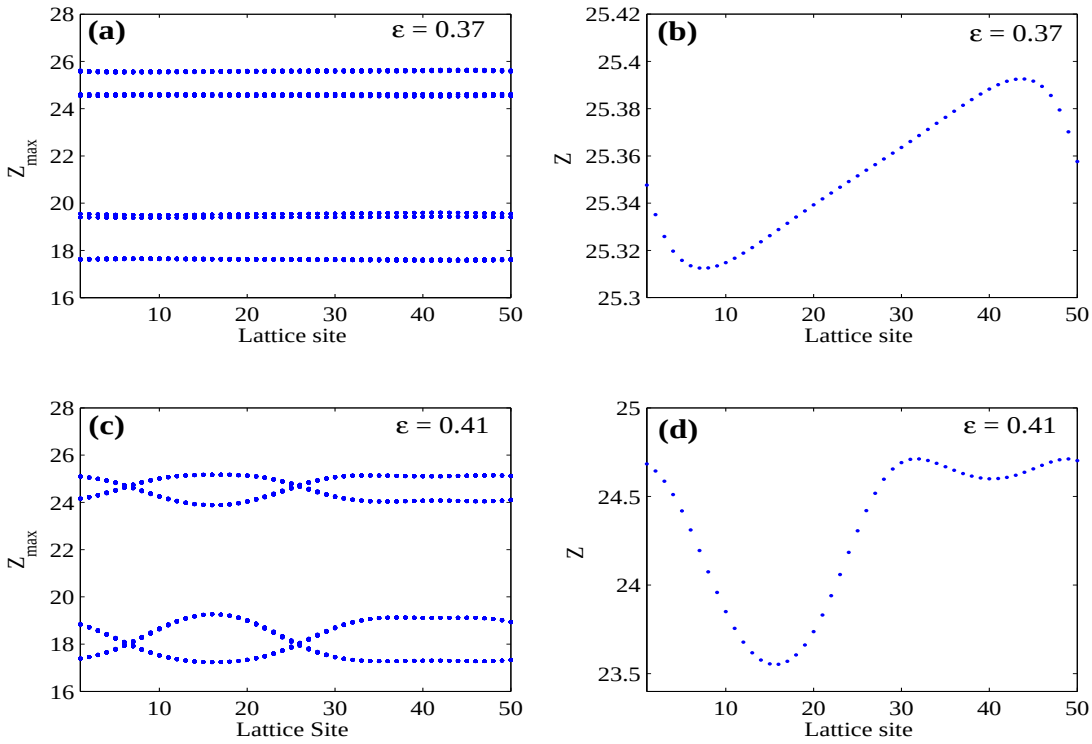

Figure 42: *Coupled cells showing spatial pattern.* $\varepsilon = 0.37$*: (a): Profile of the peaks ; (b): snapshots of the cells' profile at an arbitrary time after discarding transients ;* $\varepsilon = 0.41$*: (c): Profile of the peaks ; (d): snapshots of the cells' profile at an arbitrary time after discarding transients.*

lattice, the coupling strength and the lattice size can trigger the emergence of new spatiotemporal organization in the network of pathways, both in presence and absence of local chaos. These phenomena had not been observed in the case of homogeneous lattices where suppression of chaos was continually preceding patterning.

III.5.2 Stability of the spatially homogeneous state

With the aim of investigating the stability of the spatially homogeneous equilibrium:

$$u_s(x,y) = 1 \ \ , \ \ v_s(x,y) = 1 \ \ , \ \ w_s(x,y) = 1, \tag{58}$$

with respect to perturbations (of the form $\exp(i\overrightarrow{\kappa}.\overrightarrow{X})$) with wave vector $\overrightarrow{\kappa} = (\kappa_x, \kappa_y)$, we linearize equations (32) in the vicinity of the equilibrium state. The stability of the spatially homogeneous equilibrium state is then determined by the eigenvalues of the matrix:

$$J(\kappa^2) = \begin{bmatrix} -1-\kappa^2 & 0 & \gamma \\ \rho_{rv} & -\rho_{rv}\phi - \rho_{dv}\kappa^2 & -\rho_{rv}\psi \\ 0 & \rho_{rw}\phi & \rho_{rw}(\psi-1) - \rho_{dw}\kappa^2 \end{bmatrix},$$

where:

$$\gamma = \frac{df(w)}{dw}|_{w=1} \ \ , \ \ \phi = \frac{\partial g(v,w)}{\partial v}|_{v=1,w=1} \ \ , \ \ \psi = \frac{\partial g(v,w)}{\partial w}|_{v=1,w=1}. \tag{59}$$

It is noteworthy that, when neglecting the diffusion terms in equations (32), we obtain the Jacobian matrix for the local model given as: $J = J(0)$.

Also, the values assignments for the system parameters ψ, ϕ and γ determines the numerical assessment of U_s, V_s and W_s based on the functional kinetics of the local dynamics of the pathways. Following some mathematical treatment, we can obtain:

$$\gamma = \frac{-4W_s^4}{1+W_s^4} \quad , \quad \phi = \frac{V_s G_V(V_s, W_s)}{G(V_s, W_s)} \quad , \quad \psi = \frac{W_s G_W(V_s, W_s)}{G(V_s, W_s)}, \tag{60}$$

where $G_V(V,W) = \frac{\partial G(V,W)}{\partial V}$ and $G_W(V,W) = \frac{\partial G(V,W)}{\partial W}$.

The eigenvalue problem yields a characteristic equation which reads:

$$\lambda^3 + a_1\lambda^2 + a_2\lambda + a_3 = 0, \tag{61}$$

with the coefficients a_1, a_2 and a_3 given as:

$$\begin{aligned}
a_1(\kappa^2) &= \rho_{rv}\phi + 1 - \rho_{rw}(\psi - 1) + \kappa^2(\rho_{dv} + \rho_{dw} + 1), && (62)\\
a_2(\kappa^2) &= \rho_{rv}\psi\rho_{rw}\phi + (\rho_{rv}\phi + \rho_{dv}\kappa^2)(1+\kappa^2) \\
&+ (\rho_{dw}\kappa^2 - \rho_{rw}(\psi-1))(\rho_{rv}\phi + \rho_{dv}\kappa^2 + 1 + \kappa^2), && (63)\\
a_3(\kappa^2) &= (1+\kappa^2)[(\rho_{dw}\kappa^2 - \rho_{rw}(\psi-1))(\rho_{rv}\phi + \rho_{dv}\kappa^2) + \rho_{rv}\psi\rho_{rw}\phi] - \gamma\phi\rho_{rv}\rho_{rw}. && (64)
\end{aligned}$$

It is important to recall that, we typically seek conditions suitable for diffusion-driven instabilities. For this purpose, an essential requirement is that, the homogeneous steady state must be stable in the absence of diffusion, that is when $\kappa^2 = 0$. In this case, when $\kappa^2 = 0$, we have:

$$\begin{aligned}
a_1(0) &= \rho_{rv}\phi + 1 - \rho_{rw}(\psi - 1), \\
a_2(0) &= \rho_{rv}\phi + \rho_{rw}(\rho_{rv}\phi - \psi + 1), && (65)\\
a_3(0) &= \rho_{rv}\rho_{rw}\phi(1-\gamma).
\end{aligned}$$

According to the Routh-Hurwitz stability criteria, the spatially homogeneous steady state is

stable in the absence of diffusion whenever:

$$a_1(0) > 0 \ , \ a_3(0) > 0 \ , \ a_1(0)a_2(0) > a_3(0); \tag{66}$$

that is we have a set of three simultaneous conditions:

$$\begin{aligned} 0 &< \rho_{rv}\phi + 1 - \rho_{rw}(\psi - 1), \\ 0 &< \rho_{rv}\rho_{rw}\phi(1-\gamma), \\ 0 &< (\rho_{rv}\phi + 1 - \rho_{rw}(\psi-1))(\rho_{rv}\phi + \rho_{rw}(\rho_{rv}\phi - \psi + 1)) \\ &- \rho_{rv}\rho_{rw}\phi(1-\gamma). \end{aligned} \tag{67}$$

On the other hand, in the presence of diffusion ($\kappa^2 \neq 0$), the destabilization of the aforementioned stable homogeneous steady state occurs if:

$$a_1(\kappa^2) \leq 0 \ \text{, or } \ a_3(\kappa^2) \leq 0 \ \text{, or } \ a_1(\kappa^2)a_2(\kappa^2) \leq a_3(\kappa^2). \tag{68}$$

But $a_1(\kappa^2)$ is always strictly positive according to equations (67). Thus, diffusion-driven instabilities for the equilibrium state can occur whenever:

$$\begin{aligned} a_3(\kappa^2) &\leq 0, or \\ a_1(\kappa^2)a_2(\kappa^2) &\leq a_3(\kappa^2). \end{aligned} \tag{69}$$

Therefore, the likelihood of the emergence of diffusion-driven patterns in our biochemical networks relies on the simultaneous fulfillments of the sets of conditions (67) and (69). This set

of requirements becomes necessary whenever perturbations with suitable wave numbers (κ^2) are chosen, in order to destabilize the equilibrium state, within some given parameters conditions.

In order to highlight the possibility of occurrence of such instabilities, we plot on Fig. (43) the curves of $a_1(\kappa^2)$, $a_3(\kappa^2)$ and $a_1(\kappa^2)a_2(\kappa^2) - a_3(\kappa^2)$ as functions of κ^2.

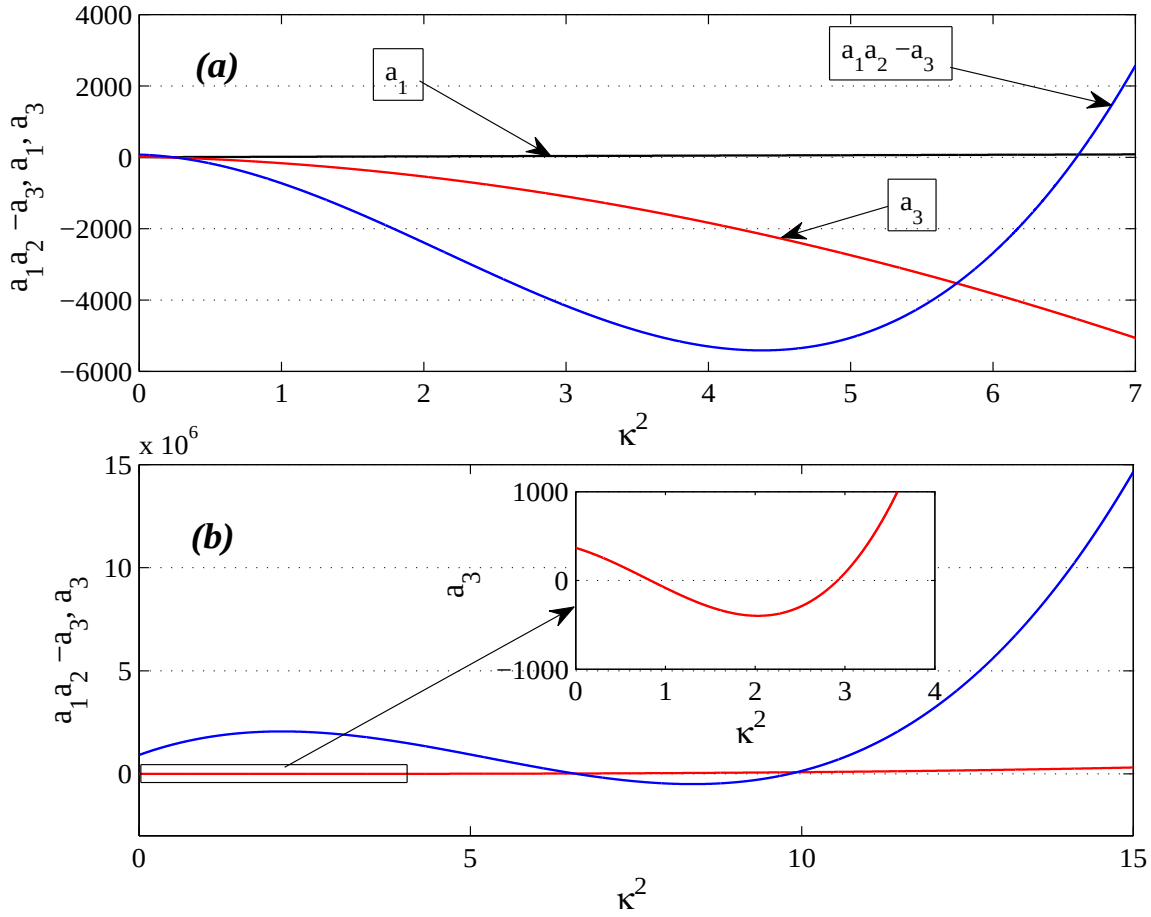

Figure 43: *Plots of the instability criteria for $a_1(\kappa^2)$ in black, $a_3(\kappa^2)$ in red, and $a_1(\kappa^2)a_2(\kappa^2) - a_3(\kappa^2)$ in blue. The parameter values are: (a): $\gamma = -2.0$, $\psi = 10.1$, $\phi = 1.12$, $\rho_{rv} = 12.5$, $\rho_{rw} = 1.1$, $\rho_{dv} = 10.1$, $\rho_{dw} = 0.1$; (b): $\gamma = -2.0$, $\psi = 100.1$, $\phi = 1.12$, $\rho_{rv} = 6.5$, $\rho_{rw} = 10.1$, $\rho_{dv} = 1.1$, $\rho_{dw} = 100.1$.*

On Fig. (43a), we observe that there is a wide range of values of κ^2 for which either $a_3(\kappa^2) \leq 0$ or $a_1(\kappa^2)a_2(\kappa^2) \leq a_3(\kappa^2)$, indicating that the spatially homogeneous steady state is unstable with respect to the related perturbation, for the given set of system parameters. In this case, let us note the fact that the two instability conditions are simultaneously fulfilled on the observed range of values of κ^2. Alternatively, their fulfillments needs not to be achieved simultaneously. In this regard, Fig. (43b) shows a scenario where the fulfillment of only one of them may occur.

Therein, we see that different ranges of values of κ^2 determine whenever either $a_3(\kappa^2) \leq 0$ or $a_1(\kappa^2)a_2(\kappa^2) \leq a_3(\kappa^2)$, implying instability set-ups for the equilibrium state. In the view of this, we can confidently assert that the destabilization of the spatially homogeneous steady state of our networks of diffusely connected biochemical pathways is possible in some given parameters conditions.

Next, we extend our investigation about the requirements for the emergence of instabilities for our homogeneous steady state, in different parameters planes. In this framework, we plot in Fig. (44) the parameters domains favorable for the presence of instabilities of our equilibrium state. It is noteworthy that these domains include all regions of occurrence of instabilities, diffusion-driven or not. The parameter domains include the (ρ_{dv}, ρ_{dw}), (ρ_{dv}, ψ), (ρ_{dv}, ϕ), (ρ_{dw}, ψ), (ρ_{dw}, ϕ) and (ϕ, ψ) parameters spaces presented in Fig. (44a), (44b), (44c), (44d), (44e) and (44f) respectively. In what proceeds, we have taken the value of $\kappa^2 = 1.0$, commonly obtained as destabilizing factor during our simulations, and equally for the sake of simplicity. These diagrams present colored regions, which are favorable for instabilities and related to the fulfillment of each instability condition: $a_1 \leq 0$ (brown), $a_3 \leq 0$ (green) and $a_1 a_2 \leq a_3$ (Yellow).

Equally important, the curves on these diagrams indicates frontiers along which $a_1 = 0$ (black), $a_3 = 0$ (red) and $a_1 a_2 = a_3$ (blue), and which determines the limits of the instability domains. From Fig. (44), we acknowledge the prevalence of conditions conducive for the destabilization of the spatially homogeneous steady state of our biochemical networks. This depicts the richness in the opportunities to prospect patterns development in our cellular system. In the next section, we shall explore the different patterning scenarios that may result from a survey of some relatively large sets of such biochemical pathways.

III.5.3 Spatiotemporal patterns

At this stage, it is necessary to reiterate how important patterns generation and wave phenomena are in biology. Although this is clear from the previously discussed facts, they are probably even more crucial in tissue communication, as it is the case during the process of embryological development for instance. The generation of steady state spatial pattern and form is, in this regard, a concept of high relevance. The patterning issues are quite diverse and are found in several different fronts such as in bacterial patterns, spatial patterning in slime molds, and in the early patterning in the embryo of the fruit fly [146].

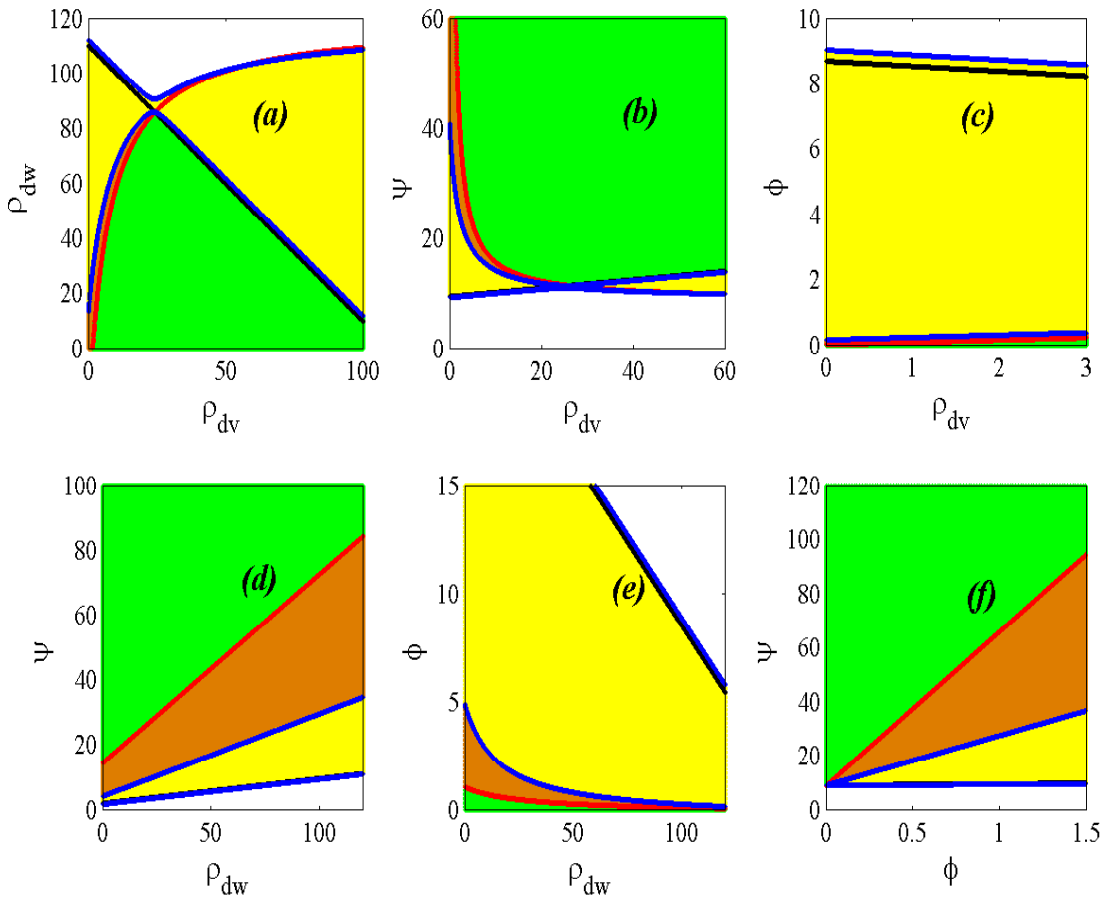

Figure 44: *Instability domains for the spatially homogeneous steady state in different parameter spaces: (a):* (ρ_{dv}, ρ_{dw})*; (b):* (ρ_{dv}, ψ)*; (c):* (ρ_{dv}, ϕ)*; (d):* (ρ_{dw}, ψ)*; (e):* (ρ_{dw}, ϕ)*; (f):* (ϕ, ψ)*. The parameter values are:* $\gamma = -2.0$, $\psi = 10.1$, $\phi = 1.12$, $\rho_{rv} = 6.5$, $\rho_{rw} = 10.1$, $\rho_{dv} = 1.1$, $\rho_{dw} = 100.1$.

It is well known that cellular division begins after fertilization. When sufficient cell division has taken place in a developing embryo, the foremost concern is about the way the homogeneous biochemical mass of the cells are spatially organized so that the sequential process of development can progress. Cells differentiate, in a biological sense, depending on where they are in the spatial organization. They also move around the embryo. This latter phenomenon is a relevant factor in morphogenesis, and has given rise to a new perspective to the generation of patterns and forms.

A phenomenological concept of pattern formation and differentiation called *"positional information"* was proposed by Wolpert (1969) [147]. He suggested that cells are preprogrammed to react to a chemical (or morphogen) concentration, and differentiate accordingly, into differ-

ent kind of cells such as cartilage cells. Indeed, it is a simple and attractive concept, which has resulted in significant advances in our knowledge of certain aspects of development. For this reason, we propose ourselves to take our reaction-diffusion model of two-dimensional spatial networks of diffusely connected cells with activator-inhibitor pathways as a possible framework for generating biological patterns.

The chemical pre-pattern view point of embryogenesis separates the process of development into several steps, among which the essential first step is the creation of a morphogen concentration spatial pattern. The name "*morphogen*" is used for such a chemical because it effects morphogenesis. The notion of "*positional information*" relies on a chemical pre-specification, so that the cell can read out its position in the coordinates of chemical concentration, and differentiate, undergo appropriate cell shape change, or migrate accordingly. Therefore, once the spatial pre-pattern of morphogen is established, morphogenesis becomes a slave process.

A crucial point arising from theoretical models is that any pattern contains its own history. Let us consider the following simple engineering analogy in our attempt to understand a biological process. It is one thing to suggest that a bridge requires a thousand tons of steel, that any less will result in a too weak structure, and any more will result in excessive rigidity. It is quite another matter to instruct the works on how best to put the pieces together. In morphogenesis, for example, it is conceivable that the cells involved in tissue formation and deformation have enough expertise that, given the right set of ingredients and initial instructions, they could be persuaded to construct whatever element one wants. It is in this perspective that, starting from our initial spatially homogeneous steady state, and given the right set of instructions via suitably chosen parameter conditions, we then hope to unveil some interesting events of pattern formation scenarios. In this regard, we present in Fig. (45) some notable structures emanating from the diffusion-driven instability of the spatially homogeneous equilibrium state of our biochemical networks.

Fig. (45a) displays the spatially homogeneous state of the biochemical network which is stable within some given parameters conditions. These plots have been generated with respect to the normalized variable w. Fig. (45b) and Fig. (45c) depict typical examples of inhomogeneous stationary (Turing) spatial patterns on which the system can collapse after being driven away from the unstable equilibrium state by diffusion. On Fig. (45b), we can observe long stripes structures paraded by the morphogen concentrations all over the spatial domain. Also Fig. (45c)

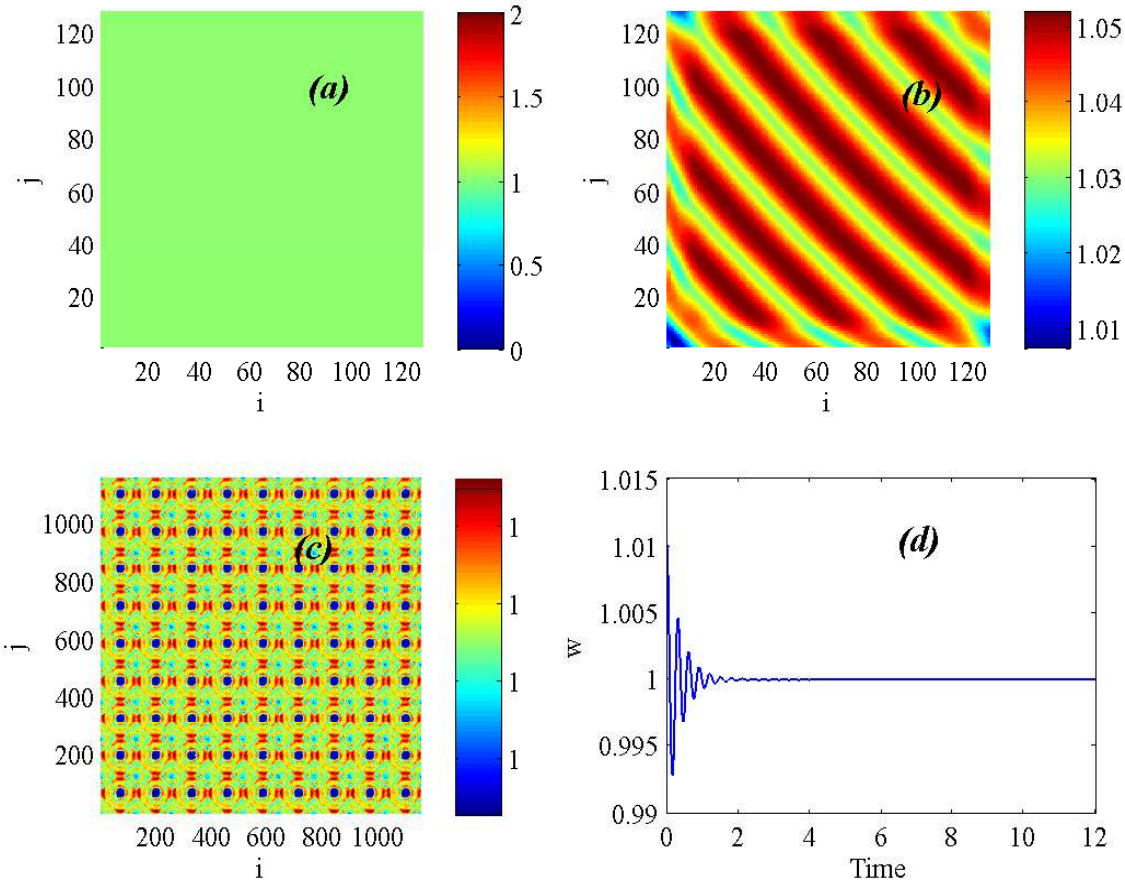

Figure 45: *Stationary Patterns: (a): Spatially homogeneous steady state:* $\gamma = -2.0$, $\psi = 10.1$, $\phi = 1.12$, $\rho_{rv} = 6.5$, $\rho_{rw} = 10.1$, $\rho_{dv} = 1.1$, $\rho_{dw} = 115.1$. *(b): Spatially inhomogeneous stationary pattern with stripes:* $\gamma = -2.0$, $\psi = 10.1$, $\phi = 1.12$, $\rho_{rv} = 17.9$, $\rho_{rw} = 115.1$, $\rho_{dv} = 1.1$, $\rho_{dw} = 100.1$. *(c): Spatially inhomogeneous stationary pattern with spots:* $\gamma = -2.0$, $\psi = 10.1$, $\phi = 1.12$, $\rho_{rv} = 6.5$, $\rho_{rw} = 10.1$, $\rho_{dv} = 0.0$, $\rho_{dw} = 110.1$. *(d): Local time series of the first cell in the lattice: Same parameter values as in (b).*

shows that the biochemical pathways of the cells can converge towards another form of stationary pattern exhibiting dark spots and circular stripes. Fig. (45d) presents the local time series of a biochemical unit when the lattice converges towards a stationary Turing structure. We observe that after being initially deviated away from its original state value of $w = 1.0$, it evolves over the time and settles on a value $w \simeq 1.0$ when the system stabilizes in a spatially inhomogeneous stationary state.

It is important to reiterate the fact that these patterns are obtained from the normalized system of equations (32), which mimics the original system of equations (14). In this regard, if the normalized model can generate such patterns, it suggests too that even the original one can dis-

play similar characteristics. In order to bring this fact to light, we present in Fig. (46) and Fig. (47), the stationary Turing patterns obtained from equations (14) based on the end-product concentrations W. These patterns include among others undulating stripes on Fig. (46a), Fig. (46d) and Fig. (47a); bright and dark spots structures on Fig. (46d), Fig. (47b), Fig. (47d); and dappling structures on Fig. (46b), Fig. (46c) and Fig. (47c).

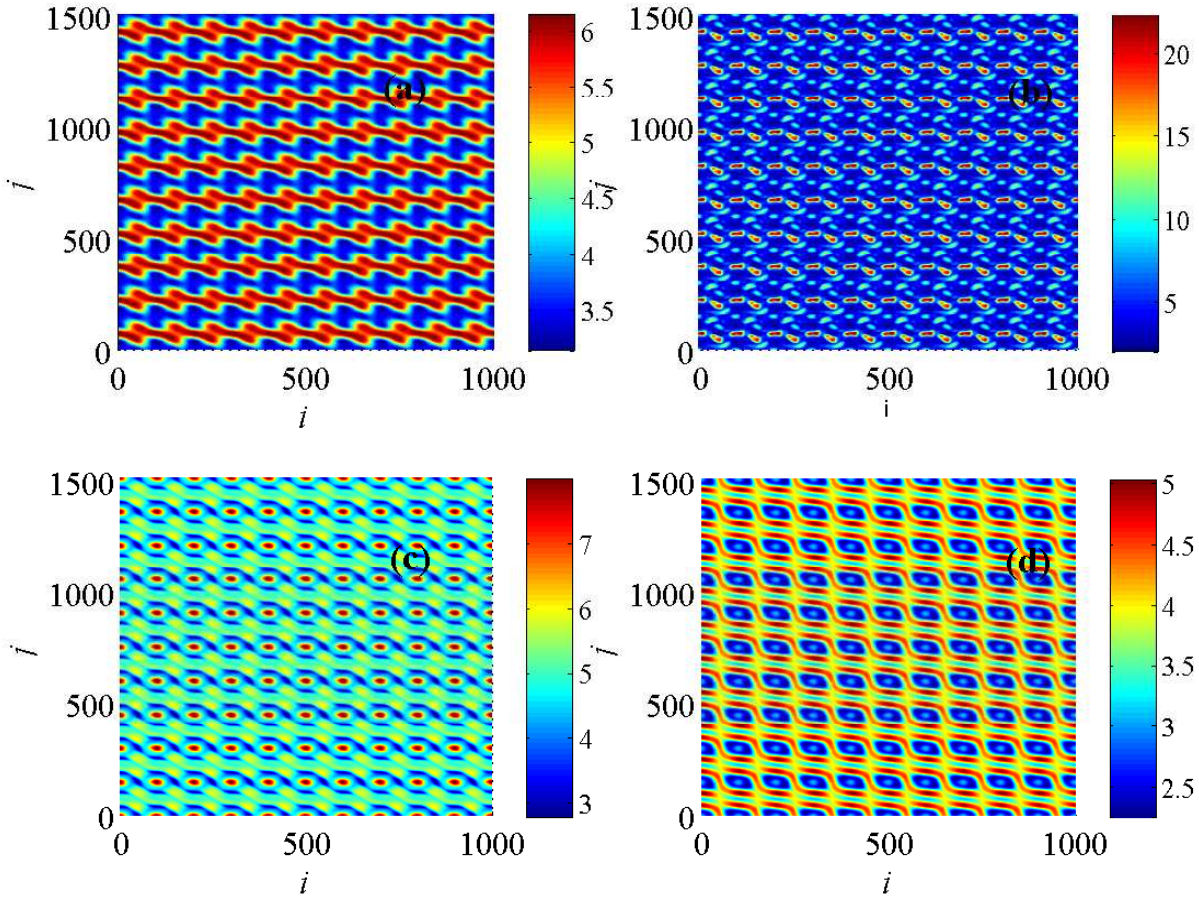

Figure 46: *Stationary Turing patterns: (a):* $D_u = 1.98$, $D_v = 2.0$, $D_w = 0.72$; *(b):* $D_u = 0.0$, $D_v = 0.05$, $D_w = 0.72$; *(c):* $D_u = 0.9$, $D_v = 1.0$, $D_w = 0.72$; *(d):* $D_u = 0.9$, $D_v = 1.0$, $D_w = 1.72$. *The other parameter values are* $k = 0.003$, $q = 0.1$, $T = 10.0$ *and* $L = 10^6$.

An extensive analysis of this cellular system under appropriate conditions shows that it displays more than just stationary patterns. Indeed, oscillatory patterns could equally be ascertained. Among them, we discern both regular and irregular oscillatory patterns disseminating all over the spatial domain. Fig. (48) reveals a typical example of regular oscillatory spatial patterns that emerge in the form of travelling wave structures propagating continuously all over

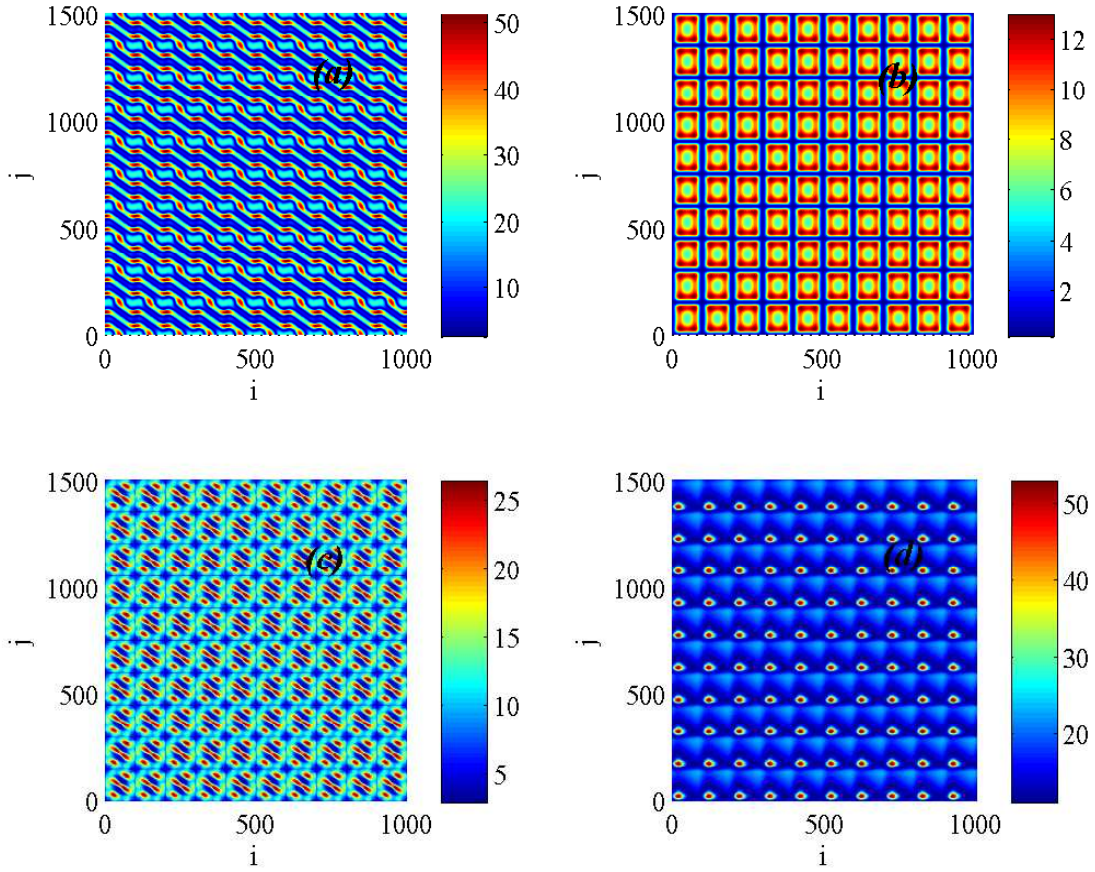

Figure 47: *Stationary Turing patterns: (a):* $D_u = 0.0$, $D_v = 0.0$, $D_w = 0.72$; *(b):* $D_u = 0.03$, $D_v = 0.1$, $D_w = 0.84$; *(c):* $D_u = 0.1$, $D_v = 0.1$, $D_w = 0.72$; *(d):* $D_u = 1.03$, $D_v = 1.2$, $D_w = 1.52$. *The other parameter values are* $k = 0.003$, $q = 0.1$, $T = 10.0$ *and* $L = 10^6$.

the two-dimensional spatial networks of biochemical pathways. Fig. (48a) shows a snapshot of the lattice at a particular time, after the transients have been discarded. Fig. (48b) presents the local time series of the midpoint of the lattice, as an indicator of the transition (subsequent to perturbation) of the local dynamics from an initial unstable steady equilibrium state $w = 1.0$ for the system, towards a regular oscillatory dynamics that persists over time. This is suggestive of what happens all over the spatial domain.

In the same footing, Fig. (49) presents an archetype of irregular oscillatory pattern arising from our biochemical ensemble in the form of spatiotemporal chaos. Fig. (49a) displays a snapshot of the array of biochemical pathways at a particular time after transients have been discarded. Fig. (49b) shows the local time series of the midpoint of the lattice as an indicator of

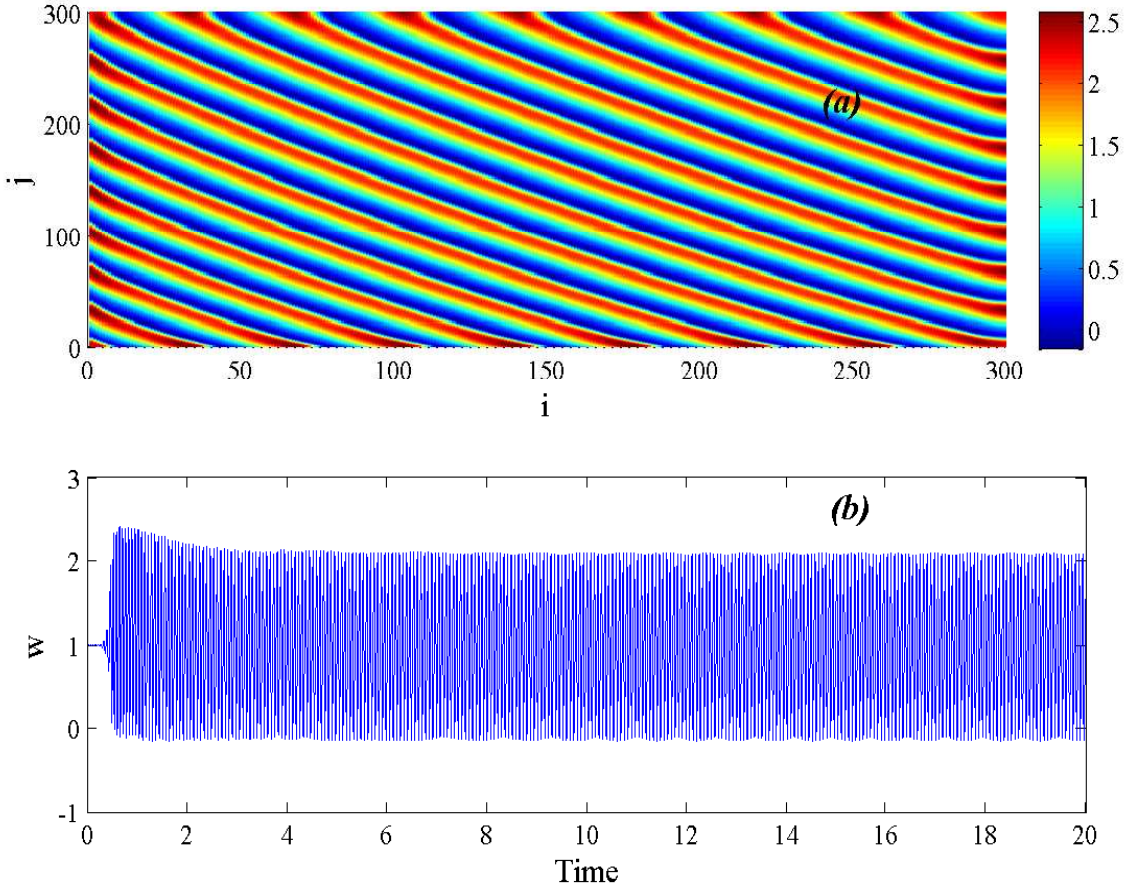

Figure 48: *Travelling waves propagating over the spatial domain of the biochemical pathways. The parameter values are* $\gamma = -2.0$, $\psi = 10.1$, $\phi = 1.12$, $\rho_{rv} = 15.5$, $\rho_{rw} = 10.1$, $\rho_{dv} = 101.1$, $\rho_{dw} = 120.1$.

the transition (subsequent to perturbation) of the local dynamics from an initial unstable steady equilibrium state $w = 1.0$ for the system, towards a chaotic dynamics that persists over time. This is symptomatic of what happens all over the spatial domain for the given set of parameters values.

The previously reported facts derived from our inquiry enable us to assert that our biochemical networks are capable of engendering stunning patterns, both stationary and oscillatory. As predicted earlier, it is then a good candidate model for the exploration of such spatiotemporal phenomena in biological systems. the patterns presented here don't have the claim to be exhaustive enough. However, we believe that they judiciously serve us right to highlight the propensity of sets of such biological units to come together and generate complex structures during the biochemical processes taking place through the developmental stages of living beings.

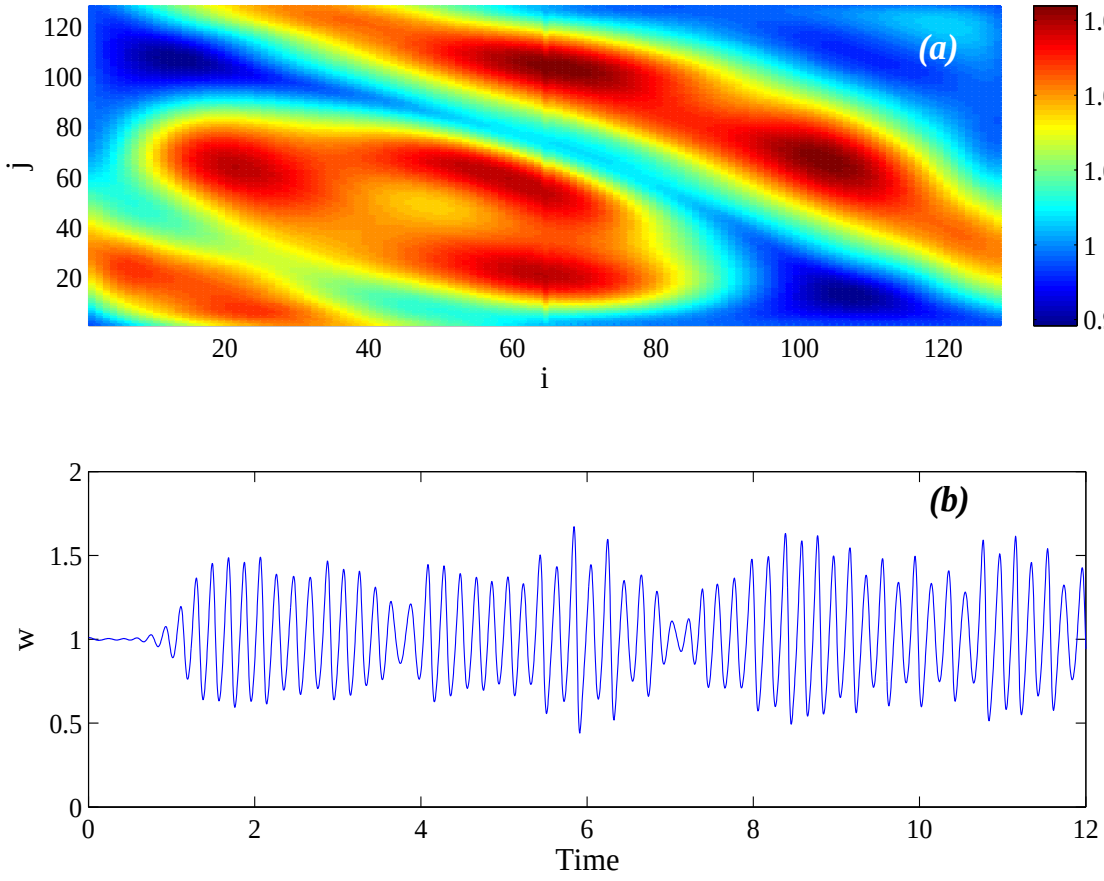

Figure 49: *Spatiotemporal chaos spreading over the spatial domain of the biochemical pathways. The parameter values are* $\gamma = -2.0$, $\psi = 10.1$, $\phi = 1.12$, $\rho_{rv} = 6.5$, $\rho_{rw} = 10.1$, $\rho_{dv} = 1.1$, $\rho_{dw} = 120.0$.

III.6 Discussions

The foregone outcomes derived from our models provide good reenactments about the internal processes pertaining in high quality physiological activities occurring in living beings, as observed through many practical inspections. In the specific case of the environmentally relayed signalling scheme with regulatory mechanisms, it is worth mentioning that our model, which is inspired by several preceding works addressing a broad area of valid problems encompassing indirectly coupled biological and complex systems, and sometimes unveiling prominent chaotic activities with time-delay schemes, is supported by key data collected in culture experiments [80, 148, 149, 150]. Specifically, some data have enabled the authors in [80, 148] to draw a comprehensive set of valuable assumptions on an analogous model of Gonadotropin-

Releasing Hormone(GnRH) from synchronized hypothalamic nerve cells. The analysis of the dependence of the equilibrium levels of $\alpha - subunits$, of Ca^{2+} and cAMP on G-proteins on the basis of experimental data has been implemented. This study showed the adaptive character of these elements. The simulations of many heterogeneous neurons have revealed the robustness of their synchronization mediated by a common pool of diffusible GnRH, which there plays the role of synchronizing agent in the midst of the nerve cells. Likewise, [151] proposes a similar approach to model biochemical signal transduction systems based on a defined aggregate objective function that likely accounts for the evolutionarily optimized efficiency in signal transmission in the extracellular medium. Starting from the ground that concentration adjustment in the cellular milieu exists to maintain effective signal transmission, the author showed that her model is self-organizing, as perturbations in proteins concentrations or changes in extracellular signalling automatically lead to adaptation. After systematic perturbations in the protein concentrations, she observed the responses and reaction times(that is the delays) of 27 molecular species involved in a set of 23 chemical reactions seemingly driving the optimization. Hypothesizing that an efficient signal transmission would maximize the responses of the molecular species to the input, she defined the objective function so as to minimize the delay and maximize the response. This procedure had pertinence in explaining the adaptation scenarios.

Also, Reference [10] clearly reports some experimental observations obtained about the functional responses of the environmental properties, with relevance in the instatement of a harmonious development in the cellular milieu. Therein, it is clearly given account about the fact that the animal body has evolved over a long period of time, and specialization(that is the richness in the diversity of species) has increased. With pertinence in each specie, cells are found to be sophisticated machines finely tuned to carry out a precise role within the body. Such specialization of cells is possible only when extracellular conditions are kept within narrow limits. Temperature, pH, the concentration of glucose and oxygen, and many other factors must be kept constant for cells to function efficiently and interact properly with one another. Homeostasis, which is essential for life, may then be defined as the dynamic constancy of the internal environment. The term *dynamic* is used because conditions are never absolutely constant, but fluctuate continuously within narrow limits. However, in the present analysis we ideally assume through our model their constancy for the sake of simplicity, that is the constancy of the damping parameter κ of the environment whenever complete synchronization is achieved, as shown in fig(**??**(b)). This

optimal value of κ helps stabilizing the environmental conditions and concomitantly annihilates the cellular differentiation. In order to maintain homeostasis, vertebrates possess several sensors that are able to measure each environmental condition. They constantly monitor the extracellular conditions and relay this information, usually(via nerve signals) to an *integrating center* which contains the *set point*, that is the proper value for that condition (see Chapter 58:*"Maintaining the internal environment"* in [10]).

The *integrating center* is often a particular region of the brain or spinal cord, but it can also sometimes be cells of the endocrine glands. It receives messages from several sensors, weighing the relative strengths of each sensor inputs, and then determines whether the value of the condition is deviating from the set point. When a deviation in a condition occurs, which is referred to in this case as a *stimulus*, the *integrating center* sends a message to increase or decrease the activity of particular effectors, which are generally muscles or glands that can change the value of the condition in question, back towards to the set point value: This is referred to as the *response*. The effectiveness of this mechanism relies on a type of control system known as *negative(or reverse) feedback loop*. For example, it is well known that if the body(or blood) temperature(which fundamentally determines the fate of biochemical reactions in the intra-inter cellular medium, cells being osmoregulator) exceeds $37°C(98.6°F)$, sensors in a part of the brain detect this deviation. Acting via an *integrating center* also located in the brain(namely the hypothalamus), these sensors stimulate effectors, including sweat glands, that lower the temperature, thereby protecting the set points of the body against deviations. Conversely, if the temperature happens to go below $37°C$, a different set of responses is generated, such as shivering and the constriction of blood vessels in the skin, which help to raise the body temperature and correct the initial challenge to homeostasis. These regulations are in the reverse (or negative) directions, and are therefore referred to as negative feedback loops crucial for the maintenance of homeostasis, and that ultimately cause the effectors to be turned off. In this way, constancy in environmental conditions is maintained, thereby enhancing a coordinated collective agreement among the environmentally connected biochemical pathways of the cells. Therefore, the regulation of body temperature, blood glucose and other environmental parameters in the cellular milieu has as end objective the stabilization of environmental patterns aiming at ensuring optimal conditions for the emergence of a harmonious cellular development.

Subsequent to this perusal of experimental observations, and all together with our theoretical

results, it appears evident that our proposed model reliably depicts a fairly faithful description of the importance of the steadiness in an optimal level(set point), of the parameter values of the environment, herein portrayed by its damping parameter κ, and achieved via adaptive feedback control mechanisms. Its regulatory feature has as an end result the promotion of a robust synchronized dynamics among the cells with activator-inhibitor pathways, which can efficiently communicate via stable environmentally relayed signallings.

Furthermore, the life of an organism starts from a single cell. This cell has virtually no pattern to it. Yet, it evolves to a very complicated organism, sometimes exhibiting complex patterns. These patterns are often the same across species. The subject of pattern formation is of central interest in the field of reaction-diffusion systems.

It is noteworthy that morphogenesis is the study concerned with the shapes of tissues, organs and entire organisms, and the position of the various specialized cell types. Correspondingly, a *morphogen* is a substance governing the pattern of tissue development, and the position of various specialized cell types within a tissue. It spreads from a localized source, and forms a concentration gradient across a developing tissue. In developmental biology, a *morphogen* is rigorously used to mean a signaling molecule that acts directly on cells to produce specific cellular responses dependent on the *morphogen* concentration. Therefore, any substance that diffuses into the cellular tissue and somehow persuades it to develop along different lines from those which would have been followed in its absence, qualifies as a *morphogen*.

Looking at each cell as a single biochemical unit, diffusion means that if there is a high concentration of a material in one cell, it will flow to another cell that has less concentration. Fundamentally, the process of diffusion is a destabilizing mechanism, sometimes naturally leading to the instatement in cellular tissues of a steady state, but one which varies in space, thereby resulting in a spatially inhomogeneous pattern. The key idea behind these processes is that a state which is stable in the local system, should become unstable in the presence of diffusion, which is commonly associated with a globally stabilizing effect. This fact has pertinence in yielding adequate treatments and giving satisfactory explanations to some undeniably captivating phenomena observed in animals, insects and plants such as gastrulation, polygonally symmetrical structures, leaf arrangements and color patterns in some animals and insects, emerging in the forms of stripes, spots, dappling, etc. Equally, the important feature of nonlinearity, typically peculiar to many biological systems, inherently plays a crucial role in the emergence of such

patterns. These nonlinearities are usually embedded in the kinetic functions describing the local dynamics of the biochemical systems.

The reaction-diffusion theory, which now has a relatively vast literature, is a field of research in its own right. It must be stressed that, strictly speaking, the mathematical and phenomenological descriptions of patterning scenarios are not explanations to the biochemical mechanisms pertaining in their generations. Yet, they are generally accepted, as these studies serve to highlight where our knowledge is deficient, since none of the individual models found in the literature can be considered so far as a complete model. These studies, including the present work, suggests directions in which fruitful experimentation might lead us. Indeed, a critical probe of these theoretical constructs, is in their impact on the experimental community.

III.7 Conclusion

In conclusion, in this chapter we have dealt with the analytical and numerical studies of the synchronization dynamics of cells with activator-inhibitor pathways based on distinct models emulating some pertinent signalling schemes that have relevance in cellular communication, namely the chemical, electrical and adaptive environmentally relayed connections. The advent of spatiotemporal organization in two-dimensional spatially extended networks of such biochemical pathways has equally been appraised in the presence of diffusion phenomena.

The chapter begins with the exposure of the complex oscillatory regimes which are inherent in the pathway. By using the linear stability analysis approach, we have investigated the existence and stability of its equilibrium states. A comprehensive bifurcation analysis of the system's state has been conducted with respect to both the rate of degradation of the first substrate and the maximum velocity of the enzyme. The findings show the abundance of biochemical rhythms within the cell. At a collective level, the Runge-Kutta scheme has been used to integrate the coupled system. First, the chemical coupling has been shown to able to instate a phase synchronized regime among the coupled pathways. The stability analysis of the complete synchronous solution has been performed based on the master stability function approach. It was numerically shown that the chemical coupling is unable to foster a completely synchronous regime amid the cells. However, numerical simulations suggest that the interplay between the chemical and electrical coupling schemes can tremendously enhance the synchronization dynamics of the pathways by establishing a complete synchronous regime among the cells. Next,

the parameter requirements necessary for the emergence of high quality synchronization between the pathways are obtained by means of the Lyapunov function used as a powerful tool for the detection of robust synchrony. Interestingly, via some bifurcation analysis, the dynamics of the synchronization manifold has been shown to be determined mainly by the strength of the synaptic coupling.

We have also examined propensity of the adaptive environment-mediated coupling scheme, though weak because of the indirect connections it establishes among the pathways, to promote a robust chaotic synchronization dynamics in their midst. A stability analysis of the complete synchronous solution is carried out both analytically and numerically in this framework, by using respectively the linear stability analysis method, the dichotomy scheme for the obtention of the coupled system eigenvalues, the master stability function approach based on a variational analysis method for a comprehensive calculation of the complete Lyapunov spectrum of the coupled system. Several prerequisites that favor this desired collective dynamical regime were found. The concept of phase synchronization has also been assessed based on indicators such as the Kuramoto parameter for phase entrainment, the calculation of the phase difference, the construction of stroboscopic localized maps and the occupational phase diagrams correlation parameter, in the phase space. The parameter conditions favoring this synchronous state were found to be abundant.

Next, the predisposition of large networks of diffusively connected cells with activator-inhibitor pathways to patterning phenomena was investigated. On one-dimensional spatial domains, heterogeneous lattices have shown to be capable of yielding spatial patterns, both with and without suppression of chaos. On two-dimensional homogeneous lattices, a generalized normalization procedure of the coupled system has been analytically implemented in this context. The linear stability analysis of the spatially homogeneous steady state of the system is conducted and numerical results provide the conditions under which diffusion-driven instabilities, crucial for patterns generation can occur. Some spatiotemporal patterns are retrieved and presented. They include both stationary and oscillatory Turing patterns, with some interesting events of occurrence of travelling waves and spatiotemporal chaos.

It is noteworthy that all the analytical and computational techniques used within the framework of these explorations were in perfect agreement and confirmed the reliability and robustness of our results.

General Conclusion

In this thesis, the synchronization dynamics, its stability and the advent of diffusion-induced spatiotemporal patterns amid cells with activator-inhibitor pathways have been probed. The aim of this work was to use concepts and techniques from physics to throw more light on quite a number of exciting concerns raised by biology in understanding the functioning, and collapse, of the networks of nonlinear biochemical interactions inside a living cell, and which have relevance in cellular communication and tissue development. In order to achieve this goal, three major steps have been considered.

The first chapter of this treatise is devoted to a literature review on cells with activator-inhibitor pathways. A reexamination of the available key results that pertain to them has been performed based on standard models. The complex dynamics of both a single biochemical pathway and a network of electrically coupled pathways have been expounded. Several interesting cellular rhythms have been reported via numerous bifurcation scenarios. They include among others, first locally, equilibrium states, *hard excitation* state, periodic and *birhythmic* oscillatory state, quasiperiodic and *chaotic* regimes. On a larger scale, events of synchronization, travelling wave phenomena and spatial patterns emergence with suppression of chaos were noticed depending on the coupling strength and the system size.

Some limitations of the available mathematical models have been discussed and some models that go beyond their description scope have been presented. In this regard, the second chapter is keen on the presentation and description of the aforesaid models, and on some analytical and numerical methods useful for their analysis. Among these new proceedings in the context of coupled biochemical pathways, are found some specific signalling schemes which encompass the chemical coupling and the environmental coupling scheme with regulatory mechanisms. These schemes take into account the long range, and sometimes indirect natures of the interactions among cells, as well as the potential adaptive character of some cellular connections in the course of their metabolism. Some methods such as the linear stability analysis, the variational approach for the derivation of the master stability function, the fourth-order Runge-Kutta

scheme, the Newton-Raphson scheme and the dichotomy scheme were exposed.

The main results and contributions of this thesis are presented in the third chapter.

First and foremost, let us recall that from a theoretical perspective, the numerous pathways embedded within many biological systems usually experience oscillations. Some are transient while others are sustained. Researchers are still debating the cause and function of these chemical oscillations. Analyzing a large biochemical network is difficult because it is rare that all of the relevant parameters for the chemical reactions are known. For example, it is not always clear how the enzymes behave under natural conditions in the densely crowded environment of the cell. An additional difficulty that impedes both experimental and theoretical work is the dense connectivity between the elements in biochemical networks. Any attempt to study a system by artificially perturbing it will generally alter the flow of metabolites. Thus a perturbation often induces changes in all parts, which complicates inferring causal relationships, such as how accelerating one reaction influences another.

The dynamics of a metabolic pathway are typically modelled by a system of ordinary differential equations. These are constructed to give the time evolution of the concentrations of the different metabolites by following the rate laws that describe the individual chemical reactions. The dynamics of the equations are then explored by numerical simulations. However, these simulations have to run for a while to actually observe the "natural" (long term) dynamics of a particular pathway. While a simulation approaches the long-term limit, it generates at all times an instantaneous description of the system. Since this information is often not desired, it is typically discarded in the analysis. However, it costs considerable computational time and can make exploring large parameter spaces by simulation tedious. Alternatively, systems of differential equations can be studied analytically. This has the advantage of revealing the dynamics in the whole parameter space, but is limited to small pathways because of the nonlinearity and complexity of the equations.

In general, for most real systems, computing the stationary states reveals little new information, as they are often accessible by direct observation. However, analyzing the stability and dynamical transitions (bifurcations) of these stationary states, can reveal deep insights into the dynamics of the system, cutting directly to how it functions and how it could potentially fail. Once the stationary states are known, a local stability and bifurcation analysis can be carried out straightforwardly, either numerically or analytically. This procedure has been implemented in

this framework on the single cell model. The findings reveal that the equilibrium state can loose its stability and settle in various types of biochemical rhythms.

With the knowledge of these facts, the main results of this research work are postulated in the third chapter as follows. From the onset, we have explored the rich dynamical behavior of a cell with activator-inhibitor pathway. Under well defined circumstances, the system exhibits steady states, periodic oscillations as well as complex dynamics, namely a chaotic behavior. The system also exhibits reverse period doubling bifurcations when the rate of degradation of the first substrate changes. The synchronization process of two coupled cells under the chemical and the combined effects of chemical and electrical couplings is also analyzed in their chaotic regime. It is found that even though the synchronous solution affected by the chemical coupling exhibits a variety of rich dynamics, the coupled system presents some difficulties to achieve a stable complete synchronization regime under the single effect of chemical coupling scheme. This is essentially due to the fact that the fast threshold coupling scheme used in this work is on the inhibitory form. However, the pathways can enter into a stable phase synchronization state, whose importance has been shown to be crucial in cellular communication. The combined effect of both the electrical coupling and chemical coupling has been shown to enhance the synchronization dynamics by facilitating the appearance of stable complete synchronization states. The concept of high quality synchronization, initially brought to light by Gautier *et al* [160, 161] was used to find the values of the coupling parameters for robust complete synchronization in the coupled cells by calculating the average rate of change of the Lyapunov function. We believe that this is of capital importance specially for experimentalist and for chemical Engineering. The method used here is appealing due to its reliable ability to detect robust synchronization in biochemical oscillators, because the synchronization problem does not need to be framed as a tracking feedback control problem as presented in many other works ([73]and references therein).

In lattices, cells with activator-inhibitor pathways are also known to display, depending on their population size, interesting features of spatiotemporal organization, when directly interacting under steady coupling conditions [1, 11, 12, 34]. In a subsequent inquiry, we have investigated their synchronized dynamics assuming that they interact indirectly through a dynamic environment with adaptive feedback control mechanism, aiming at promoting a cooperative pattern between the biochemical pathways of the chaotic cells, by stabilizing in the phase space their trajectories that lean towards disseminating themselves along unsteady directions, setting them

to flout synchronization. Though a weak form of coupling, this coupling mode has proven itself capable of engendering robust synchrony among cells with activator-inhibitor pathways. The stability analysis of the synchronized state has been carried out in this framework and the numerical simulations suggest the existence of many suitable conditions that favor the emergence of this highly desirable collaborative arrangement among the cells.

On the same footing, we have investigated the liability of relatively large two-dimensional spatial networks of such biological units to generate some beguiling spatial patterns, forms and wave phenomena, via diffusion-driven instabilities. These patterns formation scenarios include both stationary and oscillatory Turing patterns. The latter set embraces interesting wave phenomena such as travelling wave structures and spatiotemporal chaos in two-dimensional spatial lattices. The relevance of these phenomena in biology has been highlighted and we believe that the outcomes of this work will help pave the way for scientists to take advantage of the limited opportunities we have, for communicating with the workforce underlying the emergence of patterns in science as a whole, so as to direct experiments towards an acceptable end-product.

It can't be overemphasized that several analytical and computational methods have been used in the course of these investigations, and their mutual agreements all through the analysis are in favor of bestowing a valuable degree of consistency to the obtained outcomes.

Open problems and future directions

Though this thesis presents many interesting new results, there still remains numerous important issues that need to be addressed in future works.

♠ In any physical or biological system, time delays are unavoidable in signal transmission. Neural synchronization for instance was reported to occur between the brain areas separated by distances up to several centimeters [169, 170, 171]. Time delay seems to facilitate synchronization between the distant cortical areas. These facts may equally suggest that long range cellular synchronization is possible between areas which are coupled with predominantly low connectivity strengths [172]. Investigating this phenomenon in cells with activator-inhibitor pathways may bring significant insights on the mechanisms pertaining in cellular functions.

On the same footing, the concept of time delayed coupling in physical systems usually leads to the typical issue of anticipating synchronization. This synchronization regime has been often

described as a rather counterintuitive phenomenon because of the possibility of a slave system anticipating the evolution of the master [173, 175, 177]. However, not long ago, the synchronization of chaotic systems in a unidirectional coupling configuration has attracted great interest due to its potential applications to secure communication systems [22]. Particular attention has been paid to this so called "*anticipating synchronization*" regime where two identical chaotic systems can be synchronized by unidirectional delayed coupling in such a manner that "the slave" (the system with coupling) anticipates "the master" (the one without coupling). This regime has been theoretically studied in several systems [174, 175, 176], electronic circuits [177], and chaotic semiconductors [178]. Interestingly, this regime has lately been reported in excitable systems with unidirectional delayed coupling when subjected to the same external forcing [179]. Therefore, since many biological systems such as neurons and heart cells exhibit excitable behavior and often operate in a feedback regime in a noisy environment, the study of the delayed coupling effects in the presence of noise is certainly of wide concerns. This therefore yields major perspectives in this framework such as:

♠ Investigating the mechanisms of synchronization (anticipatory or not) of cells with activator-inhibitor pathways as they communicate efficiently and constructively within a noisy environment in the presence of time delayed couplings.

♠ Examining the possibility of reasonably modelling tissues of such cells as excitable media with information processing phenomena via the generation and propagation of nonlinear localized waves of excitation.

Appendix

Definition of the functions $F_z(z)$, $G_y(y,z)$, $G_z(y,z)$ and $\Gamma_z(z)$

$$
\begin{aligned}
F_z(z) &= \frac{-4z^3}{(1+z^4)^2} \\
G_y(y,z) &= \frac{T(1+z)^2(1+2y)(L+(1+y)^2(1+z)^2)-2Ty(1+y)^2(1+z)^4}{(L+(1+y)^2(1+z)^2)^2} \\
G_z(y,z) &= \frac{2Ty(1+z)(1+y)(L+(1+y)^2(1+z)^2)-2Ty(1+y)^3(1+z)^3}{(L+(1+y)^2(1+z)^2)^2} \\
\Gamma_z(z) &= \frac{\lambda\exp\{-\lambda(z-\theta_s)\}}{[1+\exp\{-\lambda(z-\theta_s)\}]^2}
\end{aligned}
$$

Bibliography

[1] S. Sinha, R. Ramaswamy, in: H. Degn, A. V. Holden, L. F. Olsen (Eds.), *Chaos in Biological Systems* (Plenum Press, New York, 1987).

[2] D. Hebb, *The organization of behavior* (New York, Wiley, 1949).

[3] S. H. Strogatz and I. Stewat, Sic. Am. **269**, 102 (1993).

[4] D. Helbing and B.A. Huberman, Nature **396**, 738 (1998).

[5] A.T. Winfree, *The Geometry of Biology Time* (Springer,2ed, New york, 2001).

[6] I.Z. Kiss, Y. Zhai, and J.L. Hudson, Science **296**, 1676 (2002).

[7] A.T. Winfree, Science **298**, 2336 (2002).

[8] S. Nadis, Nature **421**, 780 (2003).

[9] S. H. Strogatz, *Sync: the emerging science of spontaneous order* (Hyperion, New York, 2003).

[10] P. Raven, G. Johnson, K. Mason, J. Losos, S. Singer, *Biology* (McGraw-Hill Education, New York 10ed, 2013).

[11] S Rajesh, Sudeshna Sinha and Somdata Sinha, Phys. Rev. E **75**, 011906(2007).

[12] P. Guemkam Ghomsi, F.M. Moukam Kakmeni, T.C. Kofane, and C. Tchawoua, Phys. Lett. A **378**, 2813 (2014).

[13] J. Wolf, R. Heinrich, BioSystems **43**, 1 (1997).

[14] A. Goldbeter, *Biochemical oscillations and cellular rhythms. The molecular bases of periodic and chaotic behaviour.* (Cambridge University Press, Cambridge, 1996).

[15] O. Decroly and A. Goldbeter, Proc. Natl. Acad. Sci. USA **79**, 6917 (1982).

[16] J. Higgins, Ind. Eng. Chem. **59**, 18 (1967).

[17] F. M. Moukam Kakmeni and M.S. Baptista, Pramana Vol. **70**, No. 6, 1063 (2008).

[18] E. K. Pye, Can. J. Botany **47**, 271 (1969).

[19] A. K. Ghosh, B. Chance, and E. K. Pye, Arch. Biochem. Biophys. **145**, 319 (1971).

[20] L. M. Pecora and T. L. Carroll, Phys Rev Lett. **64**, 821 (1990); L. M. Pecora and T. L. Carroll, Phys. Rev. Lett. **80**, 2109 (1998).

[21] L. Huang, Q. Chen, Y-C. Lai, and L. M. Pecora, Physical Review E, **80**, 036204(2009).

[22] L.M. Pecora, T.L. Carroll, G.A. Johnson, D.J. Mar, J.F. Heagy, Chaos **7** 520 (1997).

[23] S. Boccaletti, V. Latora, Y. Moreno, M. Chavez, D.-U. Hwang, Physics Reports **424** (2006).

[24] S. Boccaletti, J. Kurths, G. Osipov, D.L. Valladares, C.S. Zhou, Physics Reports **366** (2002).

[25] Paul So, Bernard C. Cotton, and Ernest Barreto, Chaos **18**, 037114 (2008).

[26] A. Koseska, E. Volkov, and J. Kurths, Chaos **20**, 023132 (2010).

[27] H. Ulrichs, A. Mann, and U. Parlitz Chaos **19**, 043120 (2009).

[28] Y. Sun and J. Ruan, Chaos **19**, 043113 (2009).

[29] F. Sorrentino, G. Barlev, Adam B. Cohen, and Edward Ott Chaos **20**, 013103 (2010).

[30] S. Bowong, and F. M. Moukam Kakmeni, Phys. Lett. A **316**, 206 (2003).

[31] F. M. Moukam Kakmeni, S. Bowong, D. V. Senthikumar, and J. Kurths, CHAOS **20**, 043121 (2010).

[32] D. Gonze, N. Markadieu, and A. Goldbeter, CHAOS **18**, 037127 (2008).

[33] Y. Kuramoto, Chemical Oscillations, Waves, and Turbulence (Springer, New York, 1984).

[34] C. Suguna, S. Sinha, Physica A **346**, 154 (2005).

[35] J. Garcia-Ojalvo, Michael B. Elowitz, and Steven H. Strogatz, Proc. Natl. Acad. Sci. U.S.A. **101**, 10955 (2004).

[36] J.-J. Perraud, A. De Wit, E. Dulos, P. De Kepper, G. Dewel, P. Borckmans, Phys. Rev. Lett. **71** (8), 1272 (1993).

[37] A. Rovinsky, M. Menzinger, Phys. Rev. A **46** (10), 6315 (1992).

[38] W. Just, M. Bose, S. Bose, H. Engel, E. Schöll, Phys. Rev. E **64** (026219), 1 (2001).

[39] L. Yang, I. R. Epstein, Phys. Rev. Lett. **90**, 178303 (2003).

[40] A. De Wit, D. Lima, G. Dewel, P. Borckmans, Phys. Rev. E **54** (1), 261 (1996).

[41] M. Meixner, A. De Wit, S. Bose, E. Schöll, Phys. Rev. E **55** (6), 6690-6697 (1997).

[42] J. Boissonade, E. Dulos and P. De Kepper, in *Chemical Waves and Patterns*, edited by R. Kapral and K. Showalter (Kluver, Dordrecht, 1995), P. 221.

[43] L. F. Yang, M. Dolnik, A. M. Zhabotinsky, and I. R. Epstein, J. Chem. Phys. **117**, 7259 (2002).

[44] A. M. Turing, Philos. Trans. R. Soc. London Der. B **237**, 37 (1952).

[45] M. C. Cross and P. C. Hohenberg, Rev. Mod. Phys. **65**, 851 (1993).

[46] G. Ansmann, K. Lehnertz, and U. Feudel, Phys. Rev. X **6**, 011030 (2016).

[47] B. I. Shraiman, A. Pumir, W. Van Saarloos, P. C. Hohenberg, H. Chaté, and M. Holen, Physica D **57**, 241 (1992).

[48] A. De wit, G. Dewel, and P. Borckmans, Phys. Rev. E **48**, R4191 (1993).

[49] S. Alonso, K. John, and M. Bär, J. Chem. Phys. **134**, 094117 (2011).

[50] Q. Ouyang and J. M. Flesselles, Nature **379**, 143 (1996).

[51] I. Berenstein and J. Carballido-Landeira, RSC Adv. **6**, 56867 (2016).

[52] K. Krischer, M. Eiswirth, and G. Ertl, J. Chem. Phys. **96**, 9161 (1992).

[53] D. Krefting and C. Beta, Phys. Rev. E **81**, 036209 (2010).

[54] C. Beta, A. S. Mikhailov, H. H. Rothermund, and G. Ertl, Europhys. Lett. **75**, 868 (2006).

[55] J. Davidsen and R. Kapral, Phys. Rev. Lett. **91**, 058303 (2003).

[56] M. Bär, M. Hildebrand, M. Eiswirth, M. Falke, H. Engel, and Neufeld, Chaos **4**, 499 (1994).

[57] H. Meinhardt and A. Gierer, BioEssays **22**, 753 (2000).

[58] A. Gierer and H. Meinhardt, Kybernetik **12**, 30 (1972).

[59] Y. Almirantis, S. Papageorgiou, J. Theor. Biol. **151**, 289 (1991).

[60] J. M. Chung, E. Peacock-Lpez, J. Chem. Phys. **127**, 174903 (2007).

[61] D. Fanelli, C. Cianci, F. Di Patti, Eur. Phys. J. B **86**, 1 (2013).

[62] J. Shi, Z. Xie, K. Little, J. Appl. Anal. Comput. **1**, 95 (2011).

[63] J. Bard, I. Lauder. J. Theor. Biol. **45**, 501 (1974).

[64] Q. Zheng, J. Shen, Nonlinear Dyn. **78**, 1301 (2014).

[65] M. Baurmann, T. Gross, U. Feudel, J. Theor. Biol. **245**, 220 (2007).

[66] Y. Shiferaw, A. Karma, Proc. Natl. Acad. Sci. U.S.A. **103**, 5670 (2006).

[67] I. Berenstein and J. Carballido-Landeira, Chaos **27**, 013116 (2017).

[68] T. Pereira, M. S. Baptista, and J. Kurths, Eur. Phys. J. Spetial Topics **146**, 155 (2007).

[69] M. S. Baptista, F. M. Moukam Kakmeni, C. Grebogi Physical Review E, **82**, 036203(2010).

[70] I. Belykh, E. de Lange, and M. Hasler, Phys. Rev. Lett. **94**, 188101 (2005).

[71] N. Kopell and B. Ermentrout, PNAS 101, 15482 (2004).

[72] I. Belykh and A. Shilnikov, PRL **101**, 078102 (2008).

[73] A. Bartoszewicz, Robust Control, Theory and Applications, (Published by InTech, Croatia, 2011).

[74] J.R. Collier, N.A.M. Monk, P.K. Maini, and J.H. Lewis, J. Theor. Biol. **183**, 429 (1996).

[75] J. Keener and J. Sneyd, *Mathematical Physiology* (Springer-Verlag, New York, 1998).

[76] J. Monod, J. Wyman, and J. P. Changeaux, J. Mol. Biol. **12**, 88 (1965).

[77] G. von Dassow, E. Meir, E. M. Munro, and G.M. Odell, Nature **406**, 188 (2000).

[78] M. B. Miller and B. L. Bassler, Annu. Rev. Microbiol. **55**, 165 (2001).

[79] M. Freeman and J.B. Gurdon, Annu. Rev. Cell Dev. Biol. **18**, 515 (2002).

[80] Guy Katriel, Physica D **237**, 2933 (2008).

[81] P. Guemkam Ghomsi, F.M. Moukam Kakmeni, C. Tchawoua, and T.C. Kofane, Phys. Rev. E **92**, 052911 (2015).

[82] S. A. Lazzouni, S. Bowong, F. M. Moukam Kakmeni, and B. Cherki, Commun. Nonlin. Sci. Numer. Simul. **12**, 568 (2007).

[83] F. M. Moukam Kakmeni and S. Bowong, Int. Journal of Bifurcation and Chaos **17**, 3259 (2007).

[84] S. Bowong, F. M. Moukam Kakmeni, and C. Tchawoua, Phys. Rev. E **70**, 066217 (2004).

[85] F. M. Moukam Kakmeni, S. Bowong, C. Tchawoua, and E. Kaptouom, Phys. Lett. A **322**, 263 (2004).

[86] R. Abraham, C. Shaw, The Geometry of Behavior (Studies in Nonlinearity) (Addison- Wesley, Reading, 1992).

[87] A.A. Andronov, S.E. Khaikin, Theory of Oscillations (Gostekhizdat, Moscow, 1937) (in Russian).

[88] A.A. Andronov, A.A. Vitt, S.E. Khaikin, Theory of Oscillations (Pergamon, Elmsford, 1966).

[89] R.M. May, Nature (London) **261**: 459 (1976).

[90] M.J. Feigenbaum, Commun. Math. Phys. **77**: 65 (1980).

[91] J-P. Eckmann, Rev. Mod. Phys. **53**: 643 (1981).

[92] A.V. Holden, ed.,"Chaos", University Press, Manchester and Princeton (1986).

[93] L.F. Olsen and H. Degn, Quart. Rev. Biophys. **18**: 165 (1985).

[94] M.C. Mackey and L. Glass, Science, **197**: 287 (1977).

[95] A.L. Goldberger, L.J. Findley, M.R. Blackburn and A.J. Mandell, Am. Heart J. **107**: 612 (1984).

[96] J.M. Smith and R.J. Cohen, Proc. Natl. Acad. Sci. S.A. **81**: 233 (1984).

[97] A. Babloyantz and A. Destexhe, Proc. Natl. Acad. Sci. U.S.A. **83**: 3513 (1986).

[98] D. Ruelle, Math. Intelligencer **2**: 126 (1980).

[99] A.L. Goldberger, V. Bhargava, B. West and A.J. Mandell, Physica **17D**: 207 (1985).

[100] A.L. Goldberger, B.J. West and V. Bhargava, in "Proc. 11th International Modeling and Computers in Simulation" World Congress, Oslo, Norway, **Vol. 2**, eds. B. Wahlstrom, R. Henriksen and N.P. Sundby, 239-242, North Holland Publishing Co., Amsterdam (1985).

[101] A.L. Goldberger, in "Temporal Disorder in Human Oscillatory Systems", eds. L. Rensing, U. Ander Heiden and M. Mackey, Springer, Berlin, in press.

[102] A.L. Goldberger, V. Bhargava, B.J. West and A.J. Mandell, Physica **19D**: 282 (1986).

[103] A.J. Mandell, S. Knapp, C.L. Ehlers and P.V. Russo, in "Neurobiology of the Mood Disorders", eds. R.M. Post and J.C. Ballenger, 744-776, Williams and Wilkins, Baltimore (1983).

[104] A. Pikovsky, M. Rosenblum and J. Kurths, Synchronization: a universal concept in nonlinear sciences (Cambridge: Cambridge University Press) (2001).

[105] A. Mitra and S. Sinha, National conference on nonlinear systems and Dynamics, RIASM, 1 (2006).

[106] S. Ghosh, G. Rangarajan, and S. Sinha, Eur. Phys. Lett. **92**, 40012 (2010).

[107] C. Suguna, K. K. Chowdhury and S. Sinha, Phys. Rev. E **60**, 5943 (1999).

[108] J. D. Murray , Mathematical biology (Berlin: Springer-Verlag) (1989).

[109] M. C. Cross and P. C. Hohenberg, Pattern formation outside of equilibrium. Rev. Mod. Phys. **65**: 851 (1993).

[110] P. Ball, The self-made tapestry: pattern formation in nature. Oxford Univ. Press, Oxford (2001).

[111] S. Sinha and R. Ramaswamy, BioSystems **20**, 341 (1987).

[112] M. A. Savageau, in 'Biochemical System Analysis', Addision Wesley Publ. Co., Reading (1976).

[113] C. H. Waddington, Organisers and Genes, Cambridge University Press, Cambridge (1947).

[114] E. Jr, Y. Grechkin, N. Mikhailova and E. Selkov, MPW: the Metabolic Path- ways Database, Nucleic Acids Res. **26**, 43 (1998).

[115] D. , A. M. Huerta, E. Perez-Rueda and J. Collado-Vides, From specific gene regulation to genomic networks: a global analysis of transcriptional regulation in Escherichia coli, Bioessays, **20**, 433 (1998).

[116] R. Maithreye and Somdatta Sinha, Modelling simple biochemical networks, in function and regulation of cellular systems: Experiments and Models edited by A. Deutsch, M. Falcke, J. Howard and W. Zimmerman (Basle, Birkhauser, 2003).

[117] J.J. Tyson, Periodic enzyme synthesis and oscillatory repression: why is the period of oscillation close to the cell cycle time? J. Theor. BioI., **103**, 313 (1983).

[118] S. Sinha and R. Ramaswamy, Complex Behaviour of the Repressible Operon, J. Theor. BioI., **132**, 307 (1988).

[119] S. Sinha, Theoretical study of tryptophan operon: Application in microbial technology, Biotech. and Bioengg, **31**, 117 (1988).

[120] M. Santillan and M. C. Mackey, Dynamic regulation of the tryptophan operon: A modeling study and comparison with experimental data, Proc. Natl. Acad. Sci. (U.S.A), **98**, 1364 (2001).

[121] A. K. Sen and W. Liu, Dynamic analysis of genetic control and regulation of amino acid synthesis: The tryptophan operon in Escherichia coli, Biotechnol. Bioeng., **35** (18), 5 (1989).

[122] N. Minorsky, Nonlinear Oscillations, Van Nostrand, Princeton, NJ (1962).

[123] A. Goldbeter and G. Nicolis, Progr. Theor. Biol. **4**: 65 (1976).

[124] J.J. Tyson, J. Theor. Biol. **103**: 313 (1983).

[125] C. Suguna, R Maithreye, S. Suthram and Somdatta Sinha, Dynamics of cellular processes: from single cell to collective behavior, in Recent Research Developments in Biophysical Chemistry, edited by C.A. Condat and A. Baruzzi, Research Signpost (2002).

[126] C. Suguna and Somdatta Sinha, Cellular Dynamics in Noisy Environment, Fluctuation and Noise Letters **2** (4), L313 (2002).

[127] S. Liebner, U. Cavallaro, and E. Dejana, Arterioscler., Thromb., Vasc. Biol. **26**, 1431 (2006); A. V. Panfilov, Phys. Rev. Lett. 88, 118101 (2002); Bradford E. Peercy and James P. Keener, SIAM J. Appl. Dyn. Syst. **4**, 679 (2005); Claudiu A. Giurumescu, Paul W. Sternberg, and Anand R. Asthagiri, Proc. Natl. Acad. Sci. U.S.A. **103**, 1331 (2006).

[128] G. C. Cruywagen, P. K. Maini, and J. D. Murray, J. Math. Biol. **33**, 193 (1994); S. C. Muller, T. Mair, and O. Steinbock, Biophys. Chem. **72**, 37 (1998).

[129] R. Bertram, J. Previte, A. Sherman, T. A. Kinard and L. S. Satin, The phantom burster model for pancreatic beta-cells; Biophys. J. **79**, 28802892 (2000).

[130] G. Bub, A. Shrier and L. Glass, Global organization of dynamics in heterogeneous, spontaneously active excitable media; Phys. Rev. Lett. **94**, 028105 (14) (2005).

[131] Theory and Applications of Coupled Map Lattices, edited by K. Kaneko (Wiley, New York, 1993), and references therein.

[132] C. Suguna and Somdatta Sinha, Physica A **346**, 154 (2005).

[133] P. Raven and G. Johnson, Biology (The McGraw Hill Companies, Dubuque) (2002).

[134] H. H. McAdams and A.P. Arkin, Proc. Natl. Acad. Sci. U.S.A. **94**, 814 (1997).

[135] V. Resmi and G. Ambika, Phys Rev E **81**, 046216 (2010).

[136] I. R. Epstein and K. Showalter, J. Phys. Chem. **100**, 13132 (1996).

[137] M. Alamgir and I. R. Epstein, J. Am. Chem. Soc. **105**, 2500 (1983).

[138] T. Pereira, M. S. Baptista, and J. Kurths, Eur. Phys. Lett **77**, 40006 (2007).

[139] T. Pereira, M. S. Baptista, and J. Kurths, Phys. Rev. E **75**, 026216 (2007).

[140] M. Bier, B. M. Bakker, and H. V. Westerhoff, Biophysical J. **78**, 1087 (2000).

[141] A. Wolf, J.B. Swift, H.L. Swinney, J.A. Vastano, Physica D **16**, 285 (1985).

[142] T. Pereira, M. S. Baptista, and J. Kurths, Phys. Lett. A **362**, 159 (2007).

[143] Andreas Bohn and Jordi Garcia-Ojalvo, J. Theor. Biol. **250**, 37 (2008).

[144] N. J. Balmforth, C. Pasquero, and A. Provenzale, Physica D **138**, 1 (2000).

[145] Seiji Takagi, Alain Pumir, Lorenz Kramer, and Valentin Krin- sky, Phys. Rev. Lett. **90**, 124101 (2003).

[146] J. D. Murray, *Mathematical Biology II: Spatial Models and Biomedical Applications* (Springer, Berlin, Heidelberg, 2003).

[147] L. Wolpert, J. Theor. Biol. **25**, 1 (1969).

[148] A. Khadra, Y.X. Li, Biophys. J. **91**, 74 (2006).

[149] D. Ghosh and T. Banerjee, arXiv:1409.1063v3 [nlin.CD], (2009).

[150] T. Banerjee, D. Biswas, Nonlinear Dyn. **73**, 2225 (2013).

[151] G. Scheler, F1000Research **2**, 116 (2013).

[152] V.I. Oseledec, "A Multiplicative Ergodic Theorem. Lyapunov Characteristic Numbers for Dynamical Systems," Trans. Moscow Math. Soc. **19**, 197 (1968).

[153] G. Benettin, L. Galgani, A. Giorgilli and J.-M. Strelcyn, "Lyapunov Characteristic Exponents for Smooth Dynamical Systems and for Hamiltonian Systems; A Method for Computing All of Them," Meccanica **15**, 9 (1980).

[154] I. Shimada and T. Nagashima, "A Numerical Approach to Ergodic Problem of Dissipative Dynamical Systems," Prog. Theor. Phys. **61**, 1605 (1979).

[155] R. Shaw, "Strange Attractors, Chaotic Behavior, and Information Flow," Z. Naturforsch. **36A**, 80 (1981).

[156] G. Ambika and R. E. Amritkar, Phys. Rev. E **79**, 056206 (2009).

[157] E. Gehrmann, C. Gler, Y. Jin, B. Sendhoff, B. Drossel, and K. Hamacher, Phys. Rev. E **84**, 021913 (2011).

[158] J. Wolf et al., Biophys. J. **78**, 1145 (2000).

[159] F. Hynne et al., Biophys. Chem. **94**, 121 (2001).

[160] D. J. Gautier and J. Bienfang, Phys. Rev. Lett **77**, 1751 (1996).

[161] J. N. Blakely, D. J. Gautier, G. Jonhson, T. L. Carroll, and L. M. Pecora, Chaos **10**, 738 (2000).

[162] H. Fujisaka and T. Yamada, Prog. Theor. Phys. **69**, 32 (1983); **70**, 1240 (1983).

[163] F. Argoul, A. Arneodo, and P. Richetti, Phys. Lett. A **120**, 269 (1987); F. T. Arecchi et al., J. Opt. Soc. Am. B **5**, 1153 (1988); M. Lefranc et al., ibid. **8**, 239 (1991); R. Herrero, R. Pons, J. Farjas, F. Pi, and G. Orriols, Phys. Rev. E **53**, 5627 (1996);T. Braun, J. A. Lisboa, and J. A. C. Gallas, Phys. Rev. Lett. **68**,2770 (1991); H. Herzael et al., Physica D **48**, 340 (1991); M. R. Basset and J. L. Hudson, J. Phys. Chem. **92**, 6963 (1988).

[164] S. Rajesh, S. Sinha and S. Sinha Synchronization in coupled cells with activatorinhibitor pathways; Phys. Rev. E **75**, 011906 (111) (2007).

[165] K. Kaneko, Phys. Rev. Lett. **69**, 905 (1992).

[166] J. Garcia-Ojalvo, Michael B. Elowitz, and Steven H. Strogatz, Proc. Natl. Acad. Sci. U.S.A. **101**, 10955 (2004).

[167] H. H. McAdams and A. P. Arkin, Trends Genet. **15**,65 (1999).

[168] A. Rustom, R. Saffrich, I. Markovic, P. Walther, and H. H. Gerdes, Science **303**, 1007 (2004); B. Onfelt, S. Nedvetzki, K. Yanagi, and D. M. Davis, J. Immunol. **173**, 1511 (2004); Masamichi Koyanagi, Ralf P. Brandes, Judith Haendeler, An- dreas M. Zeiher, and Stefanie Dimmeler, Circ. Res. **96**, 1039 (2005).

[169] J. E. Desmedt and C. Tomberg, Neurosci. Lett. **168**, 126 (1994).

[170] W. H. R. Miltner, C. Braun, M. Arnold, H. Witte, and E. Taub, Nature (London) **397**, 434 (1999).

[171] C. Tallon-Baudry, O. Bertrand, and C. Fischer, J. Neurosci. **21**, 1 (2001).

[172] Mukeshwar Dhamala, Viktor K. Jirsa, and Mingzhou Ding, Phys. Rev. Lett. **92**, 074104 (2004).

[173] H. U. Voss, Phys. Rev. E **61**, 5115 (2000); Phys. Rev. E **64**, 039904(E) (2001); Phys. Rev. Lett. **87**, 014102 (2001).

[174] E. Hernandez-Garcia, C. Masoller, and C. R. Mirasso, Phys. Lett. A **295**, 39 (2002).

[175] O. Calvo, D. R. Chialvo, V. M. Eguiluz, C. R. Mirasso, and R. Toral, Chaos **14**, 7 (2003).

[176] C. Masoller, Phys. Rev. Lett. **86**, 2782 (2002).

[177] H. U. Voss, Int. J. Bifurc. Chaos Appl. Sci. Eng. **12**, 1619 (2002).

[178] Y. Liu et al., Appl. Phys. Lett. **80**, 4306 (2002).

[179] Marzena Ciszak, Francesco Marino, Raul Toral, and Salvador Balle, Phys. Rev. Lett. **93**, 114102 (2004).

List of personal publications which are used in preparation of this thesis

1- **P. Guemkam Ghomsi**, F. M. Moukam Kakmeni, T. C. Kofane, and Clément Tchawoua, ***Synchronization dynamics of chemically coupled cells with activator-inhibitor pathways***, Physics Letters A **378**, 2813 (2014).

2- **P. Guemkam Ghomsi**, F. M. Moukam Kakmeni, Clément Tchawoua, and T. C. Kofane, ***Synchronization of cells with activator-inhibitor pathways through adaptive environment-mediated coupling***, Phys. Rev. E **92**, 052911 (2015).

3- **P. Guemkam Ghomsi**, F. M. Moukam Kakmeni, Clément Tchawoua, and T. C. Kofane, ***Diffusion-induced spatiotemporal patterns in cells with activator-inhibitor pathways***, Submitted for publication.

4- **P. Guemkam Ghomsi**, F. M. Moukam Kakmeni, and T. C. Kofane, ***Can chemically coupled biological systems completely synchronize?***, Submitted for publication.